

## Durham E-Theses

---

# *Emulsion-Templated Porous Polymers as Support Materials for Covalent Enzyme Immobilization*

KIMMINS, SCOTT,DAVID

### How to cite:

---

KIMMINS, SCOTT,DAVID (2011) *Emulsion-Templated Porous Polymers as Support Materials for Covalent Enzyme Immobilization*, Durham theses, Durham University. Available at Durham E-Theses Online: <http://etheses.dur.ac.uk/902/>

### Use policy

---

The full-text may be used and/or reproduced, and given to third parties in any format or medium, without prior permission or charge, for personal research or study, educational, or not-for-profit purposes provided that:

- a full bibliographic reference is made to the original source
- a [link](#) is made to the metadata record in Durham E-Theses
- the full-text is not changed in any way

The full-text must not be sold in any format or medium without the formal permission of the copyright holders.

Please consult the [full Durham E-Theses policy](#) for further details.

---

Academic Support Office, Durham University, University Office, Old Elvet, Durham DH1 3HP  
e-mail: [e-theses.admin@dur.ac.uk](mailto:e-theses.admin@dur.ac.uk) Tel: +44 0191 334 6107  
<http://etheses.dur.ac.uk>



# **Emulsion-Templated Porous Polymers as Support Materials for Covalent Enzyme Immobilization**

---

Scott D. Kimmins

Ustinov College  
Department of Chemistry  
University of Durham

June 2011

Thesis submitted to the University of Durham in partial fulfillment of the regulations for the Degree of Doctor of Philosophy.

## **Declaration**

The work reported in this thesis was carried out in the laboratories of the Department of Chemistry, University of Durham between October 2007 and December 2010. This work has not been submitted for any other degree in Durham or elsewhere and, unless otherwise stated, is the original work of the author.

## **Statement of Copyright**

The copyright of this thesis rests with the author. No quotation from it should be published without their prior consent and information derived from it should be acknowledged.

## **Financial Support**

I gratefully thank the Engineering and Physical Sciences Research Council's Doctoral Training Account (EPSRC) and (DSM) for their generous funding of this research.

# Abstract

It has been observed that poly(High Internal Phase Emulsion) (polyHIPE) materials can be used as biocatalysts, via the covalent immobilization of *Candida Antarctica* Lipase B (CAL-B). Recently, it has been shown that polyHIPEs can be prepared with epoxy functionality, which show potential for the covalent immobilization of enzymes.

The aims of our work were, firstly, to produce an open-void glycidyl methacrylate (GMA)-based polyHIPE material. Secondly, these materials were then to be developed for use within a continuous flow set-up. Thirdly, the post-polymerisation of these materials was to be investigated. Finally, these materials were to be used as a support for the covalent immobilization of enzymes.

Highly porous, open-void GMA-based polyHIPE materials were accomplished via the photo-initiation, rather than thermal initiation of the continuous phase of the emulsion. The rapid cure of the emulsion effectively 'locks' the emulsion morphology, prior to emulsion destabilisation, that is more prominent in the slower thermally initiated HIPEs. Photopolymerised GMA-based polyHIPE materials were further developed for use within a continuous flow-set up. GMA-based polyHIPE materials were functionalized post-polymerisation with tris(2-aminoethyl)amine, morpholine and *O,O'*-bis(3-aminopropyl)polyethylene glycol. The functionalization of these GMA-based materials was observed via a number of analysis techniques, such as FT-IR spectroscopy, XPS spectroscopy, elemental analysis, Fmoc number determination, <sup>1</sup>H HR-MAS NMR spectroscopy, and the covalent attachment of ninhydrin and FITC. Elemental analysis of the morpholine and tris(2-aminoethyl)amine polyHIPE showed that a near quantitative conversion, of 72 and 82 % respectively, was accomplished via the reaction being conducted at reflux for 24 hours. The enzymes, Lipase from *Candida Antarctica* and Proteinase K from *Tritirachium album* were immobilized either directly onto the polyHIPE material or via a hydrophilic spacer group, *O,O'*-bis(3-aminopropyl)polyethylene glycol. CAL was immobilized with a loading of between 5.4 and 7.5 wt. % per g of polyHIPE material.

# Acknowledgments

Firstly, I would like to thank my supervisor Prof. Neil Cameron for his encouragement, patience and support throughout my Ph.D. In addition, I would like to also thank DSM for funding for my Ph.D. and support given by my industrial supervisors, Dr Jens Thies and Dr Paul Wyman.

A mention must be made for the technical staff at the chemistry department; Neil and Scott in the mechanical workshop for preparing the PTFE moulds for polyHIPE samples, Helen Riggs for assistance with SEM and ESEM analysis, Dr Ross Carnachan for assistance with mercury porosimetry and especially Dr Alan Kenwright for NMR analysis.

Thanks to my friends and colleagues in the NRC group and CG235 past and present, in particular, Greg, Lovelady, Lauren, Wee man, Mike, Alison, Didsey, Johnson, Adam, Jon, Bridie, Dan (Maltman), Dan (Tams), and Steve. In addition to my friends here in Durham and on the staff football team, for making my Ph.D. so enjoyable, Ian, Nippard, Nick, Chopper and Seb.

Last but not least, Sarah and Mildred who have given me endless support throughout my thesis and for having to put up with me.

# Contents

Abstract .....	ii
Acknowledgments .....	iii
Units and Symbols .....	x
List of Figures .....	xvi
List of Tables .....	xxiv
1 Introduction .....	1
1.1 Free-radical Initiated Polymerisation .....	1
1.1.1 <i>Methods for the Preparation of Free-radical Initiated Polymers</i> .....	5
1.1.2 <i>Copolymerisation</i> .....	6
1.1.3 <i>Glass Transition Temperature</i> .....	6
1.1.4 <i>Network Polymers</i> .....	7
1.1.5 <i>Photoinitiated Free-radical Crosslinking Polymerisation</i> .....	7
1.1.5.1 Oxygen Retardation .....	9
1.1.5.2 Frontal Polymerisation .....	10
1.2 Emulsions .....	10
1.2.1 <i>Emulsion Type: Hydrophile Lipophile Balance (HLB) and Phase Inversion Temperature (PIT)</i> .....	12
1.2.2 <i>Emulsion Instability</i> .....	13
1.2.3 <i>High Internal Phase Emulsions (HIPEs)</i> .....	14
1.3 Functional Porous Polymers by Emulsion Templating .....	15
1.3.1 <i>Functional Materials from Novel Emulsion Templating Systems</i> .....	16
1.3.1.1 Extending the Range of Monomers Applicable to Emulsion Templating... ..	16
1.3.1.2 Templating Particle-Stabilized High Internal Phase Emulsions .....	25
1.3.1.3 Porous Polymers by Photopolymerization of HIPEs .....	28
1.3.1.4 Emulsion Templated Porous Beads and Membranes .....	29
1.3.2 <i>Chemical Functionalization of Emulsion Templated Porous Polymers</i> .....	32
1.3.3 <i>Enzyme Immobilization</i> .....	39
1.3.3.1 Enzyme Immobilization onto Emulsion-Templated Porous Polymers ...	40
1.4 Aims and Structure of Thesis .....	43

1.5	Biobibliography.....	45
2	Preparation and Characterization of GMA-based Photoinitiated PolyHIPE Materials	54
2.1	Introduction.....	54
2.2	Experimental Section.....	55
2.2.1	<i>Materials</i> .....	55
2.2.2	<i>Photopolymerised GMA-based polyHIPE preparation</i> .....	59
2.2.3	<i>PolyHIPE Coding System</i> .....	61
2.2.4	<i>Preparation of a Hydrophilic Photopolymerised PolyHIPE Material</i> .....	61
2.2.5	<i>GMA / EGDMA HIPE preparation and thermal polymerisation</i> .....	62
2.2.6	<i>GMA/TRIM HIPE Preparation and Photopolymerisation</i> .....	63
2.2.7	<i>Preparation of Photopolymerised GMA-based Monoliths for Continuous Flow Applications</i> .....	64
2.2.7.1	Functionalization of Glass Column .....	64
2.2.7.2	Preparation of GMA/EGDMA HIPE with Photoinitiator .....	64
2.2.7.3	Preparation of Monolith within Functionalized Glass Column .....	64
2.3	Instrumentation and Characterization.....	71
2.3.1	<i>Scanning Electron Microscopy (SEM)</i> .....	71
2.3.2	<i>Environmental Scanning Electron Microscopy (ESEM)</i> .....	71
2.3.3	<i>Mercury Intrusion Porosimetry</i> .....	71
2.3.4	<i>Surface Area Analysis</i> .....	72
2.3.5	<i>FTIR Spectroscopy</i> .....	72
2.3.6	<i>Solvent Delivery System</i> .....	72
2.3.7	<i>UV-curing device</i> .....	73
2.3.8	<i>SEM analysis with Image J software</i> .....	73
2.4	Results and Discussion .....	73
2.4.1	<i>Thermally Initiated GMA-based HIPEs</i> .....	73
2.4.2	<i>Photoinitiated polymerisation of GMA-based HIPEs</i> .....	76
2.4.2.1	GMA-co-EHA-co-IBOA-co-TMPTA photopolymerised polyHIPEs .....	76
2.4.2.2	Preparation of Photopolymerised GMA-based PolyHIPE Materials with Differing Quantities of GMA .....	84
2.4.2.3	Preparation of Novel Photopolymerised Hydrophilic GMA-based PolyHIPE Materials.....	85



2.4.2.4	Preparation of a Photopolymerized GMA-based PolyHIPE Monolith for Continuous Flow Applications .....	90
2.4.2.5	Preparation of Photopolymerised GMA-co-TRIM PolyHIPE Material ....	99
2.5	Conclusion .....	102
2.6	Bibliography.....	104
3	Functionalization of GMA-based Emulsion-Templated Porous Polymers .....	108
3.1	Introduction.....	108
3.2	Experimental Section.....	109
3.2.1	<i>Materials</i> .....	109
3.2.2	<i>GMA/EGDMA HIPE preparation and thermal polymerisation</i> .....	110
3.2.3	<i>Photopolymerised GMA-based polyHIPE preparation</i> .....	110
3.2.4	<i>Functionalisation of GMA-based PolyHIPE materials</i> .....	110
3.2.4.1	O, O'-Bis (3-aminopropyl) polyethylene glycol.....	110
3.2.4.1.1	Thermally polymerised GMA/EGDMA polyHIPE .....	110
3.2.4.1.2	Photopolymerised GMA-based polyHIPE.....	110
3.2.4.2	Morpholine and Tris(2-aminoethyl)amine (Trisamine) .....	111
3.2.4.2.1	Method 1 .....	111
3.2.4.2.2	Method 2 .....	111
3.2.4.2.3	Method 3 .....	112
3.2.5	<i>Quantification of Amine Loading</i> .....	112
3.2.5.1	O,O'-Bis(3-aminopropyl)polyethylene glycol - Determination of amine loading from Fmoc number determination.....	112
3.2.5.2	Determination of Morpholine Loading.....	113
3.2.6	<i>Qualification of Amine Loading</i> .....	114
3.2.6.1	Ninhydrin (Kaiser Test[18]).....	114
3.2.6.2	Fluorescein 5(6) – isothiocyanate (FITC) .....	114
3.2.7	<i>Instrumental</i> .....	115
3.2.7.1	Fourier Transform Infrared Spectroscopy (FTIR) .....	115
3.2.7.2	X-ray Photoelectron Spectroscopy (XPS).....	115
3.2.7.3	Nuclear Magnetic Resonance (NMR) Spectroscopy.....	116
3.2.7.3.1	O,O'-Bis(3-aminopropyl)polyethylene glycol .....	116
3.2.7.3.2	High Resolution Magic Angle Spinning (HR-MAS) NMR Spectra of PEGylated PolyHIPE .....	116

3.2.7.4	UV-Vis Spectrophotometer.....	117
3.2.7.5	Elemental Analysis .....	117
3.2.7.6	Freeze Dryer.....	117
3.3	Results and Discussion .....	117
3.3.1	<i>Functionalization of GMA-based PolyHIPEs with Tris(2-aminoethyl)amine and Morpholine .....</i>	<i>117</i>
3.3.1.1	X-ray Photoelectron Spectroscopy (XPS) of Trisamine Functionalized GMA/EGDMA polyHIPE.....	122
3.3.2	<i>Functionalization of GMA-based PolyHIPEs with O,O'-Bis (3-aminopropyl) polyethylene glycol.....</i>	<i>126</i>
3.3.2.1	Functionalization of PEGylated PolyHIPE with Ninhydrin (Kaiser Test[18]) .....	127
3.3.2.2	Functionalization of PEGylated PolyHIPE with Fluorescein 5(6)-isothiocyanate.....	129
3.3.2.3	Fmoc Number Determination and Element Analysis (CHN).....	131
3.3.2.4	X-ray Photoelectron Spectroscopy (XPS).....	133
3.3.2.5	High Resolution Magic Angle Spinning (HR-MAS) Nuclear Magnetic Resonance (NMR) Spectroscopy.....	134
3.4	Conclusion .....	139
3.5	Bibliography.....	140
4	Enzyme Immobilization onto GMA-based Emulsion-Templated Porous Polymers ...	144
4.1	Introduction.....	144
4.2	Experimental Section.....	145
4.2.1	<i>Materials .....</i>	<i>145</i>
4.2.2	<i>GMA/EGDMA HIPE Preparation and Thermal Polymerisation .....</i>	<i>146</i>
4.2.3	<i>Photopolymerised GMA-based polyHIPE preparation .....</i>	<i>146</i>
4.2.4	<i>Functionalization of GMA-based PolyHIPE materials .....</i>	<i>147</i>
4.2.4.1	O,O'-Bis-(3-aminopropyl) polyethylene glycol .....	147
4.2.5	<i>Enzyme Immobilization onto GMA-based Emulsion-Templated Porous Polymers.....</i>	<i>147</i>
4.2.5.1	Lipase from Candida Antarctica.....	147
4.2.5.2	Proteinase K from Tritirachium Album .....	147

4.2.5.2.1	GMA/EGDMA thermally polymerised and GMA-based photopolymerised polyHIPE material.....	147
4.2.5.2.2	PEGylated photopolymerised GMA-based polyHIPE material.....	147
4.2.6	<i>Enzyme Loading</i> .....	148
4.2.6.1	Bradford Protein Assay .....	148
4.2.6.2	Determination from CAL solutions .....	149
4.2.7	<i>Enzymatic Assay</i> .....	151
4.2.7.1	CAL discontinuous photometric assay.....	151
4.2.7.2	Pro K continuous titrametric assay .....	152
4.2.8	<i>Instrumental</i> .....	153
4.2.8.1	UV-Vis Spectrophotometer.....	153
4.2.8.2	pH-Stat Autotitrator.....	153
4.3	Results and Discussion .....	153
4.3.1	<i>Lipase Immobilization onto GMA/EGDMA PolyHIPE Material</i> .....	153
4.3.1.1	Lipase loading onto GMA-based Emulsion-Templated Porous Polymers .. .....	154
4.3.1.2	Enzymatic activity of Lipase Immobilized GMA/EGDMA PolyHIPE Material.....	158
4.3.2	<i>Proteinase K Immobilization onto GMA-based PolyHIPE Materials</i> .....	162
4.4	Conclusion .....	166
4.5	Bibliography.....	168
5	Conclusions and Future Work.....	171
5.1	Preparation of GMA-based PolyHIPE Materials.....	171
5.2	Functionalization of GMA-based PolyHIPE Materials .....	174
5.3	Covalent Enzyme Immobilization onto GMA-based PolyHIPE Materials.....	179
5.4	Bibliography.....	181
	Conferences, Seminars, Publications and Awards.....	183
A1.1	Conferences .....	183
A1.1.1	Oral Contribution .....	183
A1.1.2	Poster Presentations.....	183
A1.1.3	Attended .....	184
A1.2	Seminars .....	185

A1.3	Publications.....	185
A1.4	Awards .....	185

# Units and Symbols

AIBN	Azobisisobutyronitrile
APS	Ammonium persulfate
ASAP	Accelerated Surface Area and Porosimetry
ATEE	N-Acetyl-L-tyrosine ethyl ester monohydrate
ATRP	Atom transfer radical polymerisation
BCA	Bicinchoninic acid
BET	Brunauer-Emmett-Teller
BJH	Barrett-Joyner-Halenda
B <sub>0</sub>	Permeability
BSA	Bovine serum albumin
c/w	Super-critical carbon dioxide-in-water
CAL	<i>Candida Antarctica</i> Lipase
CAL-B	<i>Candida Antarctica</i> Lipase B
CIM	Convective interaction media
COSY	Correlation Spectroscopy
<d>	Average Window Diameter
<D>	Average Void Diameter
<d>/<D>	Average Degree of Interconnectivity
DMF	<i>N,N</i> -Dimethylformamide
DMSO	Dimethyl sulfoxide
DVB	Divinyl benzene
E <sub>binding</sub>	Binding energy
EBPs	Elastin-based side chain polymers

EGDMA	Ethylene glycol dimethacrylate
EHA	2-Ethylhexyl acrylate
$E_{\text{kinetic}}$	Kinetic energy of the ejected electron
ELP	Elastin-like peptide
ENZ	Enzyme
EO	Ethylene oxide
ESEM	Environmental scanning electron microscopy
$f$	Initiator efficiency
FAT	Fixed analyser transmission
FITC	Fluorescein 5(6) - isothiocyanate
Fmoc	Fluorenylmethyloxycarbonyl
FTIR	Fourier transform infra-red spectroscopy
FWHM	Full width half maximum
GMA	Glycidyl methacrylate
$h$	Planck's constant
HEMA	Hydroxyethyl methacrylate
HIPE	High internal Phase emulsion
HIPRE	High internal Phase ratio emulsion
HLB	Hydrophile lipophile balance
HPLC	High performance liquid chromatography
HR-MAS NMR	High resolution magic angle spinning NMR
$I$	Initiator
IBOA	Isobornyl acrylate
$I_0$	Intensity of the incident light
IPA	Isopropanol

$k_d$	Rate constant of initiator dissociation
$k_p$	rate constant of propagation
$k_t$	Rate constant of termination
L	Length of column
LCST	Lower critical solution temperature
M	Monomer
MA	(Meth) acrylate
MAS	Magic angle spinning
MBAM	<i>N,N'</i> -Methylenebisacrylamide
MIPE	Medium internal phase emulsion
$M_n$	Number average molecular weight
Mol.	Mole
$M_w$	Weight average molecular weight
mwCNTs	Multi-walled carbon nanotubes
4-NPac	4-Nitrophenyl acetate
NASI	<i>N</i> -Acryloxysuccinimide
NHS	<i>N</i> -Hydroxysuccinimide
NIPAM	<i>N</i> -Isopropyl acrylamide
NMR	Nuclear magnetic resonance
NPA	4-Nitrophenyl acrylate
OR	Oil red
o/w	Oil-in-water
$P/P_0$	Relative pressure
PASP	Polymer-assisted purification techniques
PCL	Polycaprolactone

PEG	Polyethylene glycol
PEG-MA	Poly(ethylene glycol) methacrylate
PEO	Polyethylene oxide
PGA	Polyglutaraldehyde
PHEMA	Poly(hydroxyethyl methacrylate)
PHP	PolyHIPE
PHPX	where X represents the formulation used in Table 2:1, 2:2, 2:3, and 2:4
PHS	Poly(12-hydroxystearic acid)
PIT	Phase inversion temperature
PMMA	Poly(methyl methacrylate)
PNIPAM	Poly(N-isopropyl acrylamide)
PNPA	<i>Paranitrophenyl acetate</i>
PO	Propylene oxide
P <sub>PC</sub>	Percentage porosity
PPF	Poly(propylene furmarate)
ppm	Part per million
PPO	Polypropylene oxide
pro K	Proteinase K
PTFE	Poly(tetrafluoroethylene)
PVA	Poly(vinyl acetate)
R	Rate of free radical polymerization
RAFT	Reversible addition fragmentation chain transfer
rpm	Revolutions per minute
scCO <sub>2</sub>	Super-critical carbon dioxide
SEM	Scanning electron microscope



St	Styrene
TCPA	2,4,6-Trichlorophenyl acrylate
$T_g$	Glass transition temperature
THF	Tetrahydrofuran
TMEDA	<i>N,N,N',N'</i> -Tetramethylethylenediamine
TMPTA	Trimethylolpropane triacrylate
TRIM	Trimethylolpropane trimethacrylate
$T_t$	Transition temperature
$u_F$	Superficial velocity
UHP	Ultra high purity water
UV	Ultra violet
V	Void
$V_{\%I}$	Internal phase volume ratio
$v/v$	Volume per volume
$V_b$	Bulk volume
VBC	Vinylbenzyl chloride
$V_e$	Volume of the external phase of the emulsion
$V_i$	Volume of the internal phase of the emulsion
Vol.	Volume
$V_{tot}$	total intrusion volume
W	Window
w/o	Water-in-oil
w/v	Weight per volume
w/w	Weight per weight
Wt.%	Weight percent

Wt.	Weight
XPS	X-ray photoelectron spectroscopy
$\Delta P$	Change in pressure
$\epsilon$	Molar absorption of the initiator
$\eta$	Viscosity of the mobile phase
$\nu$	Frequency of the incident radiation
$\Phi$	Quantum yield of the photoinitiator

# List of Figures

Figure 1:1 – Homolytic cleavage of A) azobisisobutyronitrile and B) potassium persulfate forming two free radicals.....	2
Figure 1:2 – Mechanism of free-radical polymerisation.....	3
Figure 1:3 – Typical photoinitiators used in the preparation of photopolymerised crosslinked polymers. A) benzil ketals B) hydroxyalkylphenones C) acylphosphine oxides D). $\alpha$ – amino ketones .....	8
Figure 1:4 – Norrish type I reaction .....	9
Figure 1:5 – Schematic representation of two emulsion types A) o/w direct emulsion and B) w/o inverse emulsion. ....	11
Figure 1:6 – SEM of a typical polyHIPE material. V indicates void, W indicates window – see text description. Scale bar = 10 $\mu\text{m}$ .....	16
Figure 1:7 - a) Optical microscopy images showing the controlled increase in droplet size of the HIPE over time b) SEM images of HEMA polyHIPEs showing the increase in void and interconnect size on increasing the time between the preparation of the HIPE and its subsequent polymerisation. Reprinted with permission [55]. Copyright 2007, American Chemical Society. ....	19
Figure 1:8 - Images showing the release of OR nanoparticles from a poly(acrylamide) polyHIPE (a non-stimuli responsive polymer) (left) in comparison to the release of OR nanoparticles from a PNIPAM polyHIPE (a stimuli responsive polymer) (right) a) 50 minutes after the addition of water at 18 $^{\circ}\text{C}$ . b) 3 minutes after the addition of water at 45 $^{\circ}\text{C}$ . Reproduced with permission [56].....	21
Figure 1:9 - SEM image of a 92 % porosity gelatin-methacrylate polyHIPE prepared via free-radical polymerisation in the presence of the additives NaCl and 1% v/v dimethyl sulfoxide (DMSO) [67]. Copyright 2006, American Chemical Society. ....	23
Figure 1:10 - SEM image of a Pickering polyHIPE stabilised with titania particles. Reproduced with permission [83]. Copyright 2007, Royal Society of Chemistry.....	27
Figure 1:11 – Schematic of formation of beaded polyHIPE by a w/o/w emulsion suspension polymerisation technique. Reproduced with permission [104]. Copyright 2005, Elsevier.....	30
Figure 1:12 – Schematic of the formation of beaded polyHIPEs via the photopolymerisation of a HIPE prepared with a microfluidic device. Reprinted with permission [90]. Copyright 2009, American Chemical Society.....	31

Figure 1:13 - a) Optical microscopy image showing monodisperse beaded polyHIPEs prepared by the photopolymerisation of a HIPE formed using a microfluidic device and b) SEM image of the surface of one of these polyHIPE beads. Reproduced with permission [90]. Copyright 2009, American Chemical Society.....	31
Figure 1:14 - SEM images of polyHIPE membrane prepared by casting technique a) cross-section. b) surface. Reproduced with permission [105]. Copyright 2008, Royal Society of Chemistry.....	32
Figure 1:15 – Schematic of the reversible immobilization by peptide-mediated co-assembly: a) poly(VPGVG) functionalised PEG polyHIPE; b) poly(VPGVG) functionalised PEG polyHIPE soaked in a EBP solution at pH 3.2; c) After lowering the pH of the solution to pH 1.5; d) polyHIPE after washing in a pH 3.2 buffer. Reproduced with permission [106]. .....	34
Figure 1:16 - a) Left: poly(VPGVG) functionalised PEG based polyHIPE mixed with a fluorescently labelled EBP solution at pH 1.5; right: unfunctionalised PEG based polyHIPE mixed with a fluorescently labelled EBP solution at pH 1.5. b) left: poly(VPGVG) functionalised PEG based polyHIPE mixed with a fluorescently labelled EBP at pH 1.5; right: EBP functionalised PEG based polyHIPE mixed with a fluorescently labelled EBP which has been then washed with a pH 3.2 buffer. PolyHIPE samples illuminated under ultraviolet (UV) light ( $\lambda=254$ nm). Reproduced with permission [106]. .....	34
Figure 2:1 – Chemical structures of monomers used to prepare polyHIPE materials. A) Glycidyl methacrylate B) <i>N</i> -acryloxysuccinimide C) poly(ethylene glycol) methacrylate ( $M_n$ 360) D) ethylene glycol dimethacrylate E) trimethylolpropane trimethacrylate F) trimethylolpropane triacrylate G) dipentaerythritol penta-/hexa-acrylate F) isobornyl acrylate G) 2-ethylhexyl acrylate .....	57
Figure 2:2 – Chemical structures of the photoinitiators used for preparation of polyHIPE materials. A) 2-hydroxy-4'-(2-hydroxyethoxy)-2-methylpropiophenone and a photoinitiator consisting of a 50:50 blend of B) diphenyl(2,4,6-trimethylbenzoyl) phosphine oxide and C) 2-hydroxy-2-methylpropiophenone .....	58
Figure 2:3 – Chemical structures of surfactants used to stabilize HIPEs. A) Synperonic PEL 121, A-B-A block copolymer with a HLB number of 0.5 (A is poly(ethylene oxide) block length 5 and B is poly(propylene oxide) block length 70) B) Hypermer B246, an A-B-A	

block copolymer with a HLB number of 6 and $M_w$ of 7500 (A is poly(12-hydroxystearic acid) and B is poly(ethylene oxide)).....	58
Figure 2:4 – Equipment for polyHIPE synthesis. A) Glycidyl methacrylate B) trimethylolpropane triacrylate C) 2-ethylhexyl acrylate D) isobornyl acrylate E) diphenyl(2,4,6-trimethylbenzoyl) phosphine oxide F) 2-hydroxy-2-methylpropiophenone G) Hypermer B246 A-B-A block copolymer PHS-PEG-PHS .....	59
Figure 2:5 - Image showing the set-up for the photopolymerisation of a HIPE. A) PTFE moulds and glass plates. B) Fusion UV Systems, Inc.®LC6E Benchtop Conveyor with Light Hammer® 6 Irradiator used for curing of a HIPE. C) Polymerisation of a HIPE placed between the two glass plates within a PTFE mould on the LC6E Benchtop Conveyor.....	61
Figure 2:6 – Photopolymerised GMA-based polyHIPE monolith covalently bound to a functionalized glass chromatography column.....	65
Figure 2:7 – FTIR spectrum of thermally initiated GMA/EGDMA polyHIPE.....	75
Figure 2:8 – SEM Images of thermally polymerised GMA/EGDMA polyHIPE A) Scale bar 50 $\mu\text{m}$ B) Scale bar 20 $\mu\text{m}$ .....	76
Figure 2:9 – FTIR spectrum (base line corrected) of GMA-based photopolymerised polyHIPE material, PHP1.....	77
Figure 2:10 – SEM images of photopolymerized GMA-based polyHIPEs A) PHP7, 73 % porosity, scale bar 20 $\mu\text{m}$ B) PHP6, 78 % porosity, scale bar 20 $\mu\text{m}$ C) PHP1, 89 % porosity, scale bar 20 $\mu\text{m}$ D) PHP5, 95 % porosity, scale bar 10 $\mu\text{m}$ .....	79
Figure 2:11 – Void diameters of photopolymerised GMA-based polyHIPEs. Void diameter distribution by analysis of SEM images, from front to back 73% porosity (PHP7), 78% porosity (PHP6), 89% porosity (PHP1) and 95% porosity (PHP5). .....	79
Figure 2:12 – Graph showing the Log differential intrusion verses void size diameter of the GMA-based photopolymerised polyHIPEs. Dashed red line and pluses represent the 73 % nominal porosity polyHIPE (PHP 7); Dash dot green line and circles represents 78 % nominal porosity polyHIPE (PHP6); Blue solid line and crosses represents 89 % nominal porosity polyHIPE (PHP1).....	81
Figure 2:13 – SEM images of varying quantities (10 – 40 % v/v of monomer phase) of GMA incorporated within photopolymerised polyHIPEs, scale bar 20 $\mu\text{m}$ A) 10 % v/v B) 20 % v/v C) 30 % v/v D) 40 % .....	84

Figure 2:14 – SEM image of GMA-based polyHIPE polymerised with an aqueous soluble photoinitiator (2-hydroxy-4'-(2-hydroxyethoxy)-2-methylpropiophenone), scale bar 20 µm .....	87
Figure 2:15 - SEM image of PEG-MA w/o polyHIPE, scale bar 20 µm.....	88
Figure 2:16 – Comparison in hydrophilicity of two 200 µm thick polyHIPE materials. 20 µl of ultra high purity water was placed on the materials A) Side-on picture of hydrophobic PHP1 polyHIPE (left) and a PHP1 polyHIPE with the addition of PEG-MA (right) B) Top view of hydrophobic PHP1 polyHIPE (left) and a PHP1 polyHIPE with the addition of PEG-MA (right) .....	89
Figure 2:17 – Schematic showing the functionalization of the Omnifit glass columns with methacrylate groups.....	91
Figure 2:18 – Schematic showing the preparation of a functional highly porous polymer that is covalently bound to a glass column .....	92
Figure 2:19 – ESEM images of photopolymerised GMA-based HPLC columns (PHP9) A) Red arrow is showing the interface between the glass and monolith, scale bar 100 µm B) Scale bar 20 µm .....	93
Figure 2:20 – SEM images of photopolymerised GMA-based polyHIPE monolith columns (PHP9). A) Scale bar 1 mm. B) Surface morphology of the monolith, with typical polyHIPE morphology below the surface, scale bar 20 µm. C) PolyHIPE covalently attached to the glass column wall, scale bar 50 µm. ....	95
Figure 2:21 – SEM images of photopolymerised GMA/EGDMA HPLC columns (PHP12). A) The glass column with monolith (centre), scale bar 1 mm. B) The surface morphology of the monolith, scale bar 20 µm. C) The internal morphology of the monolith, scale bar 10 µm.....	95
Figure 2:22 – SEM images of NASI-based photopolymerised HPLC columns (PHP11) A) Red arrow indicates to the glass column, scale bar 50 µm. B) The surface morphology of the monolith, scale bar 20 µm.....	97
Figure 2:23 –SEM images of PHP10 photopolymerised monolithic columns. A) The glass column with monolith (centre), scale bar 1 mm. B) Red arrow indicates the glass column, scale bar 50 µm. C) The surface morphology of the GMA-based monolithic column, scale bar 20 µm.....	98
Figure 2:24 – SEM images of GMA – TRIM photopolymerised polyHIPE A) Scale bar 20 µm B) Scale bar 2 µm .....	101

Figure 3:1 – <i>O,O'</i> -Bis(3-aminopropyl)polyethylene glycol .....	116
Figure 3:2 – Schematic of the functionalization of GMA-based polyHIPEs with amine nucleophiles. Reaction 1 morpholine, reaction 2 tris(2-aminoethyl) amine and reaction 3 <i>O,O'</i> -bis(3-aminopropyl)polyethylene glycol .....	118
Figure 3:3 – FTIR spectra: above (black) GMA/EGDMA functionalized with tris(2-aminoethyl) amine (see section 4.2.4.1 for reaction), below (red) GMA/EGDMA thermally polymerised polyHIPE .....	119
Figure 3:4 - XPS spectra from the surface of polyHIPE materials, above (pink spectrum) <i>O,O'</i> -Bis(3-aminopropyl)polyethylene glycol functionalized polyHIPE surface; middle: (yellow spectrum) tris(2-aminoethyl) amine functionalized polyHIPE surface; bottom: (green spectrum) GMA/EGDMA polyHIPE surface. Atoms corresponding to the peaks in the respective spectra have been shown. ....	123
Figure 3:5 – High-resolution XPS spectrum from a GMA/EGDMA polyHIPE surface showing the C 1S peak. Internal structures corresponding to atoms in different chemical environments have been shown. CPS is counts per second. ....	125
Figure 3:6 - XPS spectrum from surface of polyHIPE materials showing N 1S peak above: (yellow spectra) tris(2-aminoethyl) amine functionalized polyHIPE surface; middle: (pink spectra) <i>O,O'</i> -Bis(3-aminopropyl)polyethylene glycol functionalized polyHIPE surface; bottom: (green spectra) GMA/EGDMA polyHIPE surface. Internal structures corresponding to atoms in different chemical environments have been shown. ....	126
Figure 3:7 – Schematic of functionalization of PEGylated polyHIPE. Reaction 1 with ninhydrin and reaction 2 with fluorescein isothiocyanate.....	128
Figure 3:8 – Powdered polyHIPE materials following their reaction with ninhydrin (Kaiser test[18]) A) GMA/EGDMA polyHIPE (control) B) PEGylated polyHIPE .....	129
Figure 3:9 – Reaction of powdered thermally polymerised polyHIPE material with FITC A) Image in natural light, left: GMA/EGDMA PolyHIPE (control); right: PEGylated polyHIPE. B) Image taken with samples illuminated under UV light ( $\lambda = 254\text{nm}$ ) left: GMA/EGDMA polyHIPE (control); right: PEGylated polyHIPE .....	130
Figure 3:10 - Reaction of monolithic photopolymerized polyHIPE material with FITC A) Image in natural light, left: GMA/EGDMA polyHIPE (control); right: PEGylated polyHIPE. B) Image taken with samples illuminated under UV light ( $\lambda = 254\text{nm}$ ) left: GMA/EGDMA polyHIPE (control); right: PEGylated polyHIPE .....	131

- Figure 3:11 – Schematic showing the derivatisation of amine groups on *O,O'*-bis(3-aminopropyl)polyethylene glycol functionalized (PEGylated) GMA/EGDMA polyHIPE powder with 9-fluorenylmethyl chloroformate (Fmoc-Cl), followed by deprotection with 20 % piperidine / N,N-dimethylformamide (DMF) solution to obtain the piperidine adduct, which absorbs at  $\lambda=301$  nm (UV). Blue circles represent bulk GMA/EGDMA polyHIPE matrix. DIPEA = N,N-diisopropylethyamine.....132
- Figure 3:12 –  $^1\text{H}$  NMR spectrum of *O,O'*-bis(3-aminopropyl)polyethylene glycol at 400 MHz in  $\text{CDCl}_3$ . Inset (left) is molecular structure of *O,O'*-bis(3-aminopropyl)polyethylene glycol, numbered to indicate relevant protons that match peaks within the NMR spectrum. Inset (right) is a magnified spectrum of the peaks at 3.54, 2.78 and 1.72 ppm. Solvent peaks are indicated by an \*......135
- Figure 3:13 -  $^1\text{H}$  HR-MAS NMR spectrum of swollen *O,O'*-bis(3-aminopropyl)polyethylene glycol functionalized (PEGylated) GMA/EGDMA polyHIPE at 500 MHz in  $\text{CDCl}_3$ . Inset (left) is molecular structure of *O,O'*-bis(3-aminopropyl)polyethylene glycol functionalized (PEGylated) GMA/EGDMA polyHIPE, numbered to indicate relevant protons that match peaks in the NMR spectrum. Inset (right) is a magnified spectra of the peak at 2.82 ppm. Peaks corresponding to the polyHIPE matrix are indicated by \*. Solvent peaks are indicated by \*\*. Impurities are indicated \*\*\*.....136
- Figure 3:14 -  $^1\text{H}$  HR-MAS NMR spectra of swollen polyHIPEs at 500 MHz in  $\text{CDCl}_3$ . Blue spectrum is GMA/EGDMA polyHIPE. Red spectrum is *O,O'*-bis(3-aminopropyl)polyethylene glycol functionalized (PEGylated) GMA/EGDMA polyHIPE. Inset is molecular structure of *O,O'*-bis(3-aminopropyl)polyethylene glycol functionalized (PEGylated) GMA/EGDMA polyHIPE, numbered to indicate relevant protons that match peaks with the (red) NMR spectrum.....137
- Figure 3:15 -  $^1\text{H}$  HR-MAS NMR spectra of swollen polyHIPEs at 500 MHz in  $\text{CDCl}_3$ . Blue spectra is GMA/EGDMA polyHIPE. Red spectra is *O,O'*-Bis(3-aminopropyl)polyethylene glycol functionalized (PEGylated) GMA/EGDMA polyHIPE. Inset (left) is molecular structure of *O,O'*-Bis(3-aminopropyl) polyethylene glycol functionalized (PEGylated) GMA/EGDMA polyHIPE, numbered to indicate relevant protons that match peaks within the (red) NMR spectra. ....137
- Figure 3:16 – Two dimensional COSY  $^1\text{H}$  HR-MAS NMR spectrum of swollen *O,O'*-bis(3-aminopropyl)polyethylene glycol functionalized (PEGylated) GMA/EGDMA polyHIPE at 500MHz in  $\text{CDCl}_3$ . The molecular structure of *O,O'*-bis(3-aminopropyl)polyethylene



glycol functionalized (PEGylated) polyHIPE, numbered to indicate relevant protons that match peaks within the two dimensional COSY NMR spectra. ....	138
Figure 4:1 – Graphical illustration showing a typical data set for the hydrolysis of 4-NPac, where blank rate of hydrolysis has been subtracted. Blue line represents the lipase solution before immobilization onto the polymer, red line represents the lipase solution after immobilization, green line represents the 1 <sup>st</sup> washing of the polyHIPE material.....	150
Figure 4:2 – Schematic of the direct immobilization of enzyme onto a GMA-based polyHIPE material .....	154
Figure 4:3 – Standard curve of 2.5 mL Bradford assay procedure with BSA standard.....	157
Figure 4:4 – Typical graph showing the hydrolysis of 100 $\mu$ L 4-nitrophenyl acetate (7.25 mg/mL in absolute ethanol) at 25°C in 2.97mL 20 mM pH 8.0 phosphate buffer with 30 $\mu$ L 1 mg/ml Lipase solution in 20 mM pH 8.0 phosphate buffer before immobilization onto GMA/EGDMA polyHIPE (represented by ■), 30 $\mu$ L Lipase solution in 20 mM pH 8.0 phosphate buffer after immobilization onto polyHIPE material (represented by ▲), 30 $\mu$ L from the 1 <sup>st</sup> 10 ml 20 mM pH 8.0 phosphate buffer washing of GMA/EGDMA polyHIPE (represented by ■), 30 $\mu$ L from the 2 <sup>nd</sup> 10 ml 20 mM pH 8.0 phosphate buffer washing of GMA/EGDMA polyHIPE (represented by +), and blank 30 $\mu$ L, 20 mM pH 8.0 phosphate buffer (represented by ♦) .....	158
Figure 4:5 – Images showing the hydrolysis of pNPac at room temperature of a stirred 3 mL 20 mM pH 8.0 phosphate buffer solution containing. i) 50 mg of GMA/EGDMA powdered polyHIPE (blank), ii) 50 mg of lipase immobilized GMA/EGDMA powdered polyHIPE, iii) 20 mM pH 8.0 phosphate buffer only (blank) and iv) 30 $\mu$ L of 1mg/mL lipase. A) Before the addition of pNPac B) immediately C) 5 min. D) 10 min. E) 15 min. F) 20 min after the addition of 100 $\mu$ L 7.25 ml/mL 4-NPac in absolute ethanol. ....	159
Figure 4:6 – Graph showing the hydrolysis of 4-nitrophenyl acetate at 25 °C with 20mM pH 8.0 phosphate buffer with immobilized lipase onto powdered GMA/EGDMA polyHIPE material. Each filtrate of immobilized enzyme solution at the particular time interval was diluted tenfold; i.e 900 $\mu$ L of 20 mM pH 8.0 phosphate buffer was added to 100 $\mu$ L of filtrate. At least three points were acquired for each time interval taken. Vertical error bars represent one standard deviation of the values recorded at the particular time interval. ....	161

Figure 4:7 – Schematic of the immobilization of Pro K onto PEGylated polyHIPE material.	
Reaction 1 is the activation of the PEGylated polyHIPE with glutaraldehyde. Reaction 2 is the immobilization of pro K onto polyHIPE. Reaction 3 is the reduction of imine bonds with sodium cyanoborohydride.....	164
Figure 5:1 – Schematic showing covalent attachment of hydrazine containing dyes with glutaraldehyde functionalized polyHIPE material for qualitative colourmetric analysis of the functionalization of the material. ....	177
Figure 5:2 – Schematic showing the ring-opening of epoxy ring of GMA-based polyHIPE material with an azide, followed by further functionalization of the material via a Cu(I) catalyzed azide-alkyne click reaction .....	179

# List of Tables

Table 2:1 – Quantities of starting material required for the preparation of a photopolymerised GMA-based polyHIPE with 10% GMA v/v of monomer phase (PHP1). .....	66
Table 2:2 – Quantities of starting material used for the preparation of 10%-40% GMA (v/v of monomer phase) photopolymerised polyHIPE materials .....	67
Table 2:3 – Different formulations used for the preparation of 77-95 % nominal porosity GMA-based photopolymerised materials .....	68
Table 2:4 – Different formulations of polyHIPE used for the preparation of a continuous flow set-up .....	69
Table 2:5 - Showing the formulation for the preparation of GMA/TRIM photopolymerised polyHIPE material .....	70
Table 2:6 – Void and Window Size Characterisation Data for GMA-based polyHIPEs .....	81
Table 3:1 - Reaction 3.2.4.1 GMA/EGDMA thermally polymerised polyHIPE functionalized with morpholine and trisamine .....	120
Table 3:2 - Reaction 3.2.4.2.2 GMA-based photopolymerised polyHIPE (PHP1) functionalized with morpholine and trisamine. ....	121
Table 3:3 - Reaction 3.2.4.2.3 GMA-based photopolymerised polyHIPE (PHP1) functionalized with morpholine and trisamine. ....	121
Table 3:4 - XPS data showing the averaged relative atomic composition of A) GMA/EGDMA polyHIPE surface, B) tris(2-aminoethyl) amine functionalized polyHIPE surface. Three repeats were taken for each sample. ....	124
Table 3:5 - XPS data showing the averaged relative atomic composition of A) GMA/EGDMA polyHIPE surface, B) <i>O,O'</i> -bis(3-aminopropyl)polyethylene glycol functionalized polyHIPE surface. Three repeats were taken for each sample.....	133

# 1 Introduction

This thesis focuses on the preparation of emulsion-templated porous polymers as support materials for covalent enzyme immobilization. This section of the thesis is designed to introduce the main topics related to the preparation and use of these materials, including free-radical polymerisation, the formation and stability of emulsions and enzyme immobilization, in particular covalent enzyme immobilization and advantages of undertaking this process.

## 1.1 Free-radical Initiated Polymerisation

Free-radical initiated polymerisation is a widely used technique for the formation of porous polymers[1]. The monomers that are mainly used for the preparation are unsaturated vinyl monomers, such as styrene, acrylates and methacrylates [2]. It is required that an initiator is present to start or initiate the reaction. Initiators undergo homolytic cleavage via the application of heat or UV light forming two highly reactive species possessing un-paired electrons (called free radicals) that can then initiate polymerisation. Common initiators include, azobisisobutyronitrile (AIBN), which can undergo thermolysis and photolysis, and the aqueous soluble initiator, potassium persulfate (Figure 1:1), which is used in the emulsion polymerisation process (described below).

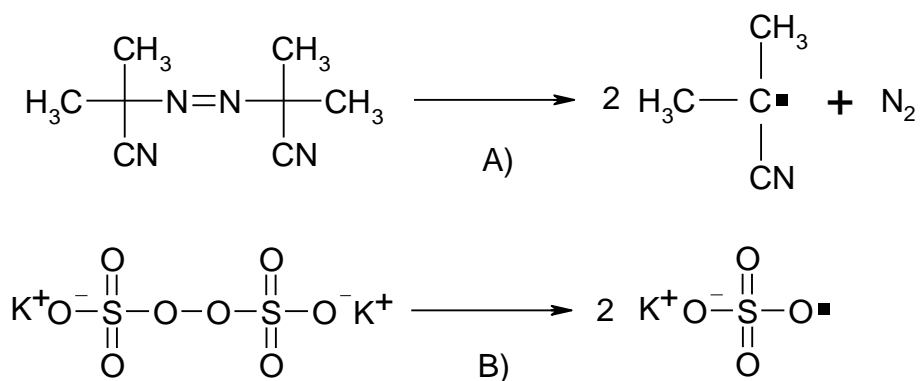


Figure 1:1 – Homolytic cleavage of A) azobisisobutyronitrile and B) potassium persulfate forming two free radicals

The mechanism of free-radical polymerisation (see Figure 1:2) involves, firstly the homolytic cleavage of the initiator to create two primary radicals [3]. This radical can then attack an unsaturated double bond of a vinyl monomer, forming a secondary initiating radical. This initiating radical then attacks a monomer and a propagating chain is formed via the addition of many monomer units to this propagating chain. Termination of the polymer chain then occurs predominately via two methods, combination, involving the coming together of two propagating chains forming one saturated polymer chain and disproportionation, which involves the hydrogen abstraction of one propagating polymer chain from another, resulting in an unsaturated and a saturated polymer chain.

**Initiation:**

Initiator

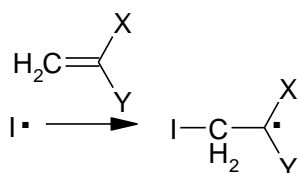
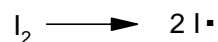
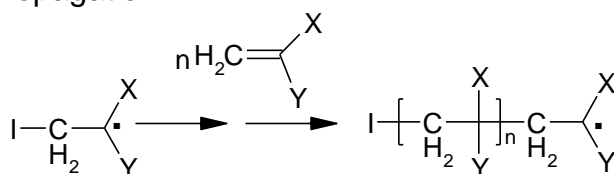
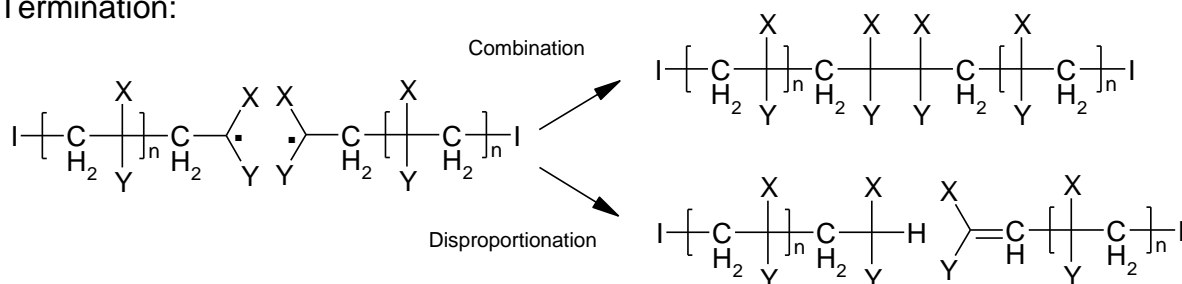
**Propagation:****Termination:**

Figure 1:2 – Mechanism of free-radical polymerisation.

Overall, the rate of free-radical polymerisation  $R_p$ , is [5]:

$$R_p = k_p \left( \frac{fk_d}{k_t} \right)^{1/2} [M][I]^{1/2} \quad \text{Equation 1:1}$$

where,  $k_p$  is the rate constant of propagation,  $f$  is the initiator efficiency,  $k_d$  is the rate constant of initiator dissociation,  $k_t$  is the rate constant of termination,  $[M]$  is the concentration of monomer, and  $[I]$  is the concentration of initiator for thermally-initiated polymerisation or

$$R_p = k_p \left( \frac{\Phi \epsilon I_0}{k_t} \right)^{1/2} [M][I]^{1/2} \quad \text{Equation 1:2}$$

where,  $k_p$  is the rate constant of propagation,  $\Phi$  is the quantum yield of the photoinitiator,  $\epsilon$  is the molar absorption of the initiator,  $I_0$  is the intensity of the incident light,  $k_t$  is the rate constant of termination,  $[M]$  is the concentration of monomer, and  $[I]$  is the concentration of initiator for a UV-initiated polymerisations. Both equations are derived assuming steady state conditions, i.e. the rate of initiation is proportional to the rate of termination.

Deviations from the steady state conditions from the rate of polymerisation described above does occur, however this is mainly due to a process called auto-acceleration (or gel effect)[3]. This process involves a lowering of the rate of termination of the propagating chain from an increase in viscosity of the medium. Overall, due to the lowering of the termination rate, the rate of polymerisation is increased, sometimes to an uncontrolled rate.

Other effects can occur during free-radical initiated polymerisation, such as chain transfer, which involves the transfer of the propagating chain to a chain transfer agent, solvent, or to another propagating polymer chain via hydrogen abstraction [6]. Overall the effect can result in the lowering of the molecular weight of the polymer, when chain transfer agents are used or can result in the formation of branched polymers.

### 1.1.1 Methods for the Preparation of Free-radical Initiated Polymers

There are four common types of methods for preparing polymers via free-radical initiation, namely, bulk, solution, suspension and emulsion polymerisation [3, 5]. Bulk polymerisation involves the free-radical initiation of a monomer mixture with initiator. Advantages of this technique are that high molecular weight polymers can be produced, although the disadvantage is that the technique suffers from auto-acceleration. Solution polymerisation involves the polymerisation of monomers within a solution, resulting in a reduction in the gel effect. Although, there are disadvantages, chain transfer of the propagating polymer chain to the solvent can occur resulting in lower molecular weight polymers, in addition to the difficulty in the separation of the polymer from the solvent used. Suspension polymerisation involves the polymerisation of a monomer mixture in the presence of a liquid, generally water, that is immiscible with the monomers and initiator used and requires the agitation of the system to produce dispersed monomer droplets. Overall, this technique lowers the effects of auto-acceleration due to heat dissipation, although one drawback is the removal of some of the surface active agents that are sometimes added to aid with the dispersion of the monomer droplets. Finally, emulsion polymerisation involves a mixture of monomer and aqueous solution with a surfactant (above its critical micelle concentration), with an aqueous soluble initiator, such as potassium persulfate, and this technique is used extensively in industry. The process involves the formation of propagating oligomeric chains from the initiation of monomer that is dissolved within the aqueous phase, these growing chains then diffuse into monomer-swollen micelles and an essentially bulk polymerisation process occurs within monomer swollen polymer micelles. The polymerisation is maintained by the diffusion of monomer from droplets in the aqueous phase into these micelles.



### 1.1.2 Copolymerisation

A copolymer is defined as a polymer derived from more than one type of monomer. There are several types of copolymers, which are determined from the arrangement of the repeat units of the different monomers along the polymer chain [2].

*Random copolymers* are formed from the random distribution of repeat units along the polymer chain.

*Alternating copolymers* are obtained from two equimolar quantities of different repeat units that are distributed in a regular alternating manner along the polymer chain.

*Block copolymers* are produced from sequences of long repeating units, of which there are two main types, di-block and tri-block copolymers.

*Graft copolymers* involve a linear main polymer of one type of monomer and the attachment as side chains of another type of monomer from this chain.

The rate of reaction of an active centre from one monomer or growing polymer chain towards another monomer (hetero-polymerisation) can be different from the rate of homopolymerisation. Hence this can lead to a polymer with different ratios of monomers compared to the feed ratio of monomers and is the reason for the production of some of the aforementioned copolymers above [2].

### 1.1.3 Glass Transition Temperature

The glass transition temperature ( $T_g$ ) is defined as the transition of a polymer from the rubbery to the glass state on the reduction in temperature [3].  $T_g$  can be explained by utilizing the concept of free volume. The free volume is the space that is not occupied by

polymer molecules in a solid or liquid. In a liquid state the polymer molecules have a lot of free volume and so can change their conformation quickly. On reducing the temperature, the polymer molecules have less thermal energy to change their conformation as quickly, hence there is a reduction in the free volume of the polymer. Eventually, the temperature will be reduced to such an extent, that the rotation or translation of the polymer chains is negligible, i.e. the polymer is effectively 'frozen' due to the reduction in the free volume, and this temperature is the  $T_g$  of the polymer. There are a number of factors that affect  $T_g$  of a polymer chain, such as flexibility, and cross-linking of the polymer chain. It is observed that the cross-linking of a polymer results in the increase of the glass transition temperature due to the restricted chain movement.

#### **1.1.4 Network Polymers**

Polymerisation of multifunctional monomers, such as ethylene glycol dimethacrylate, results in a crosslinked (or networked) material[1]. The properties of network polymers have noticeable differences in comparison with linear polymers, mainly that the polymer cannot be dissolved; it can only swell in a suitable solvent (if crosslink concentration is low), due to the covalent links between the polymer chains. In addition, a networked polymer does not melt on heating, it only degrades[7].

#### **1.1.5 Photoinitiated Free-radical Crosslinking Polymerisation**

This involves the preparation of networked polymeric materials from the UV-initiation of a multifunctional monomer system[8-10]. These polymers have a number of applications from the coating of materials to the preparation of inks[8, 11]. The main

advantage of the technique is that polymers can be prepared in seconds to minutes in comparison to hours for thermally polymerised materials, due to the ultrafast polymerisation rate of this method[8]. The two most common techniques are free-radical photoinitiated polymerisation and cationic photoinitiated polymerisation, but the latter is beyond the scope of this thesis.

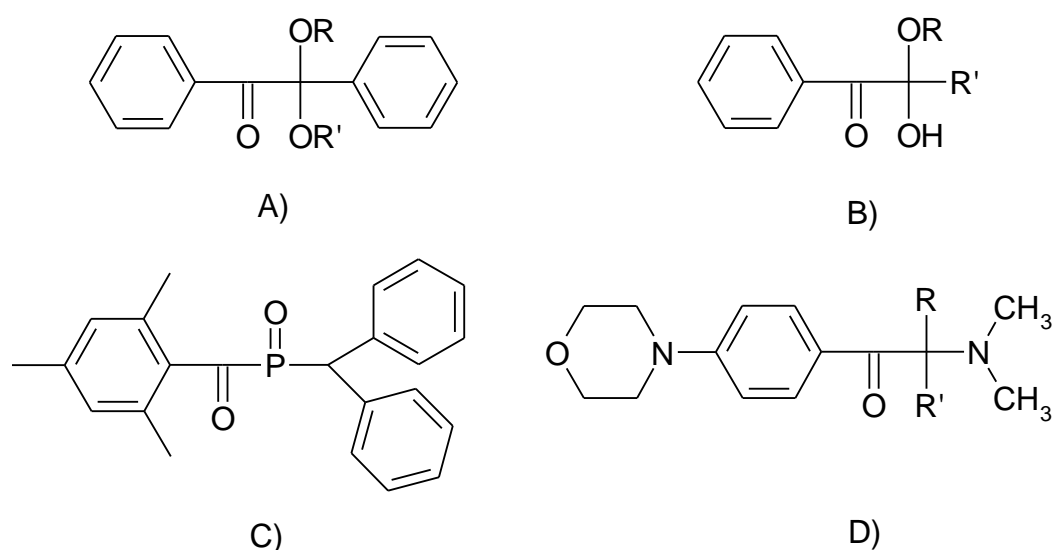


Figure 1:3 – Typical photoinitiators used in the preparation of photopolymerised crosslinked polymers. A) benzil ketals B) hydroxyalkylphenones C) acylphosphine oxides D).  $\alpha$  – amino ketones

Common monomers that are used for photoinitiated free-radical polymerisation are acrylates and methacrylates, due to their fast rate of free radical polymerisation[8]. Initiators that are usually used are aromatic carbonyl derivatives, namely hydroxyalkylphenones, benzil ketals,  $\alpha$ -amino ketones, in addition to acylphosphine oxides (see Figure 1:3) [12]. They fragment via an  $\alpha$ -cleavage (Norrish Type I) reaction (see Figure 1:4), forming two radicals, under irradiation between 300-400 nm, the major initiating moiety being the benzoyl radical[10]. The substituents attached to the aromatic carbonyl group affect the exact absorbance of UV-irradiation for the initiator in question.

It is observed that the polymerisation rate, crosslink density and the hardness increase, and the conversion decreases, on increasing the functionality of the crosslinking monomer, from a di-, to a tri-acrylate[8].

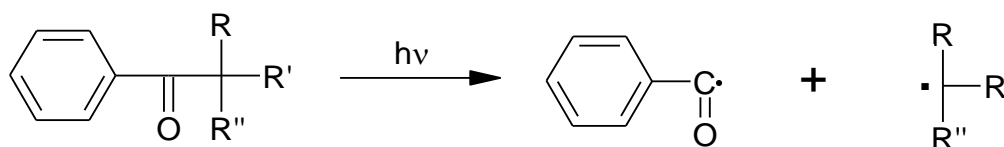


Figure 1:4 – Norrish type I reaction

The kinetics of the preparation of crosslinked polymers from the bulk free-radical polymerisation of multifunctional monomers are complicated and differ from the preparation of linear polymers[10]. For instance, due to the formation of a networked structure, at low conversion of functional groups there is an auto-acceleration effect, due to the restriction in the motion of propagating chain ends, which results in the lowering of the rate of termination by several orders of magnitude. In this regime the rate of termination is limited by reaction diffusion of the propagating chain ends [13]. This results in an increase in the rate of polymerisation. At higher conversion of the functional groups auto-deceleration is observed, as a result of the lowering of the rate of propagation from the reduction in the mobility of the propagating chain and monomers.

#### 1.1.5.1 Oxygen Retardation

Oxygen scavenges free radicals from both the initiator and propagating chains, producing the much less reactive peroxy radicals, resulting in a retardation in polymerisation[10]. Oxygen retardation occurs mainly at the air-monomer mixture interface due to a greater concentration of oxygen at the interface than in the bulk of the

monomer mixture, resulting in retardation at the surface. This problem can be overcome by the use of an intense light source, which produces an excess of free radicals to consume the oxygen, in addition to increasing the initiation rate and hence the time allowed for the diffusion of oxygen into the mixture [9].

#### **1.1.5.2 Frontal Polymerisation**

One of the main drawbacks of photoinitiated polymerisation is the penetration of UV light within the material[14]. An interesting technique, photofrontal polymerisation can be used for the production of thick polymerised materials [14]. The process utilizes the degradation of the initiator, into transparent products, described as photobleaching, which allows the penetration of UV light further into the material[15, 16]. Acylphosphine oxides (see Figure 1:3 C)) are particularly well suited initiators for this technique due to their fast rate of degradation [17].

## **1.2 Emulsions**

An emulsion is defined as an opaque mixture of two immiscible liquids, an 'oil' which encompasses hydrophobic nonpolar liquids and 'water' which represents hydrophilic aqueous solutions[18, 19]. There are two types of emulsions based on which phase (internal or external) the two immiscible liquids are within. In an oil-in-water (o/w) emulsion, called a direct emulsion, the oil is the internal (dispersed) phase and the water phase is the external (continuous) phase (see Figure 1:5 A)), whereas within water-in-oil (w/o) emulsion, called an inverse emulsion, water is the internal phase and oil is the external phase (see Figure 1:5 B)).

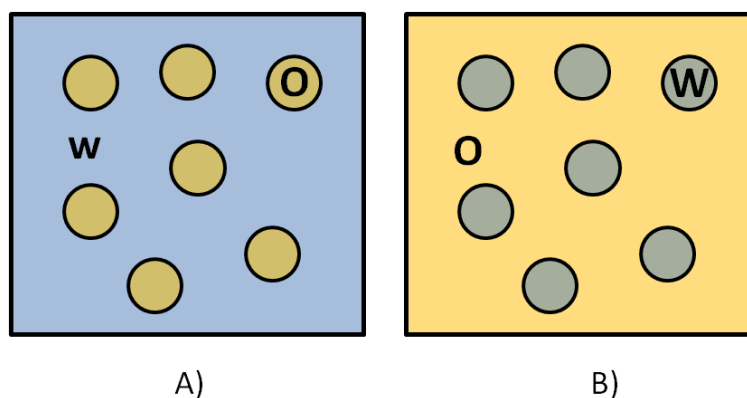


Figure 1:5 – Schematic representation of two emulsion types A) o/w direct emulsion and B) w/o inverse emulsion.

Agitation is necessary to prepare emulsions, due to the energy required for the large increase in the interfacial area of the droplets in relation to the bulk phases respectively [20]. Surface active species (surfactants), are required to stabilise emulsions, otherwise the emulsion would instantly phase separate into the two bulk phases. Surfactants are amphiphilic molecules, in that they consist of a hydrophilic part and a hydrophobic part which self assemble at the oil-water interface. There are three types of surfactants, based on the nature of the hydrophilic head group, anionic, cationic and non-ionic surfactants. Block copolymers that possess both hydrophilic and hydrophobic blocks, can also be used as surfactants to produce emulsions. Triblock copolymers of poly(ethylene oxide) (PEO) and poly(propylene oxide) (PPO) are commercially available as the Synperonic® range.

Emulsions can be further classified into macro- and micro-emulsions [19]. Macroemulsions are not thermodynamically stable, due the energy required for the increase in the interfacial area of the emulsion system, but are kinetically stable due to surfactants preventing phase separation of the emulsion, and are the focus of this thesis. Microemulsions are thermodynamically stable due to the low interfacial tension between

the two phases as a result of the high surfactant concentrations, in addition to the large entropy effect of the nanometer sized droplets that are produced. However, these are beyond the scope of this thesis.

### **1.2.1 Emulsion Type: Hydrophile Lipophile Balance (HLB) and Phase Inversion Temperature (PIT)**

Bancroft's rule states that the phase in which the surfactant is preferentially soluble becomes the continuous phase of the emulsion, for example a surfactant that is preferentially soluble in oil would lead to a w/o emulsion [21, 22].

One common method for the prediction of an emulsion type, i.e. o/w or w/o, from the surfactant used, in particular non-ionic surfactants, is the hydrophile-lipophile balance (HLB) number [19]. It is based on the weight fractions of hydrophilic and hydrophobic moieties in the surfactant. Low HLB number surfactants predominantly stabilise w/o emulsions, whereas high HLB numbered surfactants stabilise direct o/w emulsions. Whilst this technique is used extensively by emulsion scientists, it has one major flaw; it is only applicable at ambient temperatures. It can be observed that low HLB numbered surfactants can stabilise o/w emulsions at low temperatures.

Shinoda *et al.* [23-25], investigated the emulsion type produced with non-ionic, polyethoxylated surfactants  $(R-(CH_2-CH_2-O)_n-OH)$ , where R is the hydrophobic alkyl tail) at different temperatures, and came up with the concept of phase inversion temperature (PIT), also called HLB temperature. The hydrophilic tail of non-ionic surfactants is hydrated at low temperatures, resulting in the surfactant being preferentially water soluble. Following from Bancroft's rule, a direct o/w emulsion is formed [26]. As the

emulsion system is heated it reaches the PIT, where the ethoxy groups of the surfactant become dehydrated to the extent that the surfactant has no preference for either the oil or water phase and on agitation spontaneous coalescence occurs resulting in extensive phase separation. On increasing the temperature further, the surfactant is preferentially soluble in oil due to the increased dehydration of the hydrophilic head groups of the non-ionic surfactant and on agitation a w/o emulsion is prepared.

### **1.2.2 Emulsion Instability**

As macroemulsions are only kinetically stable, over time they become unstable, typically via four common processes, flocculation, coalescence, creaming and Ostwald ripening [19, 20]. Flocculation involves the coming together of droplets within a dilute emulsion, generally leading to coalescence. Coalescence involves the rupture of the surfactant film between two adjacent droplets producing one droplet due to thermal fluctuations from, initially, the formation of a molecular sized hole within the film. Creaming is the phase separation of the emulsion under gravity due to density differences within the dispersed and continuous phases. If the dispersed phase droplets are slightly soluble within the continuous phase of the emulsion, a process called Ostwald ripening may occur. This process involves the molecular diffusion from dispersed phase droplets through the continuous phase to other dispersed phase droplets. Larger sized droplets then grow preferentially over smaller droplets and the process is driven by a lowering of the interfacial area of the emulsion system. Overall, coalescence and Ostwald ripening lead to a reduction in the Gibbs free energy of the emulsion, via a reduction in the interfacial area of the emulsion system, due to the coarsening of the emulsion over time.



### 1.2.3 High Internal Phase Emulsions (HIPEs)

In addition to the division of an emulsion as macro- or micro-emulsion, and the two emulsion types, o/w and w/o, there is a further division to be made, based on the internal phase volume ratio of the emulsion.

For clarity, the internal phase volume ratio,  $V_{\%I}$  equals:

$$V_{\%I} = \frac{V_i \times 100}{(V_i + V_e)} \quad \text{Equation 1:3}$$

where,  $V_i$  is the volume of the internal phase and  $V_e$  is the volume of the external phase of the emulsion.

Emulsions with internal phase ratio less than 30 % are classed as low internal phase emulsions, between 30 and 74 %, medium internal phase emulsions, and 74 % and above as high internal phase emulsions (HIPEs) [18, 27]. For note to the reader, within the literature, HIPEs are also called, high internal phase ratio emulsions (HIPREs) [18, 28], gel emulsions[29] and (highly) concentrated emulsions [30, 31]. For clarity, throughout this thesis the term HIPE will be used.

HIPEs are classified with an internal phase ratio of 74 % and over as this represents the maximum closed-packed structure of internal phase droplets within an emulsion, above this value droplets either become polydisperse or deform into polyhedra [27]. The conventional method for their formation is the addition of the dispersed phase, to the continuous phase, to which the surfactant is added and is preferentially soluble within, under agitation [27, 30, 32]. Another method for the formation of a HIPE is the PIT method, for which non-ionic polyethoxylated surfactants are typically used [33, 34]. For the preparation of an w/o HIPE via this method, a o/w microemulsion is first prepared,

below the PIT of the emulsion system, and the temperature of the emulsion system is raised rapidly above the PIT, forming a w/o HIPE [33]. Emulsions prepared by this method are more mono-disperse than HIPEs prepared via the conventional method and internal phase droplets can be sub-micron in size [35, 36].

W/o HIPEs with non-ionic surfactants are observed to be stabilised, in terms of a reduction in internal phase droplet size on the addition of electrolytes to the aqueous phase of the emulsion in comparison with emulsions prepared with pure water [37, 38]. This stabilisation effect has been attributed to the lowering of the PIT of the w/o emulsion, due to the increased dehydration of the hydrophilic head groups of the non-ionic surfactants with the addition of salt to the aqueous phase [19, 29].

### **1.3 Functional Porous Polymers by Emulsion Templating**

A HIPE is prepared and the continuous phase is polymerised via thermal, redox, or photo-initiated free radical polymerisation forming a solid polymer and the emulsion droplets are removed yielding (in most cases) a highly interconnected network of micron sized pores of quite well defined diameter. The resulting material is often termed a polymerised HIPE, or polyHIPE. The process was developed extensively by workers at Unilever in the 1980s [40] and in recent years has seen increased interest from both academia and industry. A scanning electron microscopy (SEM) image of a typical polyHIPE material is shown in Figure 1:6 where the highly interconnected pore network can clearly be seen. The term “pore” is ambiguous when applied to such materials, since they in fact possess two distinct types of pore. For clarity, we refer to the spherical cavities created by the emulsion droplets as “voids” and the interconnecting holes as “windows” (see Figure

1:6). Note that within the literature the term “cell” is also used for the term “void”. Comprehensive reviews on polyHIPE materials were published in 2005 [41, 42]; this section of the introduction, covers advances in the synthesis, chemical functionalization and applications of emulsion templated porous polymers. Reviews on macroporous polymers prepared by other methods can be found in the literature [43-45].

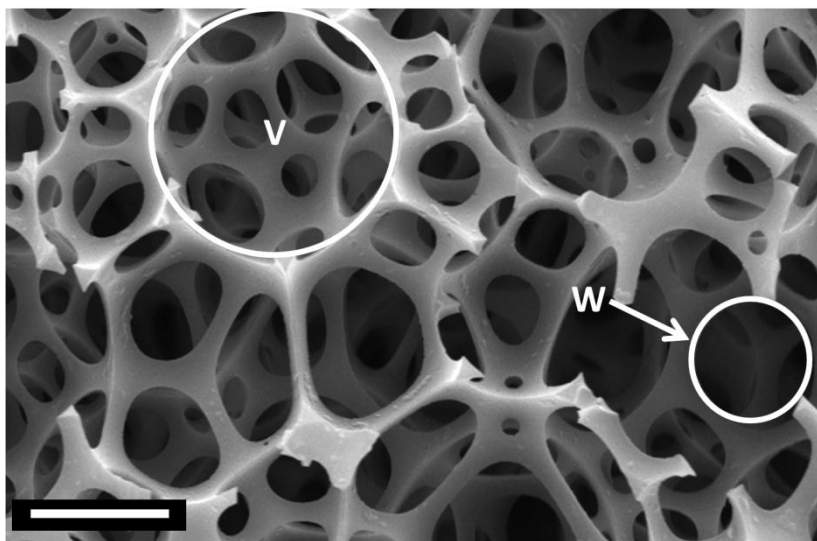


Figure 1:6 – SEM of a typical polyHIPE material. V indicates void, W indicates window – see text description. Scale bar = 10  $\mu\text{m}$

### 1.3.1 Functional Materials from Novel Emulsion Templating Systems

#### 1.3.1.1 *Extending the Range of Monomers Applicable to Emulsion Templating*

Glycidyl methacrylate (GMA) is a reactive monomer with an epoxy group that reacts readily with nucleophiles, such as amines[46]. Due to this reactivity epoxy based polymers have been used for a number of applications from the separation of biomolecules[47-49] to covalent enzyme immobilization[44]. GMA based polyHIPEs have been prepared previously, for the separation of proteins[50]. A low HLB number (0.5) surfactant (triblock copolymer of ethylene oxide (EO) and propylene oxide (PO)) was

required to produce a stable w/o polyHIPE, due to the relative hydrophilicity of GMA and ethylene glycol dimethacrylate (EGDMA) crosslinker[50].

Yao *et al.*[51], have prepared GMA-co-EGDMA polyHIPEs using triblock copolymer surfactants. The effect of the concentration of surfactant on the morphology of the resulting polyHIPE monolith was investigated. Changes were observed due to the interesting phase behaviour of triblock copolymers. The morphology changed dramatically on changing surfactant concentration from 2 % v/v of aqueous phase to 7 %, which the authors attributed to the self-assembly of the surfactant. The monolith was functionalized with ethylenediamine and used to separate the proteins bovine serum albumin, ovalbumin, lysozyme and pepsin. There are a number of advantages in using this GMA monolith for biomolecule separation. A significantly greater surface area ( $161 \text{ m}^2 \text{ g}^{-1}$ )[51] was observed in comparison to the previous GMA based polyHIPE[50] due to the formation of mesopores on the surface of the polyHIPE from the surfactant system and concentration used[51]. Secondly, flow rates of up to 3.6 L/h without compression of the monolith were observed, as a result of the macroporous morphology of the polyHIPE[51]. Permeability of the monolith increased by an order of magnitude in comparison to traditional packed bed chromatography columns[52]. Therefore, polyHIPEs are a promising solution to the problems faced by packed bed monoliths for biomolecule separation.

Barbetta *et al.* investigated the preparation and the hydrolysis of epoxy groups of thermally initiated GMA-based polyHIPEs[53]. These materials (crosslinked with DVB) could be prepared with a GMA content of up to 80 % v/v with respect to the total monomer content with a polyglycerol ester surfactant. Surface areas (measured by BET)

up to 371 m<sup>2</sup>/g were achievable with the use of toluene as the porogenic solvent. It was noticed by Fourier transform infrared (FTIR) spectroscopic analysis that hydrolysis of epoxy groups did occur on the preparation of these materials. The percentage of the epoxy groups hydrolysed was dependant on the average pore diameter (measured by Barrett-Joyner-Halenda (BJH) analysis) of these materials. Hydrolysis of epoxy groups for pores measured to be around 60 Å was noticeably less than epoxy groups within pores above this size range.

Hydroxyethyl methacrylate (HEMA) based polyHIPEs have been investigated as potential tissue engineering scaffolds. PolyHEMA foams were prepared by the thermal polymerisation of an o/w HIPE with the continuous phase containing HEMA, *N,N'*-methylenebisacrylamide (MBAM) crosslinker and a high HLB number surfactant (Triton X-405)[54]. It was observed that, as the amount of MBAM was increased, the surface area of the scaffold increased, with a maximum surface area of 17.5 m<sup>2</sup> g<sup>-1</sup> for 25 mol. % of MBAM. This was attributed to the nanometre substructure on the surface of the scaffold[54]. Water uptake of these polyHIPEs is an important factor due to the greater ability to wet the scaffold. The percentage weight increase due to water absorption within these HEMA-based scaffolds was shown to increase with the mol. % of crosslinker. This was concluded to be a result of the increase in surface area and hydrophilicity of the scaffold.

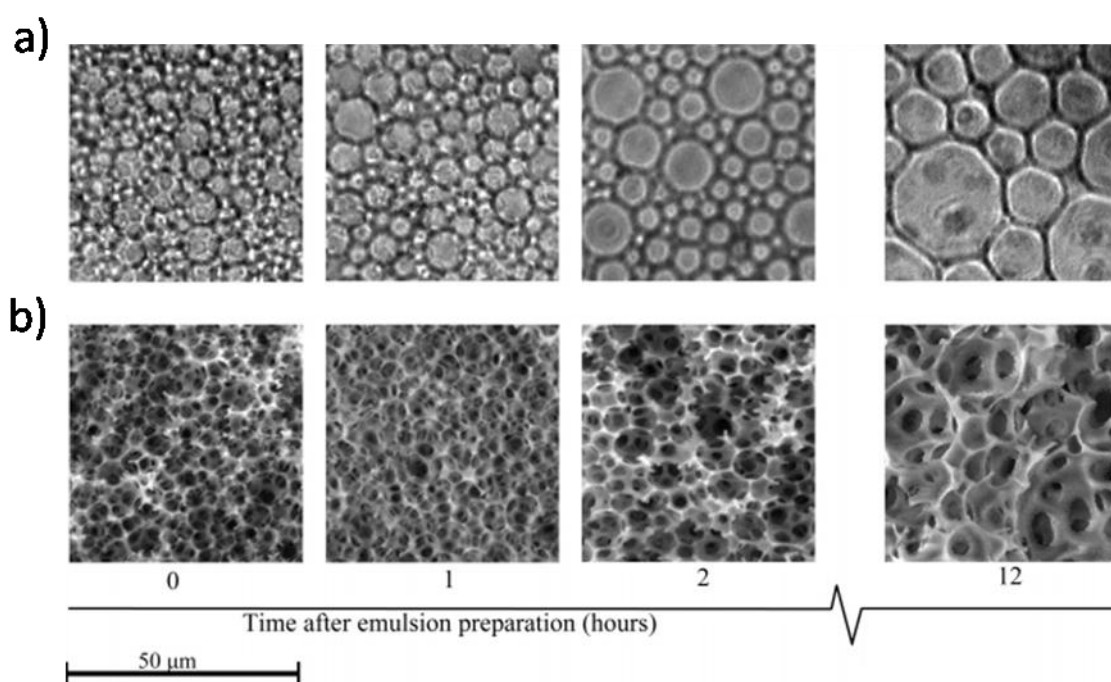


Figure 1:7 - a) Optical microscopy images showing the controlled increase in droplet size of the HIPE over time b) SEM images of HEMA polyHIPEs showing the increase in void and interconnect size on increasing the time between the preparation of the HIPE and its subsequent polymerisation. Reprinted with permission [55]. Copyright 2007, American Chemical Society.

O/w HEMA based polyHIPEs have also been prepared with a pluronic surfactant (HLB = 24) via a redox initiation system of ammonia persulfate (APS) and N,N,N',N'-tetramethylethylenediamine (TMEDA)[55]. A highly porous interconnected morphology was observed with average void and window diameters of 5.55 and 2.00 μm respectively. These HEMA based polyHIPEs were shown to absorb > 1000 % of their own weight of water. Krajnc *et al.* also developed a method for tuning the void and window diameter of the foam without using additives such as miscible solvents or salts to the o/w emulsion (see Figure 1:7). As the initiation of the emulsion is relatively fast, due to the redox initiation system, it was possible for the HIPE to be polymerized at various time intervals, which allowed the emulsion to undergo some coalescence, and/or Ostwald ripening, prior to its polymerisation. After twelve hours of gentle stirring of the HIPE at 20 rpm prior to

polymerization, average void and window diameters of 16 and 3.4  $\mu\text{m}$  were observed. Although the average void and window diameters did increase regularly over time, the degree of interconnectivity was almost halved in comparison to the emulsion which was polymerized immediately. This technique could be utilized alongside increasing the void and interconnect size via the addition of additives to the emulsion, for scaffolds for cell culture or tissue engineering.

Stimuli responsive polyHIPEs include those based on poly(N-isopropyl acrylamide) (PNIPAM)[56], a well-known thermoresponsive polymer which undergoes a lower critical solution temperature (LCST) transition in aqueous solutions at around 31  $^{\circ}\text{C}$ [57]. These polyHIPEs have been utilised to 'pump' oil red (OR) nanoparticles adhered to the internal scaffold of the foam into the surrounding environment by altering the temperature from 18  $^{\circ}\text{C}$  to 45  $^{\circ}\text{C}$  (see Figure 1:8). It was suggested, that this caused contraction of the PNIPAM polyHIPE and expulsion of the particles[56]. The formation of organic nanoparticles adhered to the polymer matrix was accomplished within one system. An o/w HIPE was prepared, with the continuous phase consisting of N-isopropyl acrylamide (NIPAM) and the crosslinker MBAM and the surfactant Triton X-405, the internal phase consisted of OR and chloroform. This emulsion was polymerised by the aqueous soluble persulfate initiation system of TMEDA and ammonium persulfate (APS) heated at 60  $^{\circ}\text{C}$  for a minimum of 12 hours. The polyHIPE material was then freeze dried to dry the material and to produce the OR nanoparticles adhered to the polymer surface[56]. A potential use of these solid foams, as suggested by Cooper *et al.*, is for the controlled delivery of water immiscible drugs in the form of organic nanoparticles within a thermoresponsive macroporous polymeric material[56].

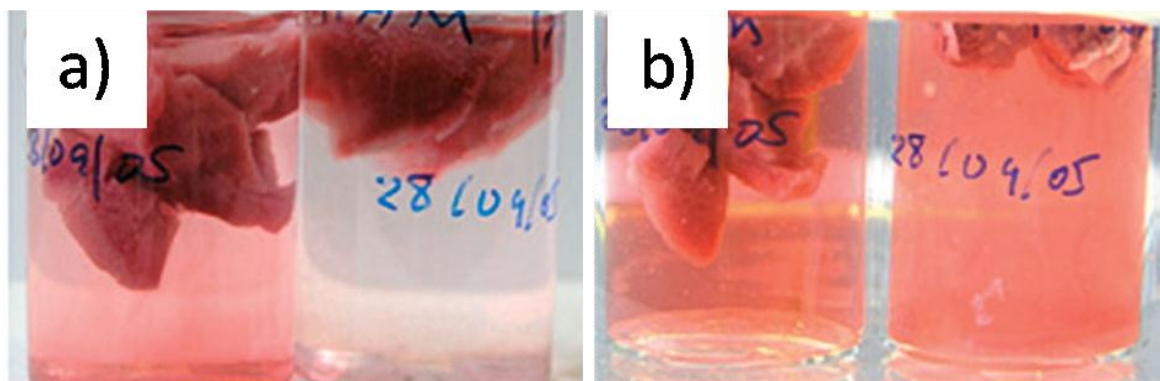


Figure 1:8 - Images showing the release of OR nanoparticles from a poly(acrylamide) polyHIPE (a non-stimuli responsive polymer) (left) in comparison to the release of OR nanoparticles from a PNIPAM polyHIPE (a stimuli responsive polymer) (right) a) 50 minutes after the addition of water at 18 °C. b) 3 minutes after the addition of water at 45 °C. Reproduced with permission [56].

PolyHIPEs prepared with acrylate monomers bearing crystallisable side groups have been observed to be semi-crystalline[58-60]. It is claimed that one of the most important factors for preparing semi-crystalline polyHIPEs is the location of where the polymerization is initiated[59]. Should the initiation occur in the internal phase rather than the continuous phase of the HIPE, semi-crystalline polyHIPEs from stearyl acrylate are observed due to the polymerization at the oil-water interface[59]. EGDMA was shown to increase the crystallinity in comparison to the DVB, due to its increased flexibility[60]. EGDMA is a relatively hydrophilic monomer, and as a result a closed void polyHIPE morphology is observed at high cross-linker concentration[60].

PolyHIPEs have been shown to be good scaffolds for *in vitro* three-dimensional (3-D) cell culture[61-63], and this has led over the last few years to investigations into biodegradable polyHIPEs as potential scaffolds for tissue engineering[64, 65]. PolyHIPEs copolymerized with 50 wt. % of biodegradable (vinyl-terminated) polycaprolactone (PCL) and 50 wt. % 2-ethylhexyl acrylate (EHA) with respect to the total monomer content have



been observed to completely degrade within 10 weeks in a sodium hydroxide solution, although a very inhomogeneous, phase separated morphology was observed[66]. Other w/o biodegradable polyHIPEs include poly(propylene furmarate) (PPF) based polyHIPEs[65]. It was shown that the stability of the precursor emulsion for these materials has a direct impact on the interconnective morphology of the polyHIPE. As the emulsion stability was increased, pore sizes decreased and when the pores were below 50  $\mu\text{m}$  in diameter windows within the pores were observed, whereas it was hypothesised that with larger pores the thickness of the film between adjacent pores was too great to form these interconnecting windows[65]. The morphology of the PPF polyHIPEs could be controlled by changing the quantity of toluene (used to dilute the continuous phase of the HIPE), the ratio of monomer to cross-linker and the molecular weight of PPF[65]. These polyHIPEs do show promise as scaffolds for tissue engineering as the pore size is adjustable and they are completely biodegradable, although the largest average pore diameters were only 49  $\mu\text{m}$ , with interconnecting windows of 3  $\mu\text{m}$ [65]. It would be interesting to study the biocompatibility of this polyHIPE and the ability of cells to penetrate and proliferate within the scaffold.

The polysaccharides gelatin and dextran have been used to prepare polyHIPEs as potential scaffolds for tissue engineering applications[64, 67-69]. Gelatin and dextran are relatively hydrophilic; therefore Barbetta *et al.* prepared these scaffolds via an o/w emulsion[64, 69]. The scaffolds were formed either by free-radical polymerization of vinyl functionalized gelatin[64] and dextran[69] or enzymatically cross-linked with unmodified gelatin and microbial transglutaminase[67]. These scaffolds were shown to have a highly porous interconnected structure with a tuneable morphology, via the addition of

additives to destabilise the emulsion (see Figure 1:9). Average pore and interconnect diameters of 84  $\mu\text{m}$  and 28  $\mu\text{m}$  could be achieved with the free-radical initiated gelatin based scaffolds[67].

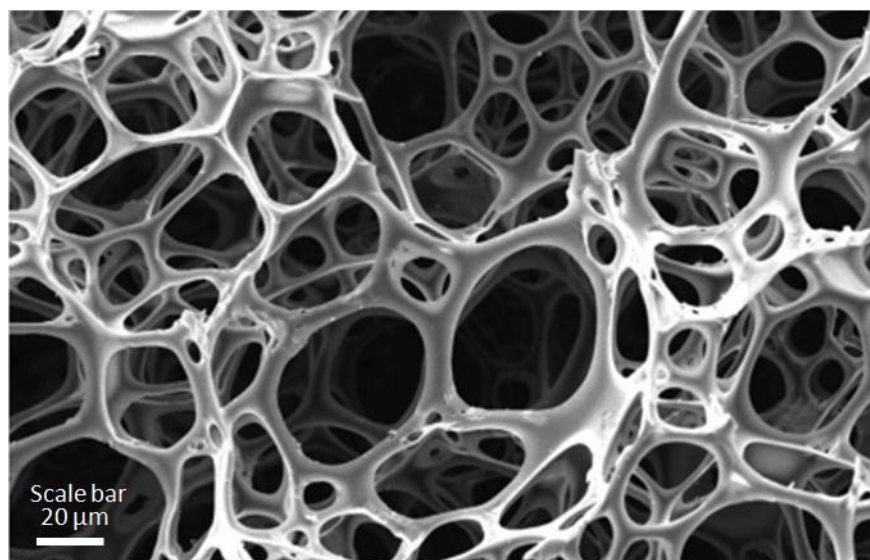


Figure 1:9 - SEM image of a 92 % porosity gelatin-methacrylate polyHIPE prepared via free-radical polymerisation in the presence of the additives NaCl and 1% v/v dimethyl sulfoxide (DMSO) [67].  
Copyright 2006, American Chemical Society.

One of the main disadvantages of o/w polyHIPEs is that a large amount of organic porogen required, for example for 10 g of a 90 % hydrophilic scaffold, approximately 90 g of organic waste is produced. This is one of the main reasons why super-critical  $\text{CO}_2$  ( $\text{scCO}_2$ ) has been investigated for the production of hydrophilic polyHIPEs.  $\text{scCO}_2$  is a clean, non-flammable, inexpensive alternative to organic solvents[70], which can be readily removed from a polyHIPE scaffold by depressurisation of the system[71]. As organic solvents are difficult to remove from polyHIPE scaffolds, the ability to remove the internal phase of the HIPE by depressurisation is an advantage not only for ease, but also for possibly improving the biocompatibility of the scaffold. Dextran-based polyHIPEs have been prepared from  $\text{scCO}_2$ -in-water (c/w) emulsions[72]. This was accomplished by using

a fluorinated surfactant which is generally used to stabilise c/w emulsions. Dextran was functionalized with methacrylate groups, so that the HIPE could be polymerized thermally at 60°C. It was observed that as the concentration of fluorinated surfactant was increased, the amount of coalescence also increased. Also it was shown that as the internal phase volume of the HIPE was increased from 75 % to 95 %, there was a marked increase in the interconnectivity of the scaffold. A c/w HIPE with 5 % (w/v) of fluorinated surfactant with respect to the aqueous phase of the emulsion with 90 % internal phase volume, produced a dextran based polyHIPE scaffold with a large proportion of voids with a diameter greater than 100  $\mu\text{m}$ .

The fluorinated surfactants that are used to produce c/w polyHIPE scaffolds are expensive, and non-biodegradable[73, 74]. In addition, thermally polymerised c/w HIPEs require high pressures (275 bar[75]) which also adds to the cost of preparing these materials. A new method for the formation of c/w polyHIPEs with non-fluorinated surfactants under lower pressures (< 120 bar) has been achieved recently. Synthesised poly(vinyl acetate)–PEG based di- and tri-block surfactants were observed to stabilise c/w HIPEs to a greater extent than fluorinated surfactants with respect to acrylamide-based emulsions[73]. Lower pressures were achieved by the lower temperature polymerization procedures such as the redox initiation of acrylamide-based HIPEs or chemical crosslinking of poly (vinyl alcohol)-based emulsions[73, 74]. Chitosan-based materials were prepared utilizing this new technique, although internal phase volumes of only 60% were investigated[74]. This technique could lead to the further development of biodegradable-based polyHIPE materials in the future.

Overall, polyHIPEs prepared with scCO<sub>2</sub> have several advantages as scaffolds for tissue engineering over those prepared by using o/w HIPEs, but the fact that their preparation involves specialist equipment and relatively high pressures (275 bar at 60 °C[75]), with fluorinated surfactants, cannot be overlooked.

### **1.3.1.2 *Templating Particle-Stabilized High Internal Phase Emulsions***

Nano- or micro-sized particles can be used to stabilize emulsions, resulting in so-called Pickering or Ramsden emulsions[76, 77]. The HLB number for a non-ionic surfactant is one of the most important criteria for determining whether a direct or an inverse emulsion formed. In the same vein, the wettability (measured by contact angles) of particles used to stabilise Pickering emulsions is the major factor that decides into which phase the particle will be preferentially solubilised. If the contact angles are lower than 90°, particles will be more soluble in an aqueous rather than oil phase, thus preferentially forming o/w, rather than w/o emulsions and *vice versa*[78, 79]. Advantages of using particles as emulsifiers rather than non-ionic surfactants include the low concentration of particles that are required (generally less than 1wt. %) to stabilize the emulsion. Pickering emulsions are generally very stable due to the adsorption of these particles at the o/w interface[79]. Multi-walled carbon nanotubes (mwCNTs) have been observed to act as surfactants and can solely stabilize emulsions with internal phase volumes of up to 0.6 (a medium internal phase emulsion or MIPE). These emulsions have been polymerized thermally to produce polyMIPEs[80]. MIPEs with mwCNTs dispersed within both the aqueous (by oxidizing the nanotubes) and monomer phase were observed to be more stable in comparison to mwCNTs dispersed within just one of the phases[80].

Pickering w/o emulsions prepared with hydrophobic silica particles were believed to phase invert at internal phase volumes of 0.7[81]. Recently it has been noticed that a range of different particles, namely titania, silica, copolymer particles and also single-walled carbon nanotubes can be used to stabilise w/o HIPEs with internal phase volumes up to 93 %[82] and these can be polymerized to form Pickering polyHIPEs[82-85]. Titania and silica nanoparticles were functionalised with oleic acid to increase their hydrophobicity to allow the formation of w/o emulsions[83, 84]. Internal phase volumes of up to 80 % are possible with 1 wt. % functionalised titania nanoparticles for a styrene (St)/DVB system[83]. However, due to the low loading ( $\sim 0.03$  wt. %) of oleic acid on these nanoparticles, internal phase volumes of 85 % could not be achieved due to the phase separation of the emulsion[83]. On the other hand, styrene/poly(ethylene glycol dimethacrylate) HIPEs with phase volumes of 85 % are achievable using oleic acid functionalised silica nanoparticles with significantly increased loading (3.5 wt. %) of oleic acid on the nanoparticle[84]. It has been noticed that Pickering polyHIPEs with porosities as high as 92 % are achievable using these functionalised silica nanoparticles[84]. Uncrosslinked poly(methyl methacrylate) (PMMA)-based w/o Pickering polyHIPEs can be produced with porosities of up to 93 % using 1wt. % of particles prepared from styrene, methyl methacrylate and acrylic acid[82]. The HIPEs are hypothesised to be stabilised not just by the copolymer particles themselves, but also by copolymer molecules from some dissolved particles. Copolymer particles dissolved within the aqueous phase prior to emulsification produced a higher porosity polyHIPE than the particles dispersed in the MMA phase. The stability of the HIPE with copolymer particles added to the aqueous phase increased with increasing NaCl concentration, which was hypothesised to be a result of the reduction of the hydrophilicity of the particles[82]. Attempts have been

made to prepare conducting Pickering polyHIPEs using single-walled carbon nanotubes (swCNTs)[85]. Previous attempts whereby the nanotubes were dispersed within the aqueous phase containing the surfactant sodium dodecyl sulphate (SDS) failed due to phase separation, as this surfactant preferentially forms o/w emulsions[86]. It has been recently noticed that swCNTs can be used as a stabiliser for the production of a 75% internal phase volume w/o Pickering polyHIPE[85]. This was accomplished by the dispersion of swCNTs only in the aqueous phase of the emulsion via the functionalisation these nanotubes within the aqueous phase by an amphiphilic block copolymer at low pH. Concentrations of 0.1 wt. % with respect to the oil phase of these functionalised swCNTs produced a highly porous open void polyHIPE. Conductivities of these polyHIPEs were  $\sim 1 \times 10^{-3}$  S/m, two orders of magnitude greater than mWCNT Pickering polyHIPEs[80, 85].

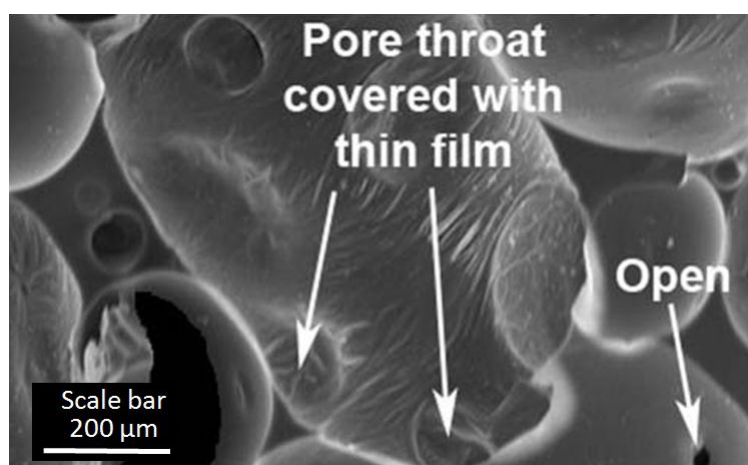


Figure 1:10 - SEM image of a Pickering polyHIPE stabilised with titania particles. Reproduced with permission [83]. Copyright 2007, Royal Society of Chemistry.

The morphology of some of these Pickering polyHIPEs (see Figure 1:10) has resulted in the mechanism of window (described as pore throats by the authors) formation to be questioned lately [82, 83, 87]. It has been hypothesized that these windows form due to

some mechanical action (vacuum) post-polymerization of the HIPE[87]. The formation of windows within a St/DVB polyHIPE stabilized with Span 80 has been shown to be due to the monomer to polymer contraction at the gel point, which has been monitored by cryo-SEM[88]. Also Gitli *et al.*[89] observed that St/DVB polyHIPEs which had not undergone Soxhlet extraction or drying *in vacuo* had an interconnected open void morphology. Some particle stabilised polyHIPEs have a thin polymeric film covering the closest point of contact between internal phase droplets, which in some instances has been partially or fully ruptured due to the drying process. One possible explanation for the different mechanisms of pore formation is that the stability of Pickering emulsions restricts the monomer to polymer contraction at the gel point and a thin polymeric film is formed instead of an open void. This can be ruptured during the post-polymerization procedures of Soxhlet extraction and drying *in vacuo*.

#### **1.3.1.3 Porous Polymers by Photopolymerization of HIPEs**

Photo-initiated polymerization can be extremely rapid, requiring on the order of a few seconds to achieve full conversion of monomer (see section 1.1.5). This polymerization technique has been applied to acrylate and methacrylate based HIPEs[90-93]. PolyHIPEs consisting of the monomers isobornyl acrylate (IBOA), EHA, N-acryloxysuccinimide (NASI), and trimethylolpropane triacrylate (TMPTA) and an organic soluble photoinitiator (Darocur 4265) were used for the immobilization of the enzyme, *Candida Antarctica* Lipase B [91]. The ultrafast curing of these emulsions potentially allows HIPEs that are too unstable to survive thermal curing to be used to prepare polyHIPEs. The only drawback of this relatively new technique for the curing of emulsions could be the thickness of the

HIPE that can be cured due to its opacity. As of yet this is a relatively under-investigated technique for the production of polyHIPEs.

#### **1.3.1.4 Emulsion Templated Porous Beads and Membranes**

One of the most common physical forms of a polyHIPE foam is a monolith, which is produced by polymerising the HIPE in a tube or column. Monoliths have applications in, chromatography and flow through chemical synthesis. Other physical forms of polyHIPEs have also been investigated, such as beads for batch type reactions[94] and membranes for cell culture[95] and electrochemical sensing[96].

PolyHIPE beads can be prepared by suspension polymerisation technique. Either a water - in-oil (w/o) or o/w HIPE is prepared with the monomers in the continuous phase, then this emulsion is added to either a water phase or oil phase respectively and the polymerisation is then initiated (see Figure 1:11) [97-100]. Beaded polyHIPEs have been prepared based on the reactive monomers 4-nitrophenyl acrylate (NPA) or 2,4,6-trichlorophenyl acrylate (TCPA)[101]. These monomers have been shown to be capable of being functionalized with a range of nucleophiles[102] and NPA based polyHIPE beads have also been used to purify contaminated water[103]. Beaded porous polymer structures were produced by a suspension polymerization technique involving a w/o/w multiple emulsion, which contained both organic and water soluble initiators and a redox initiator system (for NPA containing emulsions). NPA could be incorporated, between 25 – 60 mol. % and TCPA between 50 - 60 mol. % of the monomer mixture[101]. PolyHIPE beads were spherical with diameters between 49-105  $\mu\text{m}$  when the monomers TCPA or ethylene glycol dimethacrylate (EGDMA) were used, although rather peculiar star shaped



beads, with a core or spherical centre with diameter between 57-71  $\mu\text{m}$  and arms protruding from the core with diameter 127-285  $\mu\text{m}$ , were observed with NPA and divinylbenzene (DVB) [101]. NPA polyHIPE beads were successfully functionalized with several nucleophiles with loadings ranging from 2.6 – 6.6  $\text{mmol g}^{-1}$  [101].

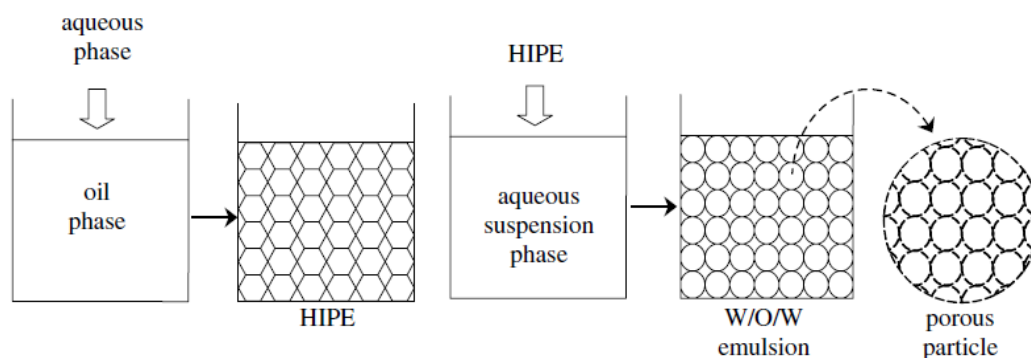


Figure 1:11 – Schematic of formation of beaded polyHIPE by a w/o/w emulsion suspension polymerisation technique. Reproduced with permission [104]. Copyright 2005, Elsevier.

Recently a new technique has been developed for the preparation of polyHIPE beads. Utilising the fast rate of polymerisation afforded by the photoinitiated free radical techniques, HIPE droplets were prepared using a microfluidic device and were subsequently photopolymerised producing monodisperse beaded polyHIPE materials (see Figure 1:12 and Figure 1:13 a)). The main advantage of this technique in comparison to beads prepared via a multiple emulsion is the surfaces of these materials are not covered with a non-porous 'skin' (see Figure 1:13 b)).

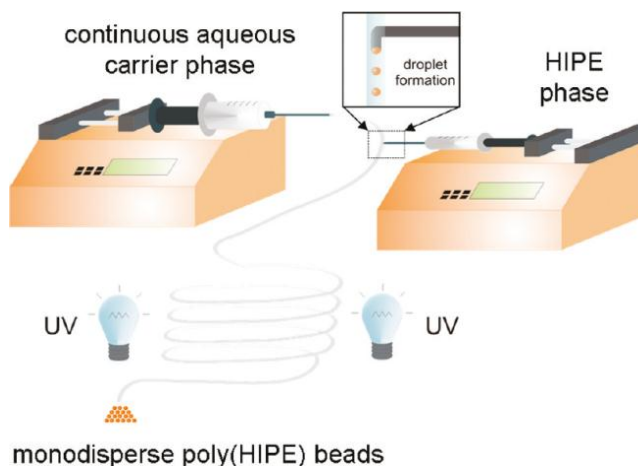


Figure 1:12 – Schematic of the formation of beaded polyHIPEs via the photopolymerisation of a HIPE prepared with a microfluidic device. Reprinted with permission [90]. Copyright 2009, American Chemical Society

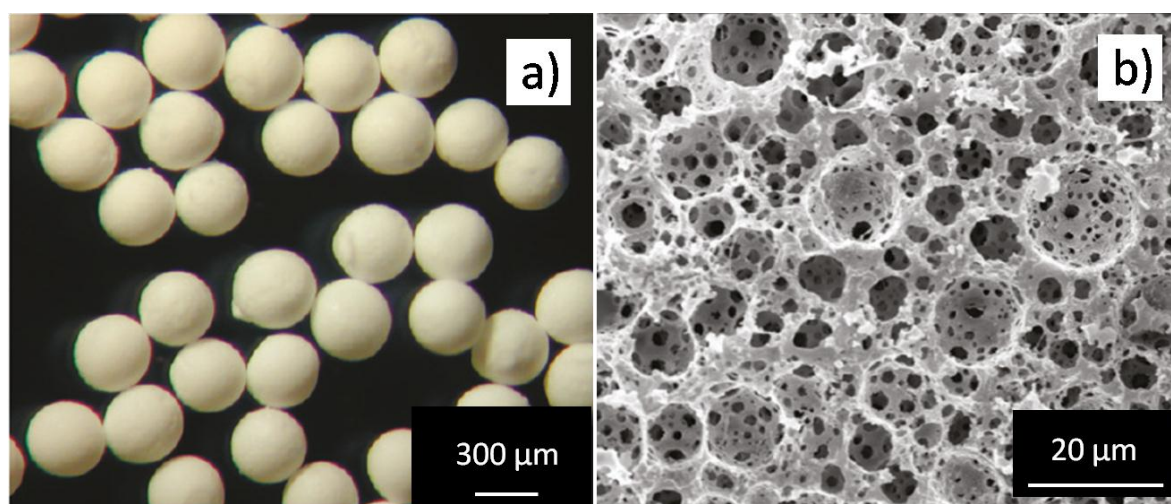


Figure 1:13 - a) Optical microscopy image showing monodisperse beaded polyHIPEs prepared by the photopolymerisation of a HIPE formed using a microfluidic device and b) SEM image of the surface of one of these polyHIPE beads. Reproduced with permission [90]. Copyright 2009, American Chemical Society.

PolyHIPE membranes used for the culture of cells for instance, are prepared by slicing a monolithic block with a fine blade called a microtome, but another technique has been developed whereby a HIPE is spread onto a glass substrate with a casting blade prior to its polymerization[105]. These highly porous polyHIPE membranes were obtained with a thickness between 200 – 400 μm (see Figure 1:14 a)). There was no observable non-

porous 'skin' on the surface of the membrane (see Figure 1:14 b)), where the HIPE was in contact with the glass substrate. Other substrates, for example poly(tetrafluoroethylene) (PTFE) were tried, as this substrate had previously been observed to form polyHIPE membranes with fewer defects in comparison to glass substrates[96]. In this instance, glass substrates were deemed to be the best substrate for polyHIPE membranes with reduced defects. The authors suggest that this could be due to the manner in which the HIPE is spread onto the substrate. Also, with the incorporation of 10 mol. % 2-ethylhexyl acrylate (EHA) (with respect to the monomer content) into the polyHIPE there was a significant improvement to the mechanical properties of this porous membrane.

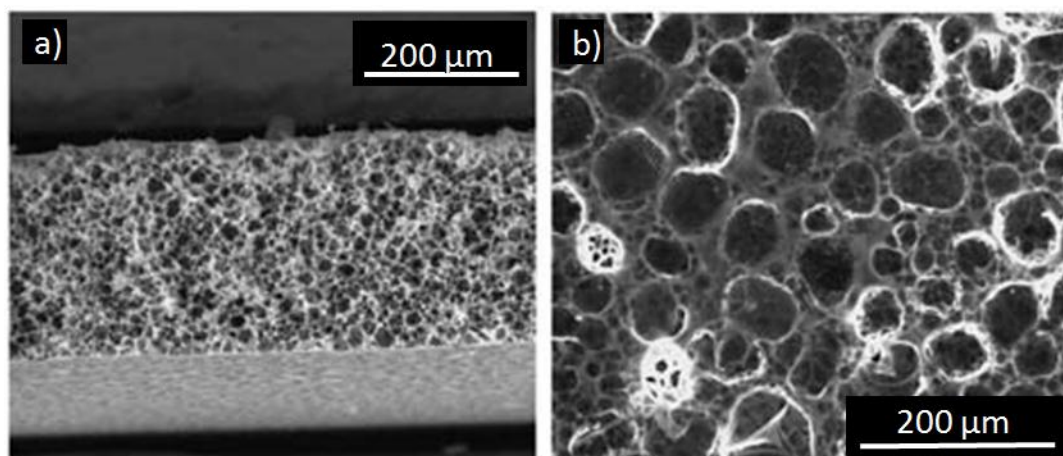


Figure 1:14 - SEM images of polyHIPE membrane prepared by casting technique a) cross-section. b) surface. Reproduced with permission [105]. Copyright 2008, Royal Society of Chemistry.

### 1.3.2 Chemical Functionalization of Emulsion Templated Porous Polymers

PolyHIPEs based on poly(ethylene glycol) (PEG)-methacrylate have been prepared for the reversible immobilization of elastin-based side chain polymers (EBPs)[106] (a stimulus-responsive polymer[107]). Stimulus-responsive polymers undergo a change in aqueous solubility on altering environmental conditions, for example solution pH or temperature and have been used to reversibly immobilize enzymes [108]. A 'short' chain

EBP was reversibly immobilized onto a porous polymer scaffold functionalized with a 'long' chain EBP. EBP-EBP co-assembly took place instead of self-assembly because the transition temperature ( $T_t$ ) of the blend was between the  $T_t$  values of the homopolymers, as has been previously observed with EBPs in solution (see Figure 1:15) [107]. These EBPs were prepared by reversible addition fragmentation chain transfer (RAFT) polymerisation of a methacrylated elastin-like peptide (ELP), VPGVG [106]. PEG-based polyHIPEs were covalently functionalized with EBPs by altering the functionality of the RAFT initiator located at the end of the polymer chain, from a thioester to a thiol and then undertaking a Michael addition onto vinyl groups (from unreacted crosslinker) within the polyHIPE [106]. It was successfully shown that EBP in solution could be co-assembled and then reversibly removed from the PEG based scaffold by controlling the pH and temperature of the solution[106] (see Figure 1:16).

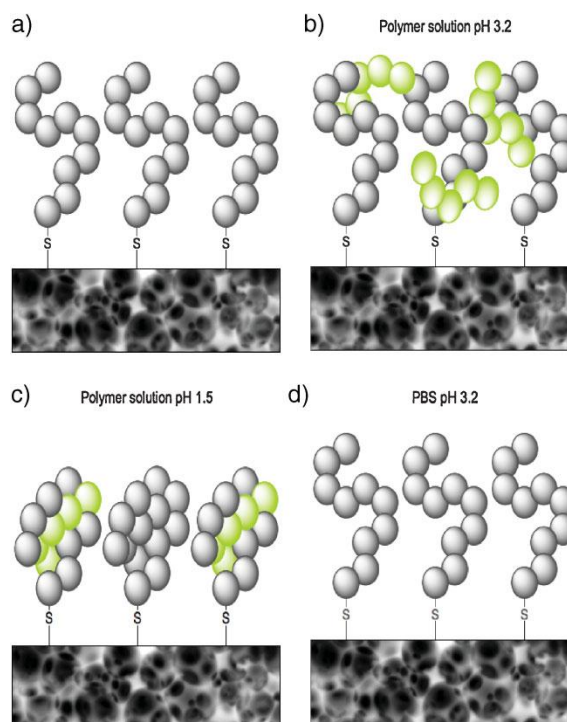


Figure 1:15 – Schematic of the reversible immobilization by peptide-mediated co-assembly: a) poly(VPGVG) functionalised PEG polyHIPE; b) poly(VPGVG) functionalised PEG polyHIPE soaked in a EBP solution at pH 3.2; c) After lowering the pH of the solution to pH 1.5; d) polyHIPE after washing in a pH 3.2 buffer. Reproduced with permission [106].

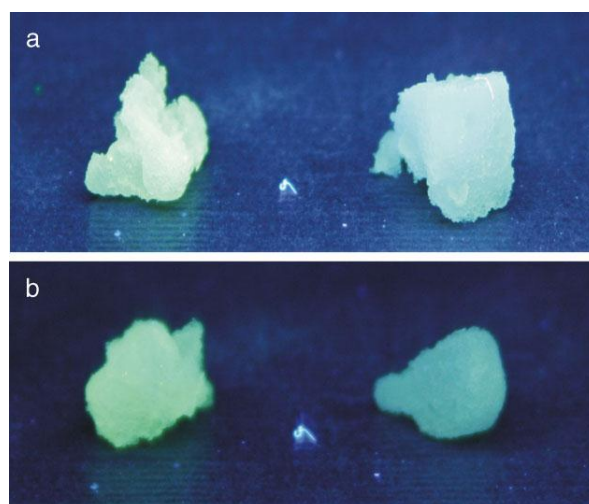


Figure 1:16 - a) Left: poly(VPGVG) functionalised PEG based polyHIPE mixed with a fluorescently labelled EBP solution at pH 1.5; right: unfunctionalised PEG based polyHIPE mixed with a fluorescently labelled EBP solution at pH 1.5. b) left: poly(VPGVG) functionalised PEG based polyHIPE mixed with a fluorescently labelled EBP at pH 1.5; right: EBP functionalised PEG based polyHIPE mixed with a fluorescently labelled EBP which has been then washed with a pH 3.2 buffer. PolyHIPE samples illuminated under ultraviolet (UV) light ( $\lambda=254$  nm). Reproduced with permission [106].

The facile preparation of polyHIPEs together with their macroporous, highly interconnected morphology has driven research on these materials. In addition, polyHIPEs can incorporate a range of different functional monomers including VBC [109, 110], GMA [50, 51, 53] and NPA [101, 102]. These subsequently can be functionalised for a variety of purposes, i.e. enzyme immobilization or water purification [91, 103]. There has been an increase in interest in functionalised monoliths due to the development of polymer-assisted purification techniques (PASP)[111]. These techniques employ polymers to purify products of chemical reactions, by sequestering reactants or products from the crude reaction mixture by reaction with a reactive group on the polymer surface. This has led to the investigation of polyHIPEs as potential substrates for PASP.

Previously, St/DVB materials have been observed to have unreacted carbon-carbon double bonds that could be used for further functionalisation[32, 112]. Reactive monomers such as VBC have been shown to be incorporated within a polyHIPE matrix without affecting the morphology. It has been demonstrated lately that VBC can be used to immobilise a Wang linker, and tris(hydroxyl methyl)aminomethane[113]. Wang resins have been used for a number of applications, from the solid phase synthesis of peptides to grafting of polymers by living free radical polymerisation[114, 115]. Species immobilised via Wang linker can be cleaved from the support or resin by post-treatment with an acid[114]. Wang resin functionalised VBC-based polyHIPEs were achieved in two steps; via the functionalisation of VBC with 4-hydroxybenzaldehyde; and the reduction of the aldehyde to deliver the Wang resin, giving loadings of 3.1 mmol/g[113]. This Wang resin functionalised support could be used to immobilize 4-iodobenzoic acid, a reagent for Suzuki-cross coupling reactions[113]. Tris(hydroxyl methyl)aminomethane

functionalised polyHIPEs were observed to have  $8.1 \text{ mmol g}^{-1}$  of hydroxyl groups within the scaffold[113]. These functionalised scaffolds were observed to have a higher conversion (82 %) for the attachment of 4-iodobenzoic acid with respect to the Wang resin scaffolds. This scaffold also scavenged acid chlorides, which are commonly used reagents in organic synthesis[113].

Other functional monomers, for example TCPA and NPA have been observed previously to be an alternative to VBC as a reactive monomer, although polyHIPEs derived from NPA were relatively inhomogeneous in their morphology [102]. TCPA based polyHIPEs with the flexible crosslinker, EGDMA, have been compared with DVB in their morphology, properties and functionalisation[116]. TCPA/DVB polyHIPEs could be prepared with Span 80, but TCPA/EGDMA polyHIPEs could only be stabilised with Synperonic PEL 121, a low HLB number triblock copolymeric surfactant, due to the increased hydrophilicity of the emulsion organic phase as a result of EGDMA. It was noticed that the reactive monomer underwent some partial hydrolysis, possibly due to the removal of inhibitors[116]. It was shown that surface area of TCPA polyHIPEs prepared with both DVB or EGDMA increased to a similar extent with the incorporation of porogenic organic solvents into the emulsion, but this increase in surface area is considerably less than other DVB based polyHIPEs with added porogenic solvents[117]. Also, the addition of the porogenic solvent increased the void size as a result of coalescence. Doubling in the average window size on increasing pore volume from 75-90 % and a tripling of the window size was observed with EGDMA. Tris(2-aminoethyl) amine functionalised polymers have been used for the removal of various reactants, such as aldehydes, imines and acid chlorides from crude final product solutions[111]. Hydrolysis of TCPA groups using sodium hydroxide solution indicated that



the monolithic forms of the polyHIPE performed to a similar extent, indicating that diffusion into the matrix did not limit reactivity. NPA polyHIPEs as mentioned above have been functionalised with piperzine and used in powdered and beaded forms for the removal of fertilizers from water samples[103].

Designing a porous polymer for further functionalisation has numerous drawbacks. Reactive monomers such as GMA can destabilise a w/o HIPE as a result of the increased hydrophilicity of the organic phase, which promotes destabilisation. Loading of functional groups from the incorporation of reactive monomers can be low as a result of inaccessibility of groups in the bulk and also because the polymer has to contain other constituents such as cross-linkers. Thirdly, high surface areas are desirable for most of the applications of solid phase chemistry, such as heterogenous catalysis, and generally polyHIPEs have relatively low surface areas, in comparison to other porous materials, such as Davankov styrene-divinyl benzene resins[1,32].

Work by Cummings *et al.* has addressed the first two drawbacks of functionalising polyHIPEs, by grafting reactive polymers onto acrylate based polyHIPEs via photoinitiation with the incorporation of an atom transfer radical polymerisation (ATRP) initiator[92]. This ATRP initiator did not affect the morphology of the polyHIPE and facilitated the surface functionalisation of poly(methyl methacrylate) (PMMA), which was observed to be able to undergo re-initiation with poly(hydroxyethyl methacrylate) (PHEMA) which is typical of a living free-radical polymerisation technique, forming a grafted block co-polymer[92]. GMA was grafted onto the photopolymerized polyHIPE and the epoxide was observed to undergo ring opening in an acidic solution, subsequently the hydroxyl groups were functionalised with a fluorinated acid chloride, which was observed to increase the



hydrophobicity of the foam[92]. ‘Click’ chemistry represents a range of reactions that exhibit mild conditions, with no byproducts and high yields. Examples include copper-catalyzed azide/alkyne cycloaddition reaction and also the thiol/ene reaction[118-120]. GMA grafted polyHIPEs can be functionalised with sodium azide, which can then be used for reaction with various alkyne containing molecules[93]. This work into ATRP surface grafting of GMA has opened up the opportunity to surface functionalise, using ATRP and/or click chemistry, with a range of other reactive monomers and molecules, without affecting the morphology of the polyHIPE. One drawback of using ATRP is that copper is incorporated into the material. Copper’s high toxicity[121] could reduce some of the potential applications of this material, particularly those of a biological nature.

A drawback of polyHIPEs for applications such as heterogeneous catalysis, chromatography and gas storage is their naturally low surface area due to their inherent macroporosity. Work has been previously carried out into increasing this surface area without affecting the polyHIPEs macroporous structure by the incorporation of porogenic solvents into the emulsion resulting in a meso- and microporous substructure within the polyHIPE[117, 122]. Recently it has been noticed that it is possible to increase the surface area of a polyHIPE via the hypercrosslinking, of DVB based polyHIPEs[123, 124]. Hypercrosslinking is a technique in which a polymer is swollen in a ‘good’ solvent, then the polymer is crosslinked, whereby on the removal of the solvent the swollen state of the polymer remains, forming a secondary pore structure[125] and resulting in high surface areas of around  $2000 \text{ m}^2 \text{ g}^{-1}$  (measured by BET)[126]. DVB-based polyHIPEs were hypercrosslinked via a “Davankov-type” method[127], by the Friedel-Crafts crosslinking of VBC which results in the formation of methylene bridges between chloromethyl groups or

the crosslinking of styrene with the addition of dimethoxymethane. These polyHIPEs have been investigated as support materials for catalysts[124] and could potentially be used for the purification of water supplies[128], as a sorbent for solid phase extraction[129-132], or as a column for high performance liquid chromatography (HPLC)[133], utilizing both the macroporous structure of the polyHIPE, allowing for high permeability of liquids through the foam and the microporous substructure which imparts the high surface contact that is desirable for the adsorption of molecules.

### **1.3.3 Enzyme Immobilization**

Enzymes are increasingly used as biocatalysts for the production of fine chemicals and pharmaceutical products [134]. The use of enzymes in industrial processes requires that they can be easily separated from the product, reused and have acceptable stability[135]. These requirements can be accomplished via immobilization of the enzyme onto a solid support [136]. The two main approaches to immobilise enzymes onto a solid support are adsorption and covalent attachment [137]. Adsorption is by far the most frequently used technique, as it is relatively simple, cheap and no other support preparation is needed. However, adsorbed enzymes tend to leach from the support [137]. Covalent attachment, generally through lysine residues on the surface of the enzyme, allows for a much stronger interaction between the enzyme and the support, resulting in a support that can be used many times without a marked reduction in enzyme activity[137]. However, sometimes this cost reduction in the reuse of the support is negated by the cost of chemicals to activate the support for enzyme immobilization.

### 1.3.3.1 Enzyme Immobilization onto Emulsion-Templated Porous Polymers

PolyHIPEs are an attractive support for enzymes due to the variety of functional groups that can be incorporated into the support for attachment of the enzyme. Furthermore, polyHIPEs can be prepared in monolithic forms, which allows for their use not just in batch but also under continuous flow.

Pierre *et al.*[91] have recently investigated enzyme immobilization onto polyHIPEs for biocatalysis. They prepared a photopolymerised polyHIPE that incorporated a reactive monomer N-acryloxysuccinimide (NASI) that was used to immobilise the enzyme, *Candida Antarctica* Lipase B (CAL-B). These polyHIPEs were reacted with a green fluorescent protein (rAceGFP) to show that an increase in NASI content from 0 to 0.74 mmol g<sup>-1</sup> resulted in a marked increase in intensity of fluorescence under a confocal microscope. Enzyme activity of the covalently immobilised lipase was compared to the enzyme in solution (Novozyme 525) and against a commercially available product Novozyme 435 (CAL-B physically adsorbed onto a macroporous acrylic resin). These results showed that the activity (in  $\mu\text{mol } \textit{paranitrophenyl acetate (PNPA)}/ \text{min}/ \text{mg}$  of CAL-B) of covalently immobilised CAL-B was comparable to the enzyme in free solution and significantly greater than that of Novozyme 435. The activity per gram of support also showed that the covalently immobilised enzyme is greater than Novozyme 435, even though the loading of CAL-B on the polyHIPE is ten times less than that of Novozyme 435. They suggested that this was due to there being more CAL-B accessible to the substrate for the covalently immobilised, rather than the adsorbed enzyme. Also the polyHIPE support showed greater potential as a biocatalyst, as there was no observable decrease in activity on reuse of the support, whereas there was 17 % decrease in initial activity with Novozyme 435.

Recently, a lipase from *Thermomyces Lanuginosus* was covalently immobilised onto a polyHIPE support via a polyglutaraldehyde (PGA) linker [138-140]. The polyHIPE was prepared from a continuous phase consisting of styrene, divinylbenzene, and Span 80, and an internal phase composition of PGA with potassium persulphate in aqueous solution. It was shown that there was a noticeable increase in the stability of the covalently immobilised lipase in comparison to adsorbed lipase on a styrene / DVB polyHIPE support. After reusing the support with adsorbed lipase just five times, there was a complete loss of enzyme activity and a 55 % reduction in original enzyme activity on storage at 4 °C in acetate buffer (25 mM, pH 6.0), due to leaching of the enzyme from the support. On the other hand, PGA attached lipase retained ~ 100 % of the initial activity after the support was reused 15 times and on storing the support for 30 days in acetate buffer. This glutaraldehyde immobilised lipase has been shown to be an effective catalyst for the production of biodiesel from sunflower, soyabean, canola, and waste cooking oils [139, 140]. The immobilization of lipase and subsequent transesterification reaction for the production of biodiesel were carried out on powdered, beaded and monolith forms of the poly (styrene / DVB / PGA) support. A continuous flow setup was possible for the monolithic form of the polyHIPE whereby it was cut into a disk and placed into a column and the substrate was passed around the system via a peristaltic pump. However, the best yields for biodiesel production were obtained from beaded or powdered forms of the support.

Recent developments in the production of emulsion templated porous polymers have resulted in a significant broadening of the scope of materials that can be prepared by this method. For example, well-defined materials can now be prepared from functional

monomers such as glycidyl methacrylate, 2-hydroxyethyl methacrylate, *N*-isopropyl acrylamide and poly(ethylene glycol methacrylate), as well as natural biomaterials such as gelatin and dextran. Advances in the emulsion templating process include the use of particulate stabilisers that eliminate the need for small molecule surfactants, together with ultra-rapid curing by photopolymerization, which means that less stable HIPEs that would not survive thermal curing can be converted into polyHIPEs. These developments facilitate the use of functional, emulsion templated porous polymers in diverse advanced material applications including as substrates for tissue engineering/cell culture and supports for biocatalysts.

## 1.4 Aims and Structure of Thesis

As was mentioned in section 1.3, recent advances in the preparation of emulsion-templated porous polymers include the formation of a greater range of functional materials, namely those with epoxy functionality, from the copolymerisation of GMA with either DVB or EGDMA. In addition to the preparation of polyHIPEs via the advantageous method of the ultra-fast photoinitiated free radical polymerisation of the continuous phase, in comparison to the more conventional thermally initiated method. Prior art within the field of emulsion-templated porous polymers does not include, to the best of the authors knowledge the development of the photopolymerisation technique for the preparation of highly porous monolithic GMA-based materials, and the investigation of the use of GMA-based polyHIPEs as supports for the covalent attachment of enzymes.

The aims of my thesis are to prepare an open-void highly porous GMA-based polyHIPE material, which can be functionalized post-polymerisation with a range of nucleophiles and used within a continuous flow set-up. In addition, the overall emphasis of the thesis is to prepare a bioreactor, via the covalent immobilization of the enzymes, onto the GMA-based emulsion-templated porous polymers.

The following chapter focuses on the preparation of GMA-based emulsion-templated materials via thermal- and photo-initiation of the HIPE and the development of these materials for use within a continuous flow system. The morphology of these materials is to be assessed via SEM, including statistical analysis of the void size and their distribution, in addition, mercury porosimetry is to be used for the quantification of the window size of GMA-based polyHIPE materials. Chapter 3 focuses on the investigation into the post-polymerisation functionalization and subsequent characterisation of GMA-based polyHIPE

materials with amine nucleophiles. A range of techniques are to be used for the characterisation of functionalized polyHIPE materials, including, FTIR, XPS, attachment of a fluorescent tag, elemental analysis and solid state  $^1\text{H}$  MAS NMR spectroscopy. The penultimate chapter concentrates on the covalent enzyme immobilization of enzymes onto GMA-based polyHIPEs, either by direct attachment of the enzyme onto the polyHIPE or via the attachment via a spacer group from the surface of the material. The activity of the immobilized enzymes are to be investigated via a discontinuous photometric and continuous titrametric assay. The final chapter gives an overall conclusion to the thesis and possible avenues of future work, such as the use of zero length linker groups from the polyHIPE support for the covalent attachment of enzymes, the development of GMA-co-TRIM polyHIPEs for continuous flow applications and the investigation into the functionalization of the polyHIPE material with a PEG spacer group with a 'clickable' moiety.

## 1.5 Bibliography

1. Buchmeiser MR. Polymeric Materials in Organic Synthesis and Catalysis. Wiley-VCH, 2003.
2. Cowie JMG. Polymers: Chemistry and Physics of Modern Materials, 2nd ed. New York: Blackie and Son Ltd, 1991.
3. Cowie JMG and Arrighi V. Polymers: Chemistry and Physics of Modern Materials. CRC Press Taylor and Francis Group, 2008.
4. Moad G and Solomon DH. The Chemistry of Radical Polymerization. Elsevier, 2006.
5. Young RJ and Lovell PA. Introduction to Polymers. Nelson Thornes, 1991.
6. Elias H-G. An Introduction to Polymer Science. VCH, 1997.
7. Nicholson JW. The Chemistry of Polymers. The Royal Society of Chemistry, 2006. pp. 54-56.
8. Decker C. Prog Polym Sci 1996;21(4):593-650.
9. Decker C. Macromol Rapid Commun 2002;23(18):1067-1093.
10. Andrzejewska E. Prog Polym Sci 2001;26(4):605-665.
11. Fouassier JP. Photoinitiated Polymerisation: Theory and Applications. Rapra Technology Limited, 1998.
12. Glockner P, Jung T, Struck S, and Struder K. Radiation Curing for Coatings and Printing Inks: Technival Basics and Applications. Hannover: Vincentz Network GmbH and Co.
13. Anseth KS, Wang CM, and Bowman CN. Macromolecules 1994;27(3):650-655.
14. Decker C. Polym Int 1998;45(2):133-141.



15. Rytov BL, Ivanov VB, Ivanov VV, and Anisimov VM. Polymer 1996;37(25):5695-5698.
16. Ivanov VV and Decker C. Polym Int 2001;50(1):113-118.
17. Decker C, Zahouily K, Decker D, Nguyen T, and Viet T. Polymer 2001;42(18):7551-7560.
18. Lissant KJ. Emulsions and Emulsion Technology. New York: Marcel Dekker, 1974.
19. Binks BP. Modern Aspects of Emulsion Science. The Royal Society of Chemistry, 1998.
20. Sjoblom J. Emulsions and Emulsion Stability. CRC Press Taylor and Francis Group, 2006.
21. Bancroft W. J Phys Chem 1913;17(6):501-519.
22. Bancroft W. J Phys Chem 1915;19(4):275-309.
23. Shinoda K and Saito H. J Colloid Interface Sci 1968;26(1):70-&.
24. Saito H and Shinoda K. J Colloid Interface Sci 1970;32(4):647-&.
25. Shinoda K and Sagitani H. J Colloid Interface Sci 1978;64(1):68-71.
26. Leal-Calderon F, Schmitt V, and Bibette J. Emulsion Science. Basic Principles: Springer, 2007.
27. Cameron NR and Sherrington DC. Biopolymers Liquid Crystalline Polymers Phase Emulsion 1996;126:163-214.
28. Caldero G, Llinas M, Garcia-Celma MJ, and Solans C. J Pharm Sci 2010;99(2):701-711.
29. Solans C, Pons R, Zhu S, Davis HT, Evans DF, Nakamura K, and Kunieda H. Langmuir 1993;9(6):1479-1482.

30. Solans C, Esquena J, and Azemar N. *Curr Opin Colloid Interface Sci* 2003;8(2):156-163.
31. Babak VG and Stebe MJ. *J Dispersion Sci Technol* 2002;23(1-3):1-22.
32. Hainey P, Huxham IM, Rowatt B, Sherrington DC, and Tetley L. *Macromolecules* 1991;24(1):117-121.
33. Kunieda H, Fukui Y, Uchiyama H, and Solans C. *Langmuir* 1996;12(9):2136-2140.
34. Ozawa K, Solans C, and Kunieda H. *J Colloid Interface Sci* 1997;188(2):275-281.
35. Esquena J, Sankar GR, and Solans C. *Langmuir* 2003;19(7):2983-2988.
36. Leal-Calderon F, Schmitt V, and Bibette J. *Emulsion Science. Basic Principles*: Springer.
37. Williams JM, Gray AJ, and Wilkerson MH. *Langmuir* 1990;6(2):437-444.
38. Aronson MP and Petko MF. *J Colloid Interface Sci* 1993;159(1):134-149.
39. Thomas A, Goettmann F, and Antonietti M. *Chem Mater* 2008;20(3):738-755.
40. Barby H and Haq Z. Patent: EP060138 1982.
41. Zhang HF and Cooper AI. *Soft Matter* 2005;1(2):107-113.
42. Cameron NR. *Polymer* 2005;46(5):1439-1449.
43. Sherrington DC. *Chem Commun* 1998(21):2275-2286.
44. Peters EC, Svec F, and Fréchet JMJ. *Adv Mater* 1999;11(14):1169-1181.
45. Okay O. *Prog Polym Sci* 2000;25(6):711-779.
46. Gauthier MA, Gibson MI, and Klok HA. *Angew Chem Int Edit* 2009;48(1):48-58.
47. Platonova GA, Pankova GA, Il'ina IY, Vlasov GP, and Tennikova TB. *J Chromatogr A* 1999;852(1):129-140.
48. Hagedorn J, Kasper C, Freitag R, and Tennikova T. *J Biotechnol* 1999;69(1):1-7.

49. Josic D, Lim YP, Strancar A, and Reutter W. *J Chromatogr B* 1994;662(2):217-226.
50. Krajnc P, Leber N, Stefanec D, Kontrec S, and Podgornik A. *J Chromatogr A* 2005;1065(1):69-73.
51. Yao CH, Qi L, Jia HY, Xin PY, Yang GL, and Chen Y. *J Mater Chem* 2009;19(6):767-772.
52. Martin C, Coyne J, and Carta G. *J Chromatogr A* 2005;1069(1):43-52.
53. Barbetta A, Dentini M, Leandri L, Ferraris G, Coletta A, and Bernabei M. *React Funct Polym* 2009;69(9):724-736.
54. Kulygin O and Silverstein MS. *Soft Matter* 2007;3(12):1525-1529.
55. Kovacic S, Stefanec D, and Krajnc P. *Macromolecules* 2007;40(22):8056-8060.
56. Zhang HF and Cooper AI. *Adv Mater* 2007;19:2439-2444.
57. Fujishige S, Kubota K, and Ando I. *J Phys Chem* 1989;93(8):3311-3313.
58. Livshin S and Silverstein MS. *Macromolecules* 2007;40(17):6349-6354.
59. Livshin S and Silverstein MS. *Macromolecules* 2008;41(11):3930-3938.
60. Livshin S and Silverstein MS. *Soft Matter* 2008;4(8):1630-1638.
61. Hayman MW, Smith KH, Cameron NR, and Przyborski SA. *Biochem Biophys Res Commun* 2004;314(2):483-488.
62. Akay G, Birch MA, and Bokhari MA. *Biomaterials* 2004;25(18):3991-4000.
63. Bokhari MA, Akay G, Zhang SG, and Birch MA. *Biomaterials* 2005;26(25):5198-5208.
64. Barbetta A, Dentini M, Zannoni EM, and De Stefano ME. *Langmuir* 2005;21(26):12333-12341.
65. Christenson EM, Soofi W, Holm JL, Cameron NR, and Mikos AG. *Biomacromolecules* 2007;8(12):3806-3814.

66. Lumelsky Y and Silverstein MS. *Macromolecules* 2009;42(5):1627-1633.
67. Barbetta A, Massimi M, Devirgiliis LC, and Dentini M. *Biomacromolecules* 2006;7(11):3059-3068.
68. Barbetta A, Massimi M, Di Rosario B, Nardecchia S, De Colli M, Devirgiliis LC, and Dentini M. *Biomacromolecules* 2008;9(10):2844-2856.
69. Barbetta A, Dentini M, De Vecchis MS, Filippini P, Formisano G, and Caiazza S. *Adv Funct Mater* 2005;15(1):118-124.
70. DeSimone JM. *Science* 2002;297(5582):799-803.
71. Butler R, Hopkinson I, and Cooper AI. *J Am Chem Soc* 2003;125(47):14473-14481.
72. Palocci C, Barbetta A, La Grotta A, and Dentini M. *Langmuir* 2007;23(15):8243-8251.
73. Tan B, Lee JY, and Cooper AI. *Macromolecules* 2007;40(6):1945-1954.
74. Lee JY, Tan B, and Cooper AI. *Macromolecules* 2007;40(6):1955-1961.
75. Butler R, Davies CM, and Cooper AI. *Adv Mater* 2001;13(19):1459-+.
76. Pickering S. *J Chem Soc* 1907;91:2001.
77. Ramsden W. *Proc R Soc London* 1903;72:156.
78. Binks BP and Lumsdon SO. *Langmuir* 2000;16(23):8622-8631.
79. Binks BP. *Curr Opin Colloid Interface Sci* 2002;7(1-2):21-41.
80. Menner A, Verdejo R, Shaffer M, and Bismarck A. *Langmuir* 2007;23(5):2398-2403.
81. Binks BP and Lumsdon SO. *Langmuir* 2000;16(6):2539-2547.
82. Zhang SM and Chen JD. *Chem Commun* 2009(16):2217-2219.
83. Menner A, Ikem V, Salgueiro M, Shaffer MSP, and Bismarck A. *Chem Commun* 2007(41):4274-4276.

84. Ikem VO, Menner A, and Bismarck A. *Angew Chem Int Edit* 2008;47(43):8277-8279.
85. Hermant MC, Klumperman B, and Koning CE. *Chem Commun* 2009(19):2738-2740.
86. Hermant MC, Verhulst M, Kyrylyuk AV, Klumperman B, and Koning CE. *Compos Sci Technol* 2009;69(5):656-662.
87. Menner A and Bismarck A. *Macromol Symp* 2006;242:19-24.
88. Cameron NR, Sherrington DC, Albiston L, and Gregory DP. *Colloid Polym Sci* 1996;274(6):592-595.
89. Gitli T and Silverstein MS. *Soft Matter* 2008;4(12):2475-2485.
90. Gokmen MT, Van Camp W, Colver PJ, Bon SAF, and Du Prez FE. *Macromolecules* 2009;42(23):9289-9294.
91. Pierre SJ, Thies JC, Dureault A, Cameron NR, van Hest JCM, Carette N, Michon T, and Weberskirch R. *Adv Mater* 2006;18(14):1822-1826.
92. Cummins D, Wyman P, Duxbury CJ, Thies J, Koning CE, and Heise A. *Chem Mater* 2007;19(22):5285-5292.
93. Cummins D, Duxbury CJ, Quaedflieg P, Magusin P, Koning CE, and Heise A. *Soft Matter* 2009;5(4):804-811.
94. Brown JF, Krajnc P, and Cameron NR. *Ind Eng Chem Res* 2005;44(23):8565-8572.
95. Bokhari M, Carnachan RJ, Przyborski SA, and Cameron NR. *J Mater Chem* 2007;17(38):4088-4094.
96. Zhao C, Danish E, Cameron NR, and Katakly R. *J Mater Chem* 2007;17(23):2446-2453.

97. Desforges A, Arpontet M, Deleuze H, and Mondain-Monval O. *React Funct Polym* 2002;53(2-3):183-192.
98. Zhang H and Cooper AI. *Chem Mater* 2002;14(10):4017-4020.
99. Zhang HF, Hardy GC, Rosseinsky MJ, and Cooper AI. *Adv Mater* 2003;15(1):78-81.
100. Zhang H, Hardy GC, Khimyak YZ, Rosseinsky MJ, and Cooper AI. *Chem Mater* 2004;16(22):4245-4256.
101. Stefanec D and Krajnc P. *Polym Int* 2007;56:1313-1319.
102. Krajnc P, Stefanec D, Brown JF, and Cameron NR. *J Polym Sci Pol Chem* 2005;43(2):296-303.
103. Pulko I, Kolar M, and Krajnc P. *Sci Total Environ* 2007;386:114-123.
104. Stefanec D and Krajnc P. *React Funct Polym* 2005;65(1-2):37-45.
105. Pulko I and Krajnc P. *Chem Commun* 2008(37):4481-4483.
106. Fernandez-Trillo F, van Hest JCM, Thies JC, Michon T, Weberskirch R, and Cameron NR. *Adv Mater* 2009;21(1):55-59.
107. Fernandez-Trillo F, Dureault A, Bayley JPM, van Hest JCM, Thies JC, Michon T, Weberskirch R, and Cameron NR. *Macromolecules* 2007;40(17):6094-6099.
108. Galaev IY and Mattiasson B. *Trends Biotechnol* 1999;17(8):335-340.
109. Barbetta A, Cameron NR, and Cooper SJ. *Chem Commun* 2000(3):221-222.
110. Krajnc P, Brown JF, and Cameron NR. *Org Lett* 2002;4(15):2497-2500.
111. Parlow JJ, Devraj RV, and South MS. *Curr Opin Chem Biol* 1999;3(3):320-336.
112. Law RV, Sherrington DC, and Snape CE. *Macromolecules* 1997;30(10):2868-2875.
113. Krajnc P, Leber N, Brown JF, and Cameron NR. *React Funct Polym* 2006;66(1):81-91.

114. Wang SS. *J Am Chem Soc* 1973;95(4):1328-1333.
115. Angot S, Ayres N, Bon SAF, and Haddleton DM. *Macromolecules* 2001;34(4):768-774.
116. Leber N, Fay JDB, Cameron NR, and Krajnc P. *J Polym Sci Pol Chem* 2007;45(17):4043-4053.
117. Cameron NR and Barbetta A. *J Mater Chem* 2000;10(11):2466-2472.
118. Kolb HC, Finn MG, and Sharpless KB. *Angew Chem Int Edit* 2001;40(11):2004-2021.
119. Hoyle CE and Bowman CN. *Angew Chem Int Edit* 2010;49(9):1540-1573.
120. Iha RK, Wooley KL, Nystrom AM, Burke DJ, Kade MJ, and Hawker CJ. *Chem Rev* 2009;109(11):5620-5686.
121. Stohs SJ and Bagchi D. *Free Radical Biol Med* 1995;18(2):321-336.
122. Barbetta A and Cameron NR. *Macromolecules* 2004;37(9):3188-3201.
123. Schwab MG, Senkovska I, Rose M, Klein N, Koch M, Pahnke J, Jonschker G, Schmitz B, Hirscher M, and Kaskel S. *Soft Matter* 2009;5(5):1055-1059.
124. Pulko I, Wall J, Krajnc P, and Cameron NR. *Chem-Eur J* 2010;16(8):2350-2354.
125. Veverka P and Jerabek K. *React Funct Polym* 1998;41(1-3):21-25.
126. Ahn JH, Jang JE, Oh CG, Ihm SK, Cortez J, and Sherrington DC. *Macromolecules* 2006;39(2):627-632.
127. Tsyurupa MP and Davankov VA. *React Funct Polym* 2002;53(2-3):193-203.
128. Fontanals N, Marcé RM, Cormack PAG, Sherrington DC, and Borrull F. *J Chromatogr A* 2008;1191(1-2):118-124.
129. Tolosa I, Douy B, and Carvalho FP. *J Chromatogr A* 1999;864(1):121-136.
130. Fontanals N, Marcé RM, and Borrull F. *J Chromatogr A* 2007;1152(1-2):14-31.

131. Fontanals N, Galia M, Cormack PAG, Marcé RM, Sherrington DC, and Borrull F. *J Chromatogr A* 2005;1075(1-2):51-56.
132. Fontanals N, Cortes J, Galia M, Marcé RM, Cormack PAG, Borrull F, and Sherrington DC. *J Polym Sci Pol Chem* 2005;43(8):1718-1728.
133. Sychoy CS, Ilyin MM, Davankov VA, and Sochilina KO. *J Chromatogr A* 2004;1030(1-2):17-24.
134. Buchholz K, Kasche V, and Bornscheuer UT. *Biocatalysts and Enzyme Technology*: Wiley-VCH, 2005.
135. Bornscheuer UT. *Angew Chem Int Edit* 2003;42(29):3336-3337.
136. Sheldon RA. *Adv. Synth. Catal.* 2007;349(8-9):1289-1307.
137. Cao L. *Carrier-bound Immobilized Enzymes, Principles, Applications and Design*: Wiley-VCH, 2005.
138. Dizge N, Keskinler B, and Tanriseven A. *Colloid Surface B* 2008;66(1):34-38.
139. Dizge N, Keskinler B, and Tanriseven A. *Biochem Eng J* 2009;44(2-3):220-225.
140. Dizge N, Aydiner C, Imer DY, Bayramoglu M, Tanriseven A, and Keskinler B. *Bioresour Technol* 2009;100(6):1983-1991.



## 2 Preparation and Characterization of GMA-based Photoinitiated PolyHIPE Materials

### 2.1 Introduction

Traditionally, polymerised high internal phase emulsions have been prepared via thermal initiation, typically with the aqueous soluble initiator potassium persulphate and the monomers styrene and divinyl benzene[1, 2]. The polymerisation can take from 24 hours to 48 hours and subsequent work-up includes the Soxhlet extraction with water and lower alcohols to remove the internal phase (including any salts used) and surfactant. Functional polyHIPE materials can be prepared via the copolymerisation of the monomer phase with a reactive monomer, such as vinylbenzyl chloride[3, 4], acrylic acid[5], 4-nitrophenyl acrylate[6] or glycidyl methacrylate[7, 8]. Inclusion of relatively hydrophilic monomers into the continuous phase of a w/o emulsion can destabilise the emulsion resulting in an inhomogeneous porous polymer[7].

Recently, functional polyHIPE materials derived from (meth)acrylates have been prepared via photopolymerisation[9, 10]. Advantages of this technique arise mainly from the rapid cure of the monomers, resulting in the preparation of emulsion-templated porous polymers in minutes rather than days and the ability to form well-defined polyHIPE morphologies from relatively unstable emulsions. *N*-Acryloxysuccinimide (NASI)-based photopolymerised polyHIPEs have been used as supports for biocatalytic reactions[9].

Monolithic materials have been used as flow-through enzymatic reactors, in particular GMA-based materials, as GMA can be functionalized post-polymerisation with a range of nucleophiles[11, 12]. Monoliths have advantages for continuous flow applications, for

example low back pressures even at high flow rates and also relatively high rate of mass transfer due to convective rather than diffusive flow (as for packed bed reactors)[13]. PolyHIPE monolithic materials are well suited as chromatographic stationary phases and flow-through systems due to their high porosity, high permeability and morphology of regular micron-sized voids with interconnecting windows [14, 15].

Preparation of novel functional GMA-based porous polymers via the photo-initiation of a HIPE and the subsequent implementation of this material for continuous flow applications is described in this chapter.

## 2.2 Experimental Section

### 2.2.1 Materials

Ethylene glycol dimethacrylate (Aldrich; 98 vol. %), glycidyl methacrylate (Fluka, 97 %), 2-ethylhexyl acrylate (Aldrich; 98%), Synperonic PEL 121 (triblock copolymer of poly(propylene oxide) and poly(ethylene oxide), with a HLB number of 0.5) (Croda), calcium chloride hexahydrate (Fluka,  $\geq 99$  %), trimethylolpropane trimethacrylate (Aldrich, technical grade), trimethylolpropane triacrylate (Aldrich, technical grade), dipentaerythritol penta-/hexa-acrylate (Sigma), isobornyl acrylate (Aldrich, technical grade), Hypermer B246 (triblock copolymer of poly(12-hydroxystearic acid) and poly(ethylene glycol) with a HLB number of 6) (Univar Ltd.), diphenyl(2,4,6-trimethylbenzoyl)phosphine oxide / 2-hydroxy-2-methylpropiophenone, blend (Aldrich), N-acryloxysuccinimide (Aldrich,  $\geq 90$  %), poly(ethylene glycol) methacrylate (Aldrich,  $M_n \sim 360$ ), sulphuric acid (Fisher Scientific,  $\geq 95$  %), 3-(trimethoxysilyl)propyl methacrylate (Aldrich,  $\geq 98$  %), acetone, potassium bromide (Aldrich,  $\geq 99$  %) and Omnifit®

chromatography columns (BenchMark Microbore 3 mm diameter 100 mm length borosilicate glass with adjustable ¼-28 fittings without frits), were used as supplied unless stipulated otherwise. See Figures 2:1, 2:2 and 2:3 for the chemical structures of the monomers, photoinitiator and surfactants used.

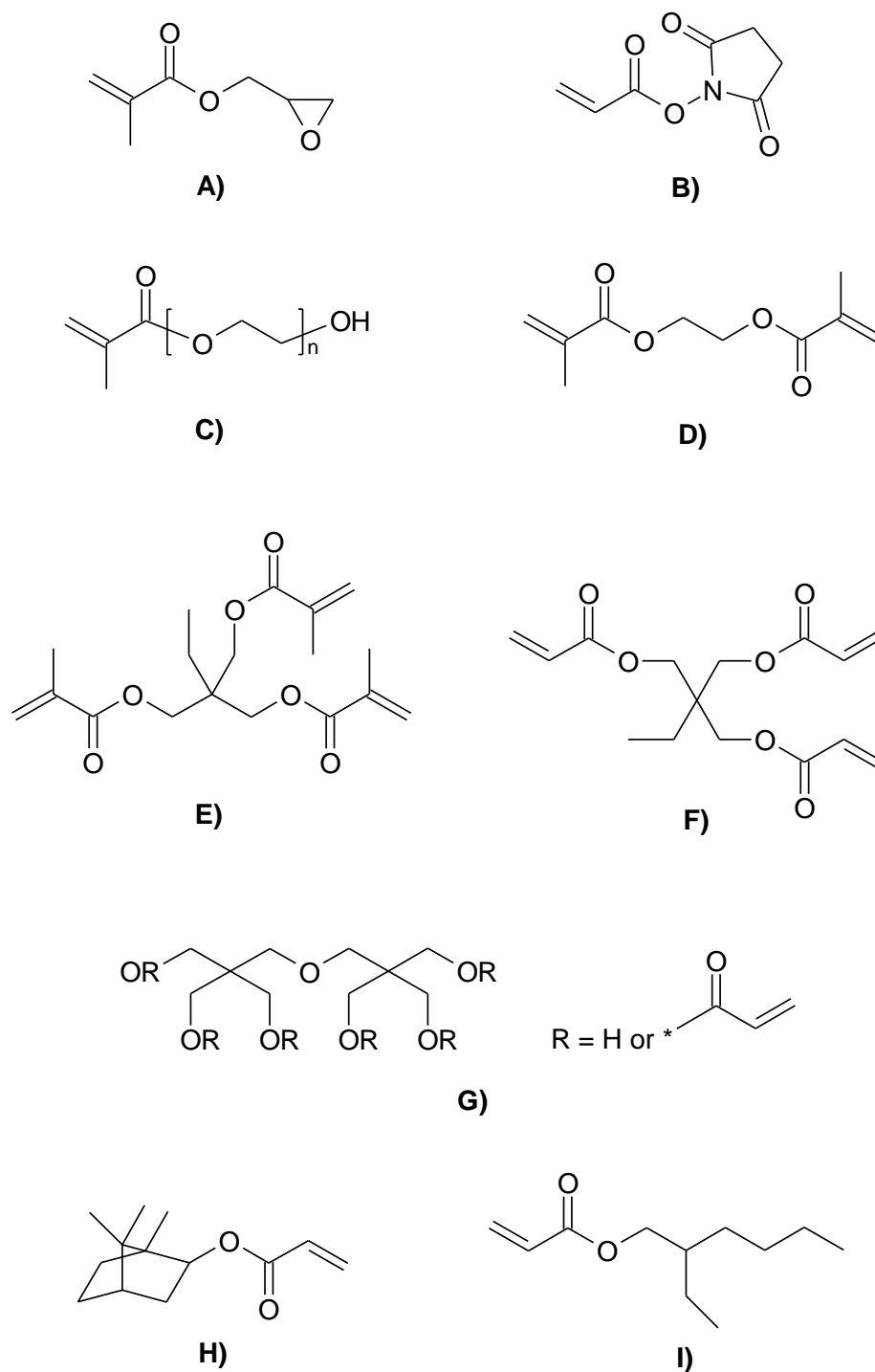


Figure 2:1 – Chemical structures of monomers used to prepare polyHIPE materials. A) Glycidyl methacrylate B) *N*-acryloxysuccinimide C) poly(ethylene glycol) methacrylate (M<sub>n</sub> 360) D) ethylene glycol dimethacrylate E) trimethylolpropane trimethacrylate F) trimethylolpropane triacrylate G) dipentaerythritol penta-/hexa-acrylate F) isobornyl acrylate G) 2-ethylhexyl acrylate

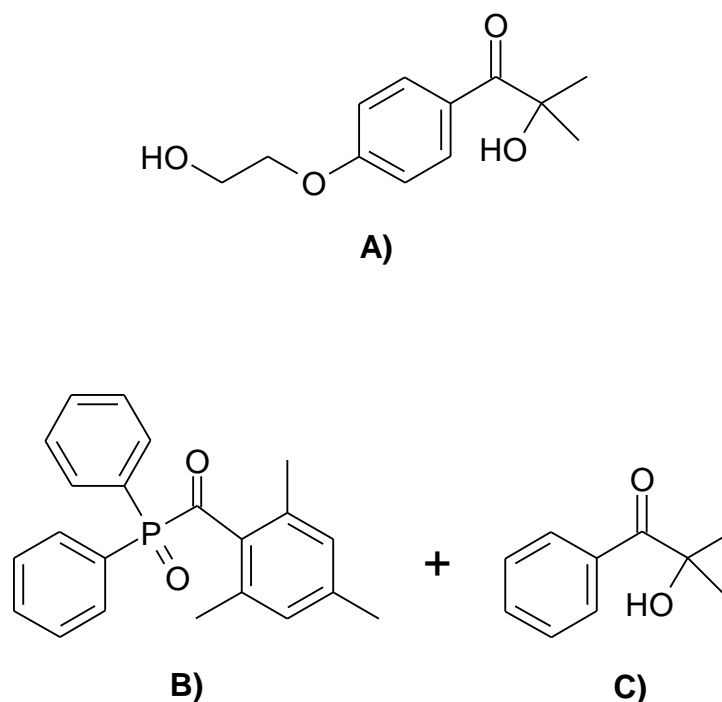


Figure 2:2 – Chemical structures of the photoinitiators used for preparation of polyHIPE materials. A) 2-hydroxy-4'-(2-hydroxyethoxy)-2-methylpropiophenone and a photoinitiator consisting of a 50:50 blend of B) diphenyl(2,4,6-trimethylbenzoyl) phosphine oxide and C) 2-hydroxy-2-methylpropiophenone

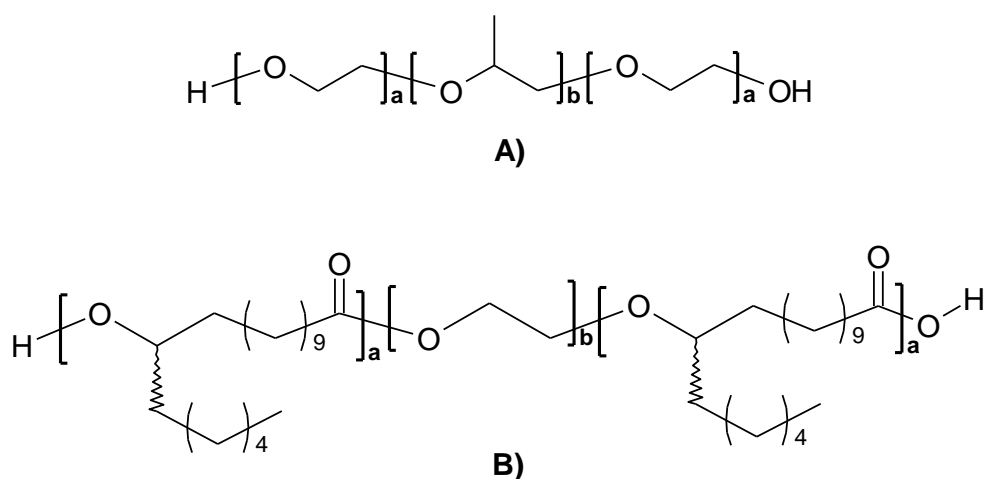


Figure 2:3 – Chemical structures of surfactants used to stabilize HIPEs. A) Synperonic PEL 121, A-B-A block copolymer with a HLB number of 0.5 (A is poly(ethylene oxide) block length 5 and B is poly(propylene oxide) block length 70) B) Hypermer B246, an A-B-A block copolymer with a HLB number of 6 and  $M_w$  of 7500 (A is poly(12-hydroxystearic acid) and B is poly(ethylene oxide))



The oil phase consisting of glycidyl methacrylate (0.70 mL, 0.73 g, 5.1mmol), 2-ethylhexyl acrylate (4.14 mL, 3.66 g, 19.9 mmol), isobornyl acrylate (0.88 mL, 0.87 g, 4.2 mmol), trimethylolpropane triacrylate (1.28mL, 1.41g, 4.8mmol), surfactant Hypermer B246 (0.2 g, 3% w/w of oil phase) and photoinitiator diphenyl(2,4,6-trimethylbenzoyl)phosphine oxide / 2-hydroxy-2-methylpropiophenone, blend (0.70 mL, 0.78 g, 10 % v/v of monomer phase) was added to a 250 mL two-necked round bottomed flask. To reduce the possibility of polymerisation due to stray light, the photoinitiator was contained in a brown glass container. Monomer, crosslinker, photoinitiator and surfactant were mixed in the dark (all laboratory lights were switched off and blinds in the laboratory were closed). The oil phase was then stirred continually in the dark at 350 rpm using a D-shaped PTFE paddle connected to an overhead stirrer. An aqueous phase consisting of 63 mL of deionised water was added dropwise to the oil phase over a period of 10 min., and then the HIPE was left to stir for an additional 10 min. to produce a homogenous emulsion (see Table 2:1, 2:2 and 2:3 for a full list of the components of this HIPE and for different formulations used). The HIPE was then placed between two glass plates within a PTFE square ring (see Figure 2:5 A)). This was then exposed to the UV lamp (see Figure 2:5 B) and C)) three times on each side at 3.5 meters per minute (conveyor belt speed) at 100 % intensity with an H-bulb ( $200 \text{ W cm}^{-2}$ ). The resulting monolith was recovered from between the glass plates and washed in acetone ( $5 \times 500 \text{ mL}$ ) and then dried *in vacuo* at  $55^\circ\text{C}$  for a minimum of 24 hours.

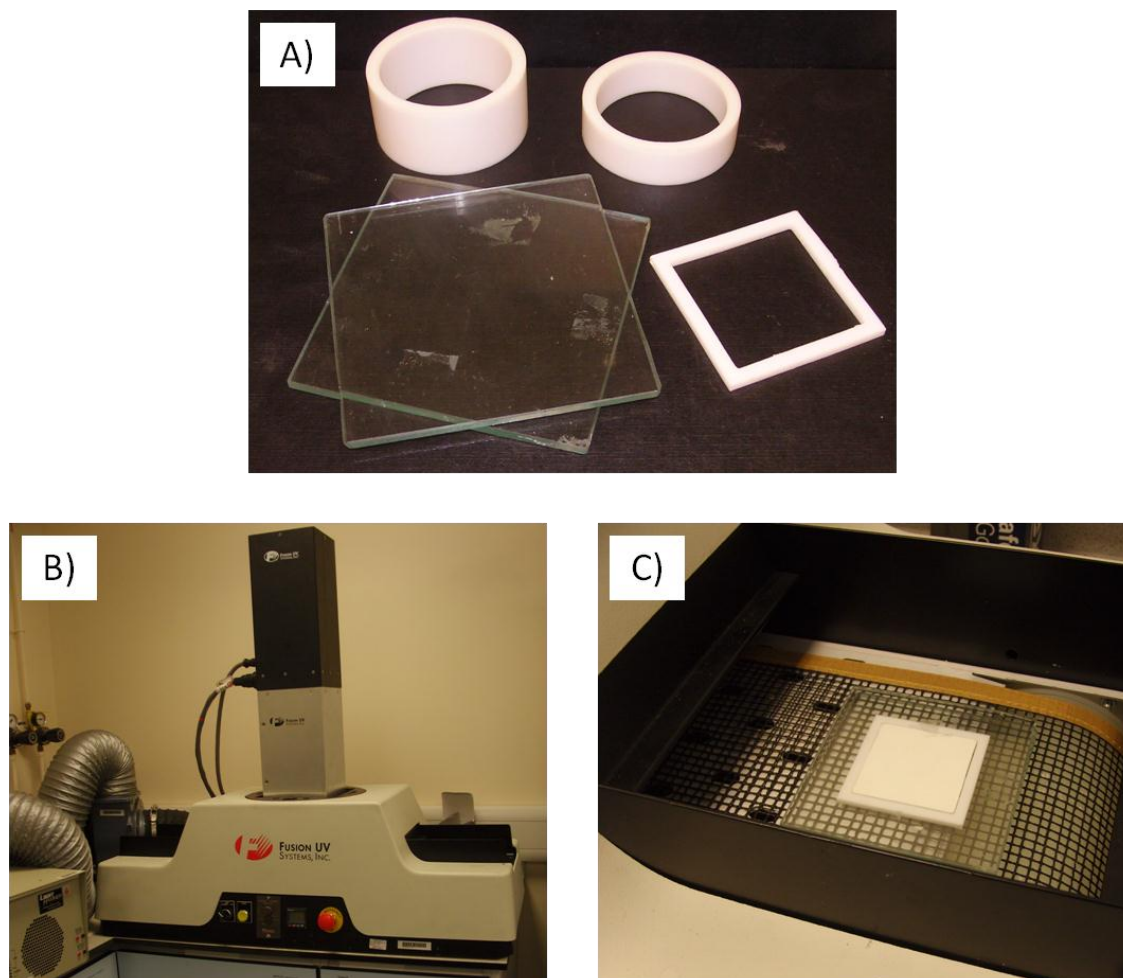


Figure 2:5 - Image showing the set-up for the photopolymerisation of a HIPE. A) PTFE moulds and glass plates. B) Fusion UV Systems, Inc.® LC6E Benchtop Conveyor with Light Hammer® 6 Irradiator used for curing of a HIPE. C) Polymerisation of a HIPE placed between the two glass plates within a PTFE mould on the LC6E Benchtop Conveyor.

### 2.2.3 PolyHIPE Coding System

PolyHIPE (PHP) materials are to be classified throughout the thesis with a code *PHPX*, where *X* represents the formulation used in Table 2:1, 2:2, 2:3, and 2:4.

### 2.2.4 Preparation of a Hydrophilic Photopolymerised PolyHIPE Material

A HIPE was prepared with the same method used in section 2.2.2 (see Table 2:1 for formulation). After 30 minutes of stirring at 350 rpm, 5 mL of 360 M<sub>w</sub> poly(ethylene



glycol) methacrylate was added dropwise into the emulsion with stirring at 350 rpm over one minute. This emulsion was then immediately polymerised with the UV curing device following the method in section 2.2.2 and then these materials were washed with copious amounts of acetone and dried in the vacuum oven at 50 °C for a minimum of 24 hours (see section 2.2.2) .

### 2.2.5 GMA / EGDMA HIPE preparation and thermal polymerisation

This procedure is based on work carried out by Krajnc *et al.*[7]. Ethyleneglycol dimethacrylate and glycidyl methacrylate were passed through a column of activated basic alumina (Aldrich; Brockmann 1) to remove any inhibitor present (hydroquinone monomethyl ether). An oil phase consisting of glycidyl methacrylate (14.51 g, 0.1 mol), ethylene glycol dimethacrylate (6.76 g, 34 mmol), and surfactant Synperonic PEL 121 (4.28 g, 20 % w/w of oil phase) was added to a 250 mL three-necked round bottomed flask. The oil was then stirred continually at 350 rpm using a D-shaped PTFE paddle connected to an overhead stirrer. An aqueous phase consisting of 80 mL of deionised water, water soluble initiator potassium persulfate (0.2 % w/v of aqueous phase), and calcium chloride hexahydrate (2 % w/v of aqueous phase) was added over a period of 30 min., then the HIPE was left to stir for an additional 30 min. The HIPE was then transferred to a polycarbonate centrifuge tube, which was then placed in an oven at 60 °C for 24 hours. The resulting monolith was recovered from the tube then extracted in a Soxhlet apparatus with deionized water for 24 hours, then with ethanol for 24 hours, and dried *in vacuo* at 55 °C for a minimum of 24 hours.

### 2.2.6 GMA/TRIM HIPE Preparation and Photopolymerisation

An oil phase consisting of glycidyl methacrylate (14.51 g, 0.1 mol), trimetholpropane trimethacrylate (TRIM) (6.76 g, 34 mmol), surfactant, Synperonic PEL 121 (4.28 g, 20 % w/w of oil phase) and photoinitiator diphenyl(2,4,6-trimethylbenzoyl)phosphine oxide / 2-hydroxy – 2 – methylpropiophenone, blend (2 mL, 2.24 g, 9.9 % v/v of monomer phase) was added to a 250 mL three-necked round bottomed flask. The oil was then stirred continually at 350 rpm using a D-shaped PTFE paddle connected to an overhead stirrer in the dark. An aqueous phase consisting of 80 mL of deionised water and calcium chloride hexahydrate (2 % w/v of aqueous phase) was added over a period of 30 min., then the HIPE was left to stir for an additional 30 min. to produce a homogeneous emulsion (PHP12, see Table 2:4 for a list of all the components of the HIPE). The oil phase was then stirred continually in the dark at 350 rpm using a D-shaped PTFE paddle connected to an overhead stirrer. The HIPE was then placed between two glass plates within a PTFE square ring (see Figure 2:5) and secured with tape. This was then exposed to the UV lamp (see Figure 2:5 B) and C)) three times on each side at 3.5 meters per minute at 100 % intensity with an H-bulb ( $200 \text{ W cm}^{-2}$ ) to ensure complete curing of the emulsion. The resulting monolith was recovered from between the glass plates and extracted in a Soxhlet apparatus with deionized water for 24 h, ethanol for 24 h, and dried *in vacuo* at 55 °C for a minimum of 24 hours.

## **2.2.7 Preparation of Photopolymerised GMA-based Monoliths for Continuous Flow Applications**

### **2.2.7.1 Functionalization of Glass Column**

Functionalization of glass columns followed the method by Uttamlal *et al.*[16]. Omnifit chromatography glass columns were immersed in concentrated sulphuric acid for a minimum of 30 min., this was followed by washing the columns with copious amounts of ultra high purity (UHP) water (Millipore) followed by acetone. The column was then placed into a 10 wt. % solution of 3-(trimethoxysilyl)propyl methacrylate in acetone for a minimum of 30 minutes. The columns were then washed with acetone and left to cure for 30 minutes at room temperature in a clean and dry environment.

### **2.2.7.2 Preparation of GMA/EGDMA HIPE with Photoinitiator**

See preparation of GMA/TRIM, section 2.2.6; ethylene glycol dimethacrylate (6.76 g, 20 mmol), (6.76g, 34 mmol) was used instead of trimetholpropane trimethacrylate (PHP12, see Table 2:4 for a list of all the components of the HIPE).

### **2.2.7.3 Preparation of Monolith within Functionalized Glass Column**

The procedure for the preparation of HIPE followed the method used in section 2.2.2 and 2.2.7.2 (for GMA/EGDMA photopolymerised monoliths) (see Table 2:4 for the different formulations of HIPE used). All polyHIPE monoliths prepared were of nominal porosity of 89 %, with the exception of the photopolymerised GMA/EGDMA polyHIPE, which had a nominal porosity of 80 %. HIPE was placed into the functionalized glass column. The column was then passed through the UV curing system six times (rotating

the column after every passage) at 3.5 meters per minute at 100 % intensity with a H-bulb ( $200 \text{ W cm}^{-2}$ ) to ensure a fully cured monolith (see Figure 2:6 for an image of a fully cured photopolymerised monolith within a functionalized glass column). The column was then connected up to a pump and washed with copious quantities of isopropanol and water. Columns were prepared for re-use by removing monoliths and placing the columns in a base bath for a minimum of 24 hours.



Figure 2:6 – Photopolymerised GMA-based polyHIPE monolith covalently bound to a functionalized glass chromatography column

Table 2:1 – Quantities of starting material required for the preparation of a photopolymerised GMA-based polyHIPE with 10% GMA v/v of monomer phase (PHP1).

Continuous Phase		PHP1					
		Weight % w/w of monomer phase	Weight/g	Volume % v/v of monomer phase	Volume/mL	Mol. % mole/mole of monomer phase	Mol./ mmoles
Monomer Phase	GMA	11	0.73	10.0	0.70	15	5.1
	IBOA	13	0.87	13	0.88	12	4.2
	EHA	55	3.66	59	4.14	59	19.9
	TMPTA	21	1.41	18	1.28	14	4.8
Surfactant	Hypermer B246	3	0.20	-	-	-	-
Initiator	Photoinitiator*	12	0.78	10	0.70	-	-

Dispersed Phase	PHP1		
	Weight % w/w of dispersed phase	Weight/g	Volume/mL
H <sub>2</sub> O	100	63	63

\*Photoinitiator is diphenyl(2,4,6-trimethylbenzoyl)phosphine oxide / 2-hydroxy-2-methylpropiophenone, blend

Table 2:2 – Quantities of starting material used for the preparation of 10%-40% GMA (v/v of monomer phase) photopolymerised polyHIPE materials

Continuous Phase	PHP1			PHP2			PHP3			PHP4		
	Volume % v/v of monomer phase of GMA within polyHIPE											
	10%			20%			30%			40%		
	Vol/mL	Wt./g	Mol./mmol	Vol/mL	Wt./g	Mol./mmol	Vol/mL	Wt./g	Mol./mmol	Vol/mL	Wt./g	Mol./mmol
GMA	0.70	0.73	5.1	1.40	1.46	10.3	2.10	2.19	15.4	2.80	2.92	20.5
IBOA	0.88	0.87	4.2	0.88	0.87	4.2	0.88	0.87	4.2	0.88	0.87	4.2
EHA	4.14	3.66	19.9	3.44	3.04	16.5	2.74	2.42	13.2	2.04	1.81	9.80
TMPTA	1.28	1.41	4.8	1.28	1.41	4.8	1.28	1.41	4.8	1.28	1.41	4.8
Hypermer B246	-	0.2	-	-	0.2	-	-	0.2	-	-	0.2	-
Photoinitiator*	0.70	0.78	-	0.70	0.78	-	0.70	0.78	-	0.70	0.78	-

Dispersed Phase	Weight % w/w of dispersed phase	PHP1	PHP2	PHP3	PHP4
		Volume % of v/v of monomer phase GMA within polyHIPE			
		10%	20%	30%	40%
		Volume/mL	Volume/mL	Volume/mL	Volume/mL
H <sub>2</sub> O	100	63	63	63	63

\* Photoinitiator is diphenyl(2,4,6-trimethylbenzoyl)phosphine oxide / 2-hydroxy-2-methylpropiophenone, blend

Table 2:3 – Different formulations used for the preparation of 77-95 % nominal porosity GMA-based photopolymerised materials

Continuous Phase	PHP1			PHP2			PHP6			PHP7		
	Nominal Porosity*											
	95 %			89 %			78 %			73 %		
	Vol./mL	Wt./g	Mol./mmol	Vol./mL	Wt./g	Mol./mmol	Vol./mL	Wt./g	Mol./mmol	Vol./mL	Wt./g	Mol./mmol
GMA	0.35	0.37	2.6	0.70	0.73	5.1	1.40	1.46	10.3	1.75	1.82	12.8
IBOA	0.44	0.44	2.1	0.88	0.87	4.2	1.76	1.74	8.3	2.20	2.17	10.4
EHA	2.07	1.83	9.9	4.14	3.66	19.9	8.28	7.33	39.8	10.35	9.16	49.7
TMPTA	0.64	0.71	2.4	1.28	1.41	4.8	2.56	2.82	9.5	3.20	3.52	11.9
Hypermer B246	-	0.1	-	-	0.2	-	-	0.4	-	-	0.5	-
Photoinitiator*	0.35	0.39	-	0.70	0.78	-	1.40	1.57	-	1.75	1.96	-

Dispersed Phase	Weight % w/w of dispersed phase	PHP5	PHP1	PHP7	PHP8
		Nominal Porosity*			
		95%	89%	78%	73%
		Volume/mL	Volume/mL	Volume/mL	Volume/mL
H <sub>2</sub> O	100	66.5	63	56	52.5

\*Nominal porosity is measured from the ratio of the dispersed phase volume with respect to the total volume of the emulsion (dispersed phase volume and continuous phase volume).

\*\*Photoinitiator is diphenyl(2,4,6-trimethylbenzoyl)phosphine oxide / 2-hydroxy-2-methylpropiophenone, blend

Table 2:4 – Different formulations of polyHIPE used for the preparation of a continuous flow set-up

Continuous Phase	PHP1			PHP8			PHP9			PHP10			PHP11			PHP12		
	Vol./mL	Wt./g	Mol./mmol	Vol./mL	Wt./g	Mol./mmol	Vol./mL	Wt./g	Mol./mmol	Vol./mL	Wt./g	Mol./mmol	Vol./mL	Wt./g	Mol./mmol	Vol./mL	Wt./g	Mol./mmol
GMA	0.70	0.73	5.1	0.70	0.73	5.1	1.40	1.46	10.3	1.40	1.46	10.3	-	-	-	13.93	14.51	102.1
NASI	-	-	-	-	-	-	-	-	-	-	-	-	0.38	0.51	3.0	-	-	-
IBOA	0.88	0.87	2.1	5.02	4.95	23.8	2.16	2.13	10.2	2.16	2.13	10.2	0.52	0.51	2.4	-	-	-
EHA	4.14	3.66	19.9	-	-	-	2.16	1.91	10.4	2.16	1.91	10.4	2.90	2.57	39.8	-	-	-
TMPTA	1.28	1.41	4.8	1.28	1.41	4.8	1.28	1.41	4.8	-	-	-	-	-	-	-	-	-
Penta-/Hexa-Crosslinker*	-	-	-	-	-	-	-	-	-	1.28	1.48	2.82	0.79	0.91	1.7	-	-	-
EGDMA	-	-	-	-	-	-	-	-	-	-	-	-	-	-	-	6.43	6.76	34.1
Hypermer B246	-	0.2	-	-	0.2	-	-	0.2	-	-	0.2	-	-	0.13	-	-	-	-
Synperonic PEL 121																-	4.28	-
Photoinitiator* *	0.70	0.78	-	0.70	0.78	-	0.70	0.78	-	0.70	0.78	-	0.32	0.36	-	2.00	2.24	-

Dispersed Phase	PHP1			PHP8			PHP9			PHP10			PHP11			PHP12		
	Wt. %***	Wt./g	Vol./mL	Wt. %	Wt./g	Vol./mL	Wt. %	Wt./g	Vol./mL	Wt. %	Wt./g	Vol./mL	Wt. %	Wt./g	Vol./mL	Wt. %	Wt./g	Vol./mL
H <sub>2</sub> O	100	63	63	100	63	63	100	63	63	100	63	63	100	45	45	98	80	80
CaCl <sub>2</sub>	-	-	-	-	-	-	-	-	-	-	-	-	-	-	-	2	1.6	-

\* Dipentaerythritol penta-/hexa-acrylate

\*\* Photoinitiator is diphenyl(2,4,6-trimethylbenzoyl)phosphine oxide / 2-hydroxy-2-methylpropiophenone, blend

\*\*\* Weight% w/w of dispersed phase



Table 2:5 - Showing the formulation for the preparation of GMA/TRIM photopolymerised polyHIPE material

Continuous Phase		Weight % w/w of monomer phase	Weight/g	Volume % v/v of monomer phase	Volume/ml	Mol. % mole/mole of monomer phase	Mol./ mmoles
Monomer Phase	GMA	68	14.51	69	13.93	83.6	102.1
	TRIM	32	6.76	31	6.34	16.4	20.0
Surfactant	Synperonic PEL 121	20	4.28	-	-	-	-
Initiator	Photoinitiator*	10.5	2.24	9.9	2.0	-	-

Dispersed Phase	Weight % w/w of dispersed phase	Weight/g	Volume/ml
H <sub>2</sub> O	98	80	80
CaCl <sub>2</sub> .6H <sub>2</sub> O	2	1.6	-

\* Photoinitiator is diphenyl(2,4,6-trimethylbenzoyl)phosphine oxide / 2- hydroxy – 2 – methylpropiophenone, blend

## **2.3 Instrumentation and Characterization**

### **2.3.1 Scanning Electron Microscopy (SEM)**

Morphologies of polyHIPE materials were observed using a FEI XL30 SEM operating between 20-25 kV. Sections of monolith were sliced and placed onto carbon fibre pads and attached to aluminium stubs and were then coated in gold using an Edwards Pirani 501 sputter coater.

### **2.3.2 Environmental Scanning Electron Microscopy (ESEM)**

Morphologies of polyHIPE materials were also observed using a FEI XL30 SEM operating at 10.0 kV in environmental scanning mode at a water vapour pressure of 3.5 Torr.

### **2.3.3 Mercury Intrusion Porosimetry**

Mercury intrusion porosimetry analysis was conducted using a Micromeritics Autopore IV. Intrusion and extrusion mercury contact angles of  $130^\circ$  were used. Intrusion pressures did not exceed 30000 psi for 73 % porosity polyHIPE material and 1600 psi for 79 % and 89 % nominal porosity polyHIPE materials. Penotrometers used had a stem and penotrometer volume of 1.190 mL and 4.2 mL respectively. Intrusion volume of mercury was between 66 % and 90 % of the stem volume.

### 2.3.4 Surface Area Analysis

Nitrogen adsorption measurements were performed at 77.3 K on a Micromeritics Accelerated Surface Area and Porosimetry (ASAP) analyser 2020 model. Samples were dried to a constant mass by heating the samples at 50 °C *in vacuo* prior to data collection. Surface area measurements utilized ten points adsorption isotherm over 0.01 to 0.30 P/P<sub>0</sub> and analyzed via the BET method[17].

### 2.3.5 FTIR Spectroscopy

Potassium bromide discs were prepared by subjecting a mixture of 1 mg of powdered polyHIPE per 100 mg of pure, dry potassium bromide to pressure under vacuum. Perkin Elmer Spectrum 100 FTIR spectrometer with a resolution of 4.00 cm<sup>-1</sup> was used for GMA-based polyHIPE materials. A background reading was acquired prior to the analysis of the polyHIPE materials. Twelve accumulations were taken for both the background and the scan. The scan range was taken between 4000 – 450 cm<sup>-1</sup>.

### 2.3.6 Solvent Delivery System

Varian 9012 solvent delivery system was used for the continuous flow analysis of the photopolymerised monolithic column. Back pressures and flow rate for each column and solvent used were taken from the solvent delivery system.

### 2.3.7 UV-curing device

Photopolymerisation was conducted on Light Hammer® 6 variable power UV curing system with LC6E benchtop conveyor from Fusion UV Systems Inc.® The curing system uses an H bulb operating at  $200 \text{ W cm}^{-2}$  when set at 100 % intensity.

### 2.3.8 SEM analysis with Image J software

Calculation of the average void size of photopolymerised materials was undertaken using the software Image J[18]. 2.5 cm depth by 7.5 cm diameter cylindrical monolithic blocks were prepared for analysis in conjunction with mercury intrusion porosimetry. SEM images were taken from three different sections of the same PolyHIPE material and random selections of 60 voids from each SEM image were used for the calculation of the average void size. A statistical correction factor[19] was used to provide accurate void diameters.

## 2.4 Results and Discussion

### 2.4.1 Thermally Initiated GMA-based HIPEs

Thermally initiated GMA-based polyHIPE materials as described by Krajnc *et al.*[7] were initially investigated as a potential material for the covalent immobilization of enzymes for biocatalytic reactions. It was shown by Krajnc *et al.* that these materials could be further functionalized with an amine and then subsequently used as a monolith for the separation of proteins. As GMA and EGDMA monomers are relatively hydrophilic, their usage for the preparation of a HIPE was accomplished with the use of a polymeric

surfactant with a very low HLB number of 0.5. The morphology of these materials was still subject to emulsion stability, presumably due still to the hydrophilic nature of the monomers used.

GMA/EGDMA polyHIPEs were characterized by FTIR spectroscopy to confirm their chemical structure (see Figure 2:7). The FTIR spectrum shows the characteristic O-H, C=O and epoxy stretching vibrations at 3517, 1732, 910 and 856  $\text{cm}^{-1}$ , respectively. Epoxy stretching vibrations at 910  $\text{cm}^{-1}$  and 856  $\text{cm}^{-1}$  confirm that unreacted epoxy groups are present after the thermal polymerisation of the material which could be used for subsequent functionalization. The FTIR spectrum is very similar to other GMA/EGDMA polyHIPEs[7], as well as monoliths produced by bulk polymerisation[20], indicating that the chemical composition of these materials is similar to the polyHIPE prepared in this work. Hydroxyl groups are present in the material as indicated from the peak at 3517  $\text{cm}^{-1}$ , which have also been observed in other GMA/EGDMA polyHIPE materials and are mainly due to the hydrolysis of GMA epoxy groups[7, 21]. However, residual surfactant (Synperonic PEL 121) containing hydroxyl groups and adsorption of moisture from the air when preparing the KBr disk for FTIR analysis could also contribute to the magnitude of this peak. It has been observed previously by the author that, when preparing these materials for nitrogen adsorption analysis, small amounts of moisture can be present within these powdered materials.

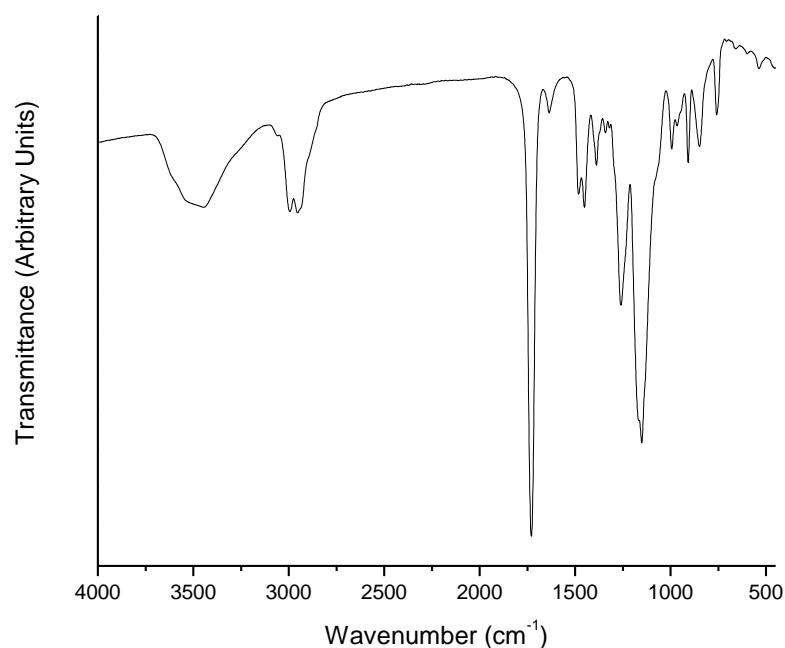


Figure 2:7 – FTIR spectrum of thermally initiated GMA/EGDMA polyHIPE

Morphology of 80 % nominal porosity GMA-co-EGDMA polyHIPE was investigated via SEM analysis. As can be seen in Figure 2:8, these materials have a closed-void morphology with a very inhomogeneous distribution of void sizes as a result of the inherent instability of the emulsion from which the material is templated. The GMA-co-EGDMA polyHIPE prepared here looks similar in morphology to the polyHIPE prepared by Krajnc *et al.*[7], with 60 % porosity, which could explain the reason for the closed void morphology. It was observed within the polycarbonate centrifuge tube that phase separated aqueous phase was present above the polyHIPE material. Comparison of the material prepared here with the materials prepared by Krajnc *et al.*[7, 8] would lead to the conclusion that the thermally initiated polymerisation of a GMA-based w/o HIPEs leads to a relatively inhomogeneous material as a result of emulsion instability.

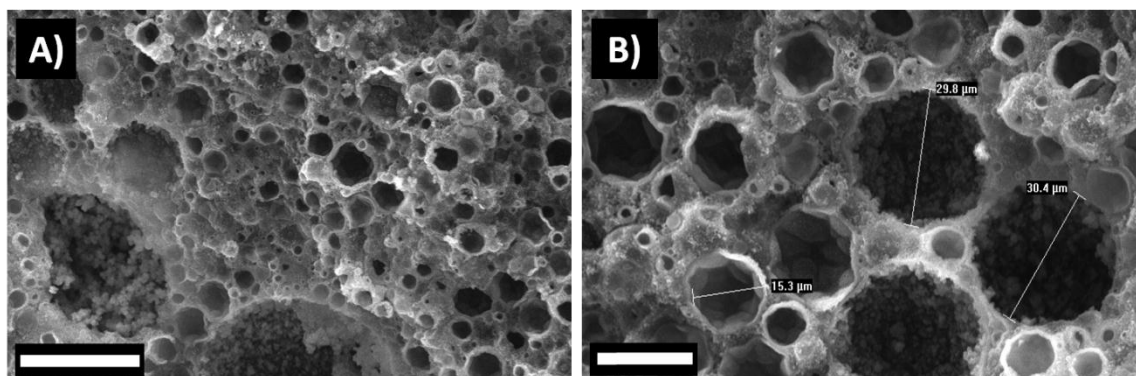


Figure 2:8 – SEM Images of thermally polymerised GMA/EGDMA polyHIPE A) Scale bar 50 µm B) Scale bar 20 µm

### 2.4.2 Photoinitiated polymerisation of GMA-based HIPEs

Photoinitiated polymerisation has been implemented as a technique for the preparation of functional polyHIPEs only recently [9, 10, 22] and is currently an under-researched technique for the preparation of these materials[23]. Advantages of this technique are the fast cure of the emulsion which potentially allows the preparation of novel functional emulsion-templated porous polymers.

#### 2.4.2.1 *GMA-co-EHA-co-IBOA-co-TMPTA photopolymerised polyHIPEs*

Following the observation that GMA-based thermally initiated polyHIPEs exhibited a closed-void and heterogeneous morphology, it was decided to investigate photopolymerisation for their preparation after being inspired by recent work on functional photopolymerised (meth)acrylate-based emulsion-templated porous polymers[9, 10]. These materials were prepared via the copolymerisation of GMA with a triacrylate crosslinker and acrylate monomers EHA and IBOA to adjust the elasticity of the polyHIPE material.

Surface area (measured by Brunauer-Emmett-Teller (BET) method[17]) of this photopolymerised polyHIPE material was  $2 \text{ m}^2/\text{g}$ , which is typical of other thermally polymerised materials[2].

FTIR analysis was carried out on PHP 1 and showed that (meth)acrylate carbonyl was present (peak at  $1730 \text{ cm}^{-1}$ ), as well as epoxy peaks at  $909 \text{ cm}^{-1}$  and  $856 \text{ cm}^{-1}$ . The FTIR spectrum (see Figure 2:9) is very similar to that of the thermally initiated GMA-based polyHIPE material, indicating a similar chemical composition to that material. Again a hydroxyl peak is present at  $3500 \text{ cm}^{-1}$ , mainly due to the hydrolysis of the epoxy group. The surfactant used for the preparation of this material also contains hydroxyl groups, so residual surfactant could increase the magnitude of this peak.

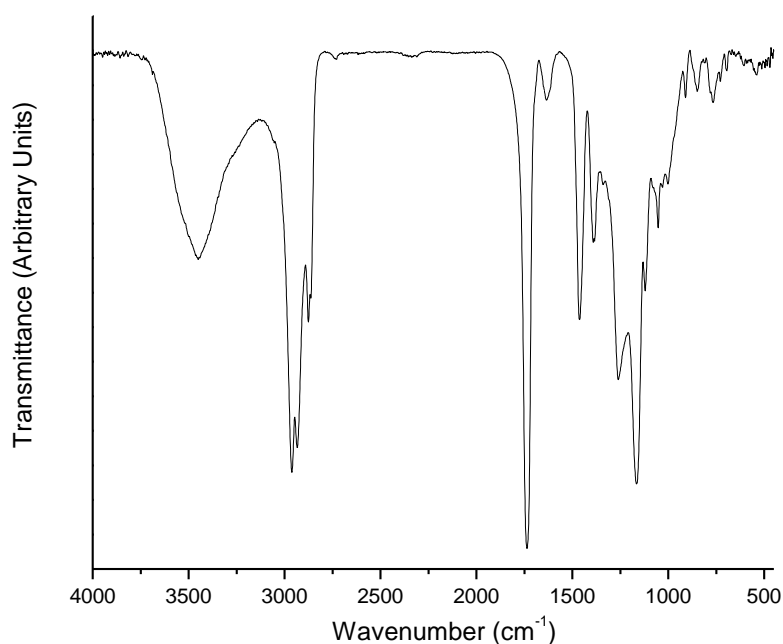


Figure 2:9 – FTIR spectrum (base line corrected) of GMA-based photopolymerised polyHIPE material, PHP1.



Investigation into the influence of the internal phase volume of the emulsion on the void diameter, window diameter and the degree of interconnectivity of these GMA-based photopolymerised materials was undertaken. PTFE moulds of 35 mm in diameter (see Figure 2:5 A)) were used for the preparation of these materials. SEM analysis and mercury intrusion porosimetry were carried out on the same piece of material to ensure the correlation between the void and window diameter. As can be seen in Figure 2:10, up to 95 % porosity GMA-based highly porous open-void emulsion-templated porous polymers with typical polyHIPE morphology[2] were prepared. Statistical analysis of these materials (see Figure 2:11 and Table 2:6) show that, as the nominal porosity of the materials is increased from 73 % to 95 %, the average void diameter increases overall from 9.6 to 17.4  $\mu\text{m}$ . This effect has been observed in thermally polymerised styrene-based polyHIPEs[19] and is attributed to coalescence of the emulsion droplets prior to the gel point, as a result of the decrease in the continuous phase layer between aqueous droplets. Distribution of void sizes of these materials is shown graphically in Figure 2:11. The void size distribution increased on increasing the internal phase volume of the HIPE. This is again indicative of an increase in coalescence on increasing the internal phase volume of the emulsion. 2-Hydroxyethyl methacrylate-based polyHIPE materials that were allowed to coarsen over time prior to rapid polymerisation were also observed to have an increased distribution of the void sizes due to coalescence[24].

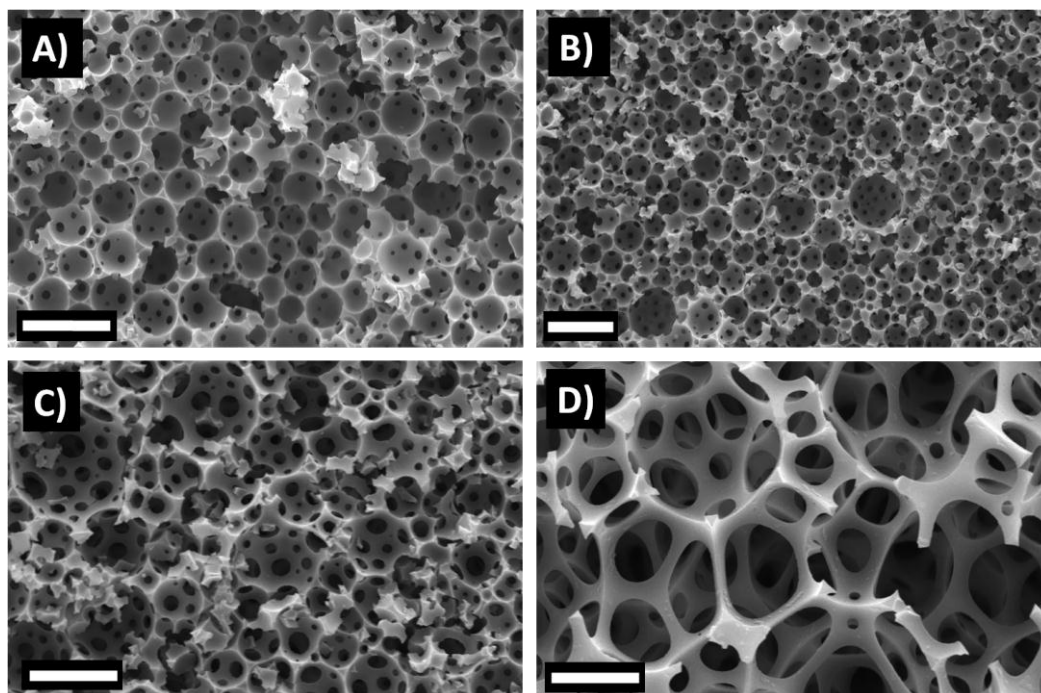


Figure 2:10 – SEM images of photopolymerized GMA-based polyHIPEs A) PHP7, 73 % porosity, scale bar 20  $\mu\text{m}$  B) PHP6, 78 % porosity, scale bar 20  $\mu\text{m}$  C) PHP1, 89 % porosity, scale bar 20  $\mu\text{m}$  D) PHP5, 95 % porosity, scale bar 10  $\mu\text{m}$

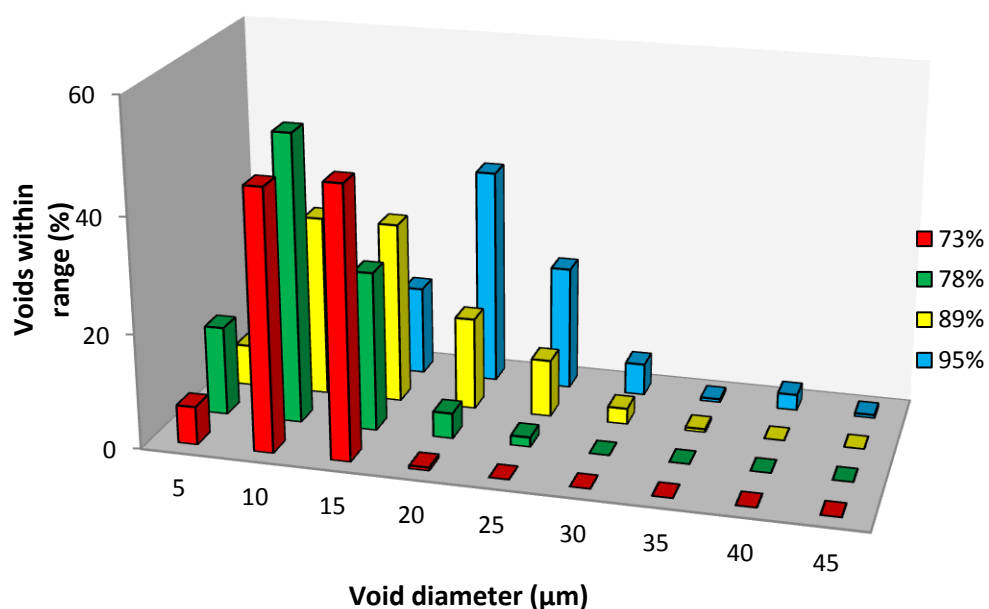


Figure 2:11 – Void diameters of photopolymerised GMA-based polyHIPEs. Void diameter distribution by analysis of SEM images, from front to back 73% porosity (PHP7), 78% porosity (PHP6), 89% porosity (PHP1) and 95% porosity (PHP5).

PHP1, PHP6, and PHP7 were analysed with mercury intrusion porosimetry (see Figure 2:12). This technique has been used extensively for the analysis of polyHIPE materials[25-27], however it should be noted that it does not provide information about the void size but only the interconnecting windows within these materials. Analysis of PHP5 was not possible due to the compression of the material during analysis. Mercury intrusion porosimetry results for GMA-based photopolymerised HIPE show that the average window diameter increases from 0.6 to 4.7  $\mu\text{m}$  on increasing the internal phase volume from 73 to 89 %. Increasing the internal phase volume results in thinning of the continuous phase layer between aqueous droplets. As the monomer phase contracts on polymerisation of the vinyl monomers[28] in combination with the thinning of the continuous phase layer, this results in larger interconnective windows within the polymer material. This is one of the first examples of mercury intrusion porosimetry analysis for photopolymerised emulsion-templated porous polymers and is made possible by curing of relatively deep (35mm) emulsion samples.

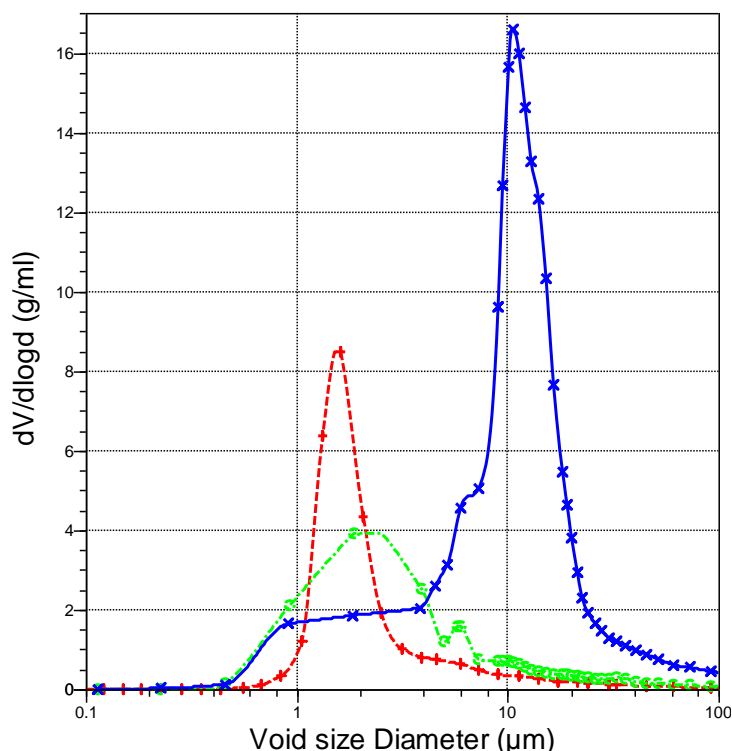


Figure 2:12 – Graph showing the Log differential intrusion verses void size diameter of the GMA-based photopolymerised polyHIPEs. Dashed red line and pluses represent the 73 % nominal porosity polyHIPE (PHP 7); Dash dot green line and circles represents 78 % nominal porosity polyHIPE (PHP6); Blue solid line and crosses represents 89 % nominal porosity polyHIPE (PHP1).

Table 2:6 – Void and Window Size Characterisation Data for GMA-based polyHIPEs

Nominal Porosity	73 %	78 %	89 %	95 %
Average Void Diameter (<D>) / $\mu\text{m}^a$	9.6	8.7	12.5	17.4
Average Window Diameter (<d>)/ $\mu\text{m}^b$	0.6	1.9	4.7	<sup>c</sup>
Average Degree of Interconnectivity (<d>/<D>)	0.07	0.22	0.37	<sup>c</sup>
Polydispersity / $\mu\text{m}^d$	2.6	3.4	5.1	6.1
Porosity <sup>b</sup>	74.9 %	79.2 %	89.8 %	<sup>c</sup>

a – determined with image J analysis; b – determined via mercury intrusion porosimetry; c – mercury intrusion porosimetry data could not be determined as the material was too elastic, i.e. the material was compressed during analysis; d – polydispersity is determined by the standard deviation in the void sizes as measured by image analysis.

The porosity (%) is calculated from the equation below:

$$P_{pc} = \frac{100 \times V_{tot}}{V_b} \quad \text{Equation 2:1}$$

where  $P_{pc}$  is the percentage porosity,  $V_{tot}$  is the total intrusion volume, and  $V_b$  is the bulk volume.

Calculated porosity values match very well with the nominal porosity of the polyHIPEs (see Table 2:6), the values are within 2 % of the intended porosity. This shows that these photopolymerised materials are a direct template from their respective emulsion.

There are several advantages of preparing GMA-based polyHIPE materials via the photopolymerisation of a mixture of GMA and acrylate monomers. Thermal polymerisation takes approximately 24 hours, whereas the preparation of GMA-based polyHIPEs via this method takes minutes. Also, this fast cure technique has allowed the preparation of a homogenous highly porous polymer with an open void morphology in comparison to the inhomogenous and mainly closed-void morphology of the thermally initiated GMA-co-EGDMA material[8]. Inhibitors were not removed from the monomers for the photopolymerised material, whereas in comparison inhibitors were removed for the thermally initiated material, thus removing another step in the preparation of the materials.

Other advantages of using this method for preparing GMA-based emulsion-templated porous polymers include the reduction in the content of the surfactant used for HIPE formation. Only 3 wt. % with respect to the monomer phase was used for the photopolymerised materials in comparison to 20 wt. % of the Synperonic PEL 121 for the

preparation of the thermally initiated GMA-based polyHIPE, thus reducing the likelihood of residual surfactant within the polymer after washing. Monomer phase and aqueous phase of other photopolymerised materials were purged with  $N_2$  prior to emulsification [9], presumably due to the possibility of oxygen retardation (with acrylate-based coatings)[29]. It was observed that oxygen did not have to be removed from the monomer or aqueous phase prior to emulsification for the preparation of GMA-based porous materials. This is possibly due to the high concentration of photoinitiator (10 % v/v of monomer phase) used, which can consume any oxygen dissolved within the continuous phase, together with intense UV radiation which generates excess free radicals, therefore increasing the rate of oxygen consumption[30]. This results in a reduction in the amount of atmospheric oxygen that can diffuse into the monomer phase[30].

It is interesting to note that thick (35 mm) opaque emulsions can be photopolymerised with no noticeable difference in the distribution of the void size from different sections of the polymer (SEMs not shown). The preparation of thick cured samples from UV radiation is usually attributed to a frontal polymerisation effect. Frontal photo-polymerisation occurs via the bleaching of the photoinitiator from its photolysis[31]. Acylphosphine oxides, in particular diphenyl(2,4,6-trimethylbenzoyl)phosphine oxide is a photoinitiator that is used for this technique, taking advantage of the fast rate of photolysis and deep cure when using this initiator[32]. Thick (up to 55 mm) hydrogel materials have also been prepared by photo-induced thermal frontal polymerisation, where UV radiation is used to initiate the polymerisation on the surface and thick materials are polymerised from the heat produced from the polymerisation with the addition of thermal initiators present within the solution[33].

#### 2.4.2.2 Preparation of Photopolymerised GMA-based PolyHIPE Materials with Differing Quantities of GMA

Following the successful preparation of functional highly porous polymers with GMA via a photopolymerisation technique, it was decided to investigate what content of GMA can be incorporated into this copolymer without affecting the morphology of the polyHIPE. GMA was incorporated from 10 to 40 vol. % with respect to the monomer phase. IBOA, TMPTA, surfactant (HB246), photoinitiator concentration and internal phase volume remained constant throughout. The volume of EHA was adjusted with the amount of GMA added to the emulsion to keep the internal phase volume at 89 % for the total emulsion.

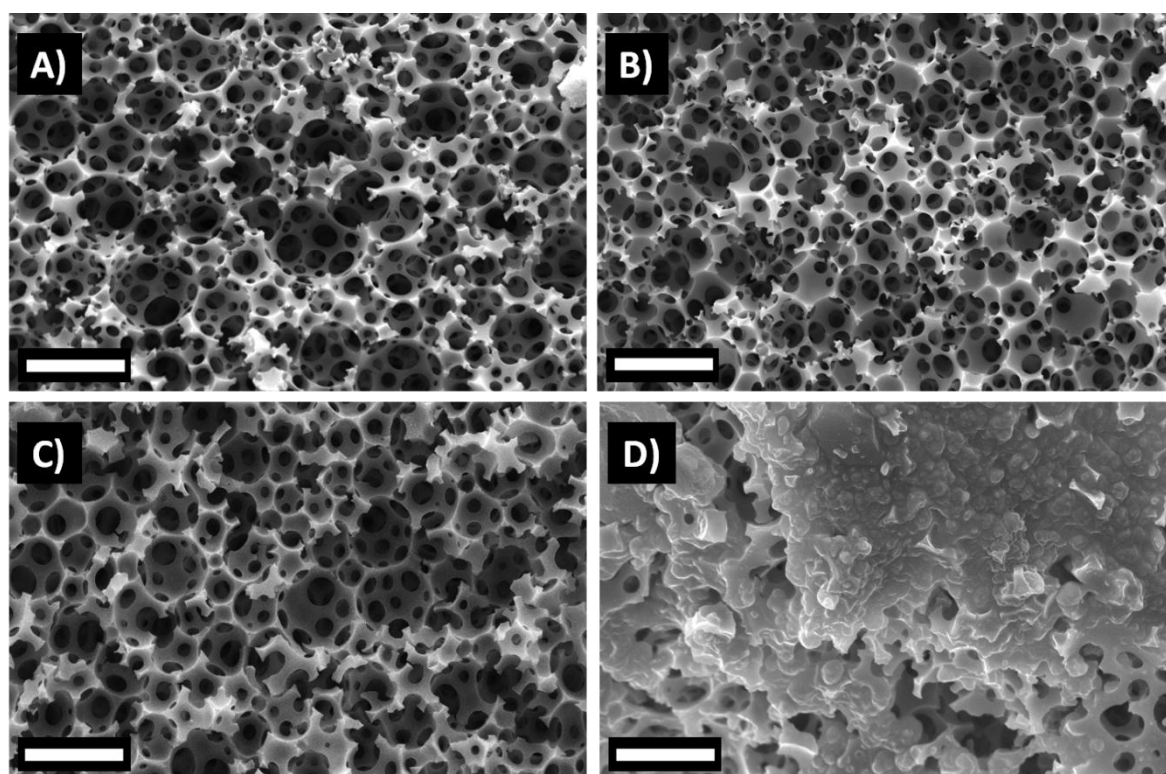


Figure 2:13 – SEM images of varying quantities (10 – 40 % v/v of monomer phase) of GMA incorporated within photopolymerised polyHIPEs, scale bar 20  $\mu\text{m}$  A) 10 % v/v B) 20 % v/v C) 30 % v/v D) 40 %



GMA could be successfully incorporated into the photopolymerised emulsion-templated porous polymer at up to 30 vol. % of the monomer phase with no obvious effect on the morphology of the material (see Figure 2:13 C)). It was observed, however, that with 30 vol. % GMA there was a very small amount of phase inverted o/w polymerised material (SEM not shown). Extensive phase separation was observed when GMA was used at levels above 30 vol. %. Figure 2:13 D) shows that for 40 vol. % GMA there are areas of non-porous polymerised material as a result of phase separation of the HIPE due to the addition of the more hydrophilic GMA monomer.

#### ***2.4.2.3 Preparation of Novel Photopolymerised Hydrophilic GMA-based PolyHIPE Materials***

Attempts were made to prepare hydrophilic functional emulsion-templated materials. This was investigated as a potential material for the immobilization of enzymes. Hydrophilicity of a material can affect the activity of immobilized enzymes[34-36]. Hydrophobic reactive materials are suitable for the immobilization of lipase[34], and in contrast hydrophilic materials have been observed to be suitable for acrylase enzymes[37].

Photopolymerisation of the HIPE was investigated to take advantage of the fast cure of the emulsion which has been observed in this thesis and in other reports to allow preparation of the polyHIPE materials from relatively unstable HIPEs[9, 10]. Initial investigation into the preparation of these materials focused on the polymerisation of o/w HIPEs, as the monomer phase consist of hydrophilic monomers. Preparation of PEG/EGDMA with the photoinitiation system of diphenyl(2,4,6-



trimethylbenzoyl)phosphine oxide and 2-hydroxy-2-methylpropiophenone, following the method by Fernandez-Trillo,[38] was unsuccessful due to the immiscibility of the photoinitiator with the internal phase (light mineral oil). An oil with a low aromatic content was successful in dissolving the photoinitiator and allowed the preparation of a o/w HIPE, however the emulsion did not polymerise, due to the absorption of UV light from the aromatic groups present within the oil.

2-Hydroxy-4'-(2-hydroxyethoxy)-2-methylpropiophenone, a water soluble photoinitiator used for the photopolymerisation of cryogels[39] and hydrogels[40-42], was investigated as a possible alternative to the oil soluble photoinitiator system used previously. PEG/EGDMA HIPE with light mineral oil as the internal phase and 2-hydroxy-4'-(2-hydroxyethoxy)-2-methylpropiophenone dissolved within the continuous phase prior to emulsification resulted in extensive phase separation of the HIPE. Polymerisation of an acrylic acid-based HIPE with toluene as the internal phase using the hydrophilic photoinitiator following the method by Krajnc *et al.*[5], was also unsuccessful due to the absorbance of the UV light from the aromatic solution used for the internal phase. However, the preparation of a resin containing the exact formulation used for the continuous phase of this HIPE was successful.

Following from the preparation of this resin and the polymerisation of the PEG/EGDMA HIPE, it was investigated if GMA-based polyHIPEs could be prepared with this aqueous soluble photoinitiator. The photoinitiator was dissolved within the aqueous phase (0.79 wt. % w/v of the aqueous phase, and 7.5 wt. % w/w of monomer phase) prior to emulsification. Figure 2:14 shows that a typical open void highly porous morphology typical of polyHIPE materials[2] can be prepared with the locus of the photoinitiation

within the aqueous phase. Overall this shows that it is possible to polymerise HIPEs with this initiator, although problems arise for the preparation of functional hydrophilic materials via an o/w HIPE, due to either emulsion instability or the absorbance of UV light from aromatic solvents used as internal phase. It can be envisaged that o/w HIPEs containing (meth)acrylates within the continuous phase could be photopolymerised with the use of this aqueous photoinitiator if a non-aromatic internal phase could be used that can stabilise these emulsions.

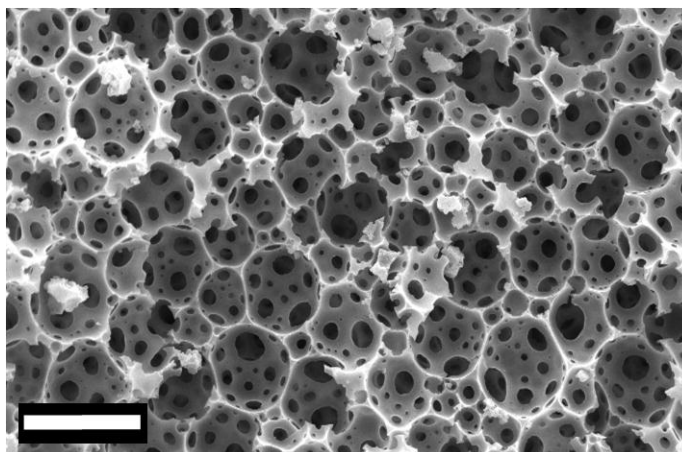


Figure 2:14 – SEM image of GMA-based polyHIPE polymerised with an aqueous soluble photoinitiator (2-hydroxy-4'-(2-hydroxyethoxy)-2-methylpropiophenone), scale bar 20  $\mu\text{m}$

Composite materials can be prepared from HIPEs, if both the continuous and internal phases contain monomers and are subsequently polymerised[43, 44]. Following from this it was investigated as to whether it could be possible to prepare a hydrophilic functional photopolymerised w/o polyHIPE material. It was decided to prepare a HIPE, consisting of a continuous phase identical to the GMA-based materials prepared previously within this thesis, and an internal phase that consisted of UHP water and a hydrophilic monomer. Poly(ethylene glycol) methacrylate ( $M_n \sim 360$ ) (PEG-MA) was the monomer of choice for

use within the internal phase of a w/o HIPE to assess if hydrophilic emulsion-templated porous polymers could be prepared.

Initial attempts concentrated on preparation of these emulsions with the PEG-MA dissolved within the aqueous phase prior to emulsification. However, this resulted in the formation of an unstable HIPE. It was observed that a stable viscous HIPE could be prepared via the preparation of a homogenous w/o HIPE, followed by the addition of PEG-MA (5 mL, 71 % v/v with respect to monomers used in the continuous phase) to the emulsion (total emulsion volume prior to addition of PEG-MA was 70.7 mL). Photopolymerisation of this emulsion after one minute following the addition of PEG-MA resulted in a highly porous emulsion-templated porous polymer (see Figure 2:15).

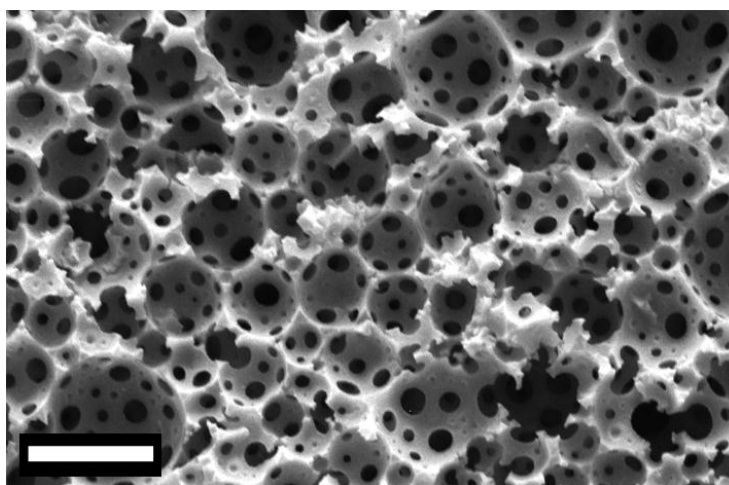


Figure 2:15 - SEM image of PEG-MA w/o polyHIPE, scale bar 20  $\mu\text{m}$

Analogous polyHIPE materials without the addition of PEG-MA were used as a control in wetting studies to assess the hydrophilicity of the PEG-MA polyHIPE materials. Monoliths were cut into 200  $\mu\text{m}$  thick membranes and were assessed by the addition of a drop of UHP water onto each polyHIPE material at the same time. Water contact angle measurements on these materials were not recorded as the materials are porous and the

water droplet penetrates the polyHIPE, therefore the contact angle can decrease over time, resulting in unreliable results. As can be seen in Figure 2:16, there is a dramatic increase in the hydrophilicity of the materials prepared with the addition of PEG-MA. The water droplet on the PEG-MA polyHIPE is absorbed into the porous membrane due to capillary action (see right image of Figure 2:16 B)) from the favourable interaction with the hydrophilic surface. These materials could be used for the immobilization of enzymes via the activation of the hydroxyl group of the PEG chain with N,N'-carbonyldiimidazole[45] or they could also be used for the preparation of scaffolds for cell culture[46-48]. To the best of the author's knowledge, this is the first example of hydrophilic polyHIPE material being prepared via this technique of preparing a homogeneous w/o HIPE prior to the addition of a hydrophilic monomer. Again this material emphasises the benefit of using the rapid cure of the emulsion to prepare novel functional materials.

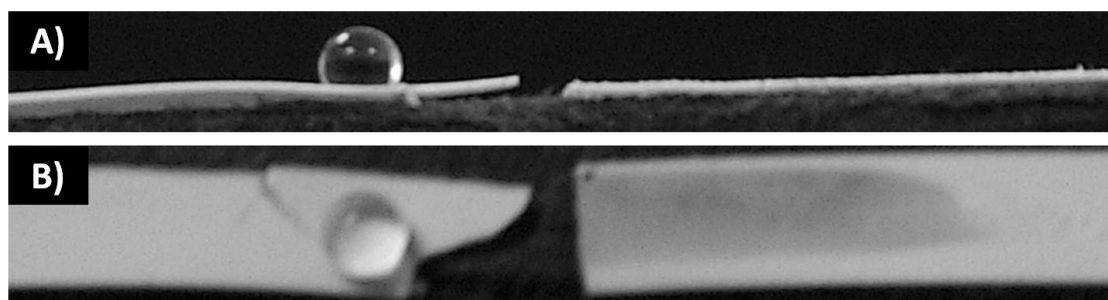


Figure 2:16 – Comparison in hydrophilicity of two 200  $\mu\text{m}$  thick polyHIPE materials. 20  $\mu\text{l}$  of ultra high purity water was placed on the materials A) Side-on picture of hydrophobic PHP1 polyHIPE (left) and a PHP1 polyHIPE with the addition of PEG-MA (right) B) Top view of hydrophobic PHP1 polyHIPE (left) and a PHP1 polyHIPE with the addition of PEG-MA (right)

PolyHIPEs typically have low specific surface areas resulting from their macroporous morphology[2]. This disadvantage has been addressed by grafting functional polymers onto the polyHIPE surface, via ATRP[22]. The novel preparation of PEG-MA polyHIPEs

prepared above could be thought of as grafting of PEG-MA chains from a polyHIPE surface. This is due to the polymerisation and crosslinking of the continuous phase, but also the polymerisation of PEG-MA within the aqueous phase. It would be interesting to observe if other hydrophilic functional monomers, such as acrylic acid or acylamide could be incorporated into polyHIPEs via this same technique. These materials need to be fully characterised, particularly by mercury porosimetry to observe the effect of increasing the PEG-MA content on porosity. In addition to this it needs to be investigated if the material's hydrophilicity decreases over time, which would indicate that the PEG-MA is adsorbed rather than covalently bound to the polyHIPE surface.

#### ***2.4.2.4 Preparation of a Photopolymerized GMA-based PolyHIPE Monolith for Continuous Flow Applications***

The overall goal for the use of these materials was as a continuous flow system. Following from the successful preparation of a GMA-based highly porous emulsion-templated polymer (see above, section 2.4.2.1 and 2.4.2.2), it was decided to utilize the photopolymerisation to prepare a monolithic material for a continuous flow set-up. This was envisaged via the functionalization of glass columns with methacrylate groups for the covalent attachment of the monolith to the column wall.

Functionalization of the glass column (see Figure 2:17) followed the procedure from Uttamlal *et al.*[16], whereby the glass surface was 'activated' with hydroxyl groups, which is subsequently reacted with 3-(trimethoxysilyl)propyl methacrylate to produce a methacrylated functionalized glass column.

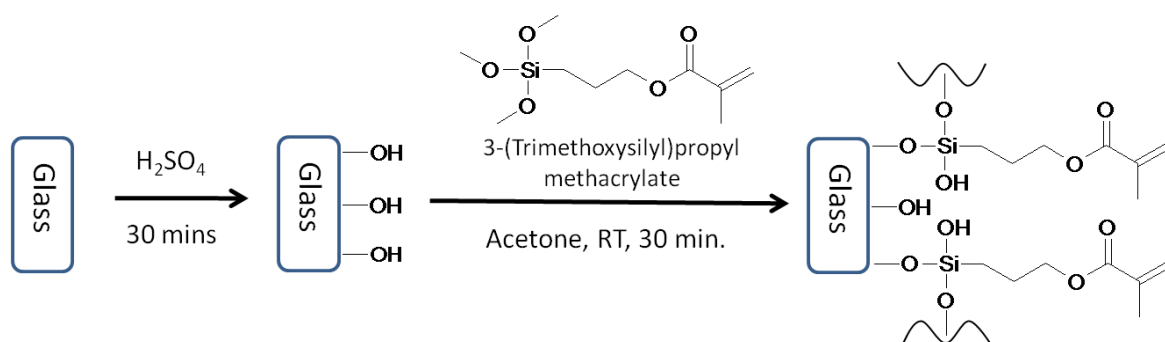


Figure 2:17 – Schematic showing the functionalization of the Omnifit glass columns with methacrylate groups

Functional highly porous monolithic columns were produced via the photopolymerisation of a HIPE within the methacrylate functionalized glass, as is schematically represented in Figure 2:18. These columns were then subsequently connected to a pump and washed with copious amounts of isopropanol and water, to remove the internal phase of the emulsion and surfactant. Monoliths were also photopolymerised within an unfunctionalized glass column to compare with functionalized columns, all such monoliths were ‘pushed’ out of the column when subjected to a water flow rate of 1 mL/min. SEM analysis (see Figure 2:19, 2:20, 2:21, 2:22 and 2:23) of the morphology of the monoliths within the columns was achieved via the functionalization of 10 mm cross-sections of glass columns with subsequent polymerisation of HIPE within these cross-sections.



monolith to dry overnight and repeating the experiment, it was observed that the dye did channel between the monolith and the column, indicating that the monolith was removed from the column on drying.

ESEM and SEM analysis of the column and monolith was undertaken to give a greater understanding of the morphology of the monolith, as well as the covalent attachment of the monolith to the glass column. Sections (1 cm in length) of glass column were used for the analysis. ESEM analysis showed that the PHP9 monolith was attached to the column wall and that the surface of the monolith had a polymerised 'skin' albeit it was porous (see Figure 2:19). SEM analysis showed that PHP9 monoliths shrank due to the vacuum process, which is necessary for the deposition of gold on the polymer surface for SEM (see Figure 2:20 A)). Although the monolith shrank on drying, polyHIPE was clearly visible on the surface of the glass column (see Figure 2:20 C)), indicating the covalent attachment of the polymer to the glass surface was successful.

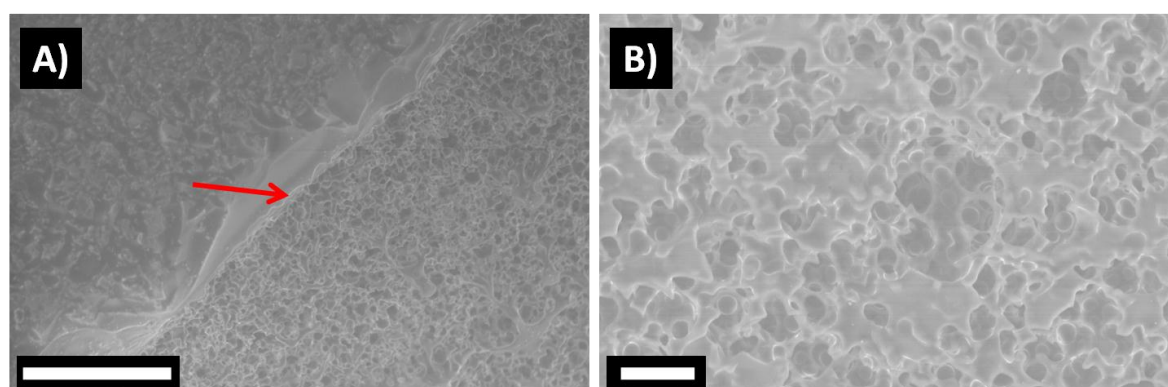


Figure 2:19 – ESEM images of photopolymerised GMA-based HPLC columns (PHP9) A) Red arrow is showing the interface between the glass and monolith, scale bar 100 µm B) Scale bar 20 µm

GMA/EGDMA HIPEs were also photopolymerised into monolithic columns (PHP12) to compare with PHP1, PHP8 and PHP9. SEM analysis showed that GMA/EGDMA monolith



did not shrink due to the rigidity of this material (see Figure 2:21 A)). The surface of both PHP9 and GMA/EGDMA monoliths were observed to have a polymerised 'skin', see Figure 2:20 B) and Figure 2:21 B). Other photopolymerised GMA/EGDMA polyHIPE materials, prepared by Gokmen *et al.* have been obtained without this polymerised 'skin', although these materials were beads and rods prepared from the addition of a HIPE to a continuous phase of a 3 wt. % PVA solution[10]. One explanation for the polymerised 'skin' on the surface of the monolithic materials could be the retardation of the polymerisation due to oxygen diffusion into the emulsion at the emulsion surface. This retardation effect has been observed to produce a 'matted' surface (in contact with air) for some photoinitiated coatings[30]. Beneath this surface layer of polymerised 'skin' a typical emulsion-templated porous polymer morphology is observed for both monoliths (see Figure 2:20 B) and 2:21 C)). Overall, PHP1, PHP8, PHP9 and GMA/EGDMA monoliths (PHP12) are not suitable for use as continuous flow systems. Both suffer from a polymerised surface skin, especially GMA/EGDMA monoliths, possible due to the lower activity of methacrylates compared to acrylates and the use of a di-acrylate rather than a tri-acrylate crosslinker. The drawback of the PHP1, PHP8 and PHP9 monoliths is the shrinkage of the material on drying, and the relatively high back pressures, possibly due to the compression of the material under flow or the polymerised 'skin' on the surface.

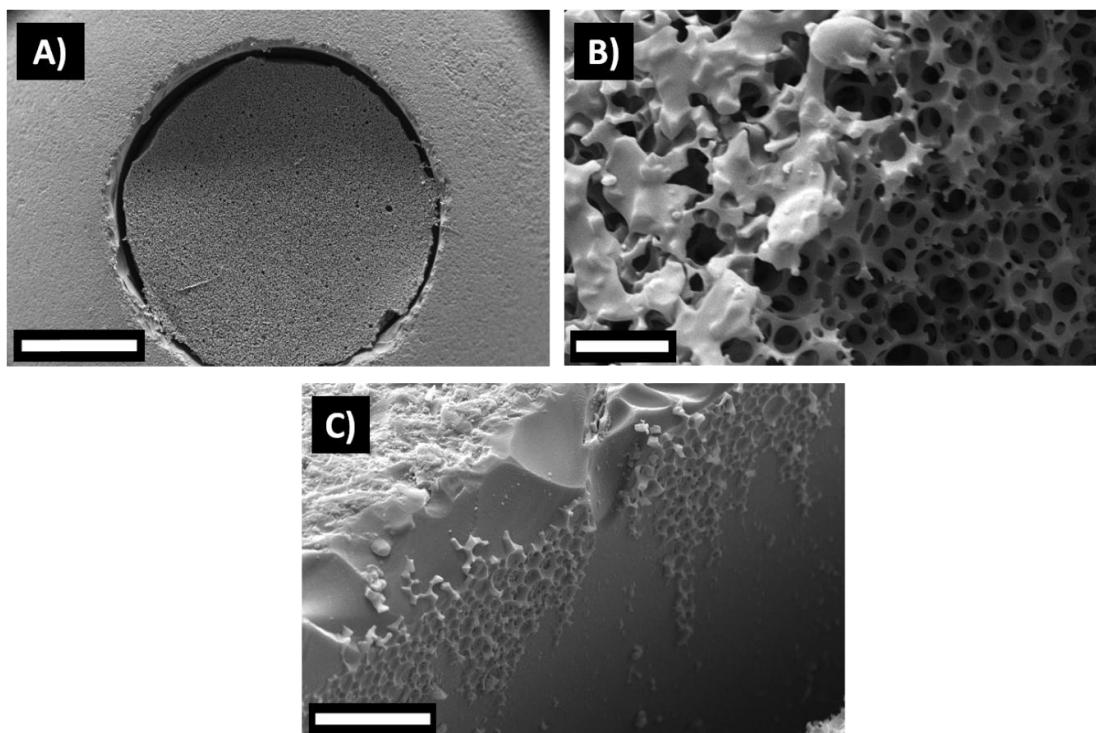


Figure 2:20 – SEM images of photopolymerised GMA-based polyHIPE monolith columns (PHP9). A) Scale bar 1 mm. B) Surface morphology of the monolith, with typical polyHIPE morphology below the surface, scale bar 20  $\mu\text{m}$ . C) PolyHIPE covalently attached to the glass column wall, scale bar 50  $\mu\text{m}$ .

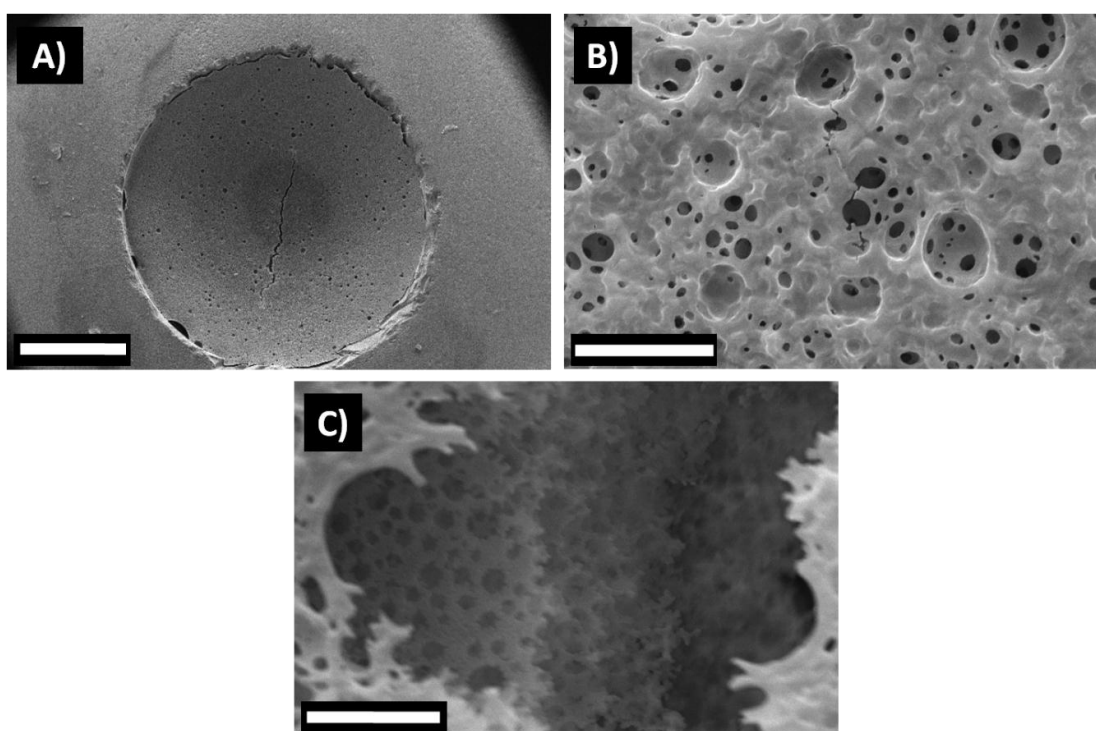


Figure 2:21 – SEM images of photopolymerised GMA/EGDMA HPLC columns (PHP12). A) The glass column with monolith (centre), scale bar 1 mm. B) The surface morphology of the monolith, scale bar 20  $\mu\text{m}$ . C) The internal morphology of the monolith, scale bar 10  $\mu\text{m}$ .

A fully acrylate, NASI-based polyHIPE, with a penta-/hexa-acrylate crosslinker instead of a tri-acrylate crosslinker (following the procedure from Pierre *et al.*[9]) was investigated for the formation of the monolith (PHP11). Increasing the functionality of the monomers used in photopolymerised materials, for example from a di- to a tri-acrylate, is known to increase the polymerisation rate, crosslink density and rigidity of the materials [29]. As the PHP9 monolith was shown to shrink on drying, increasing the functionality of the crosslinker in these NASI-based materials could be beneficial. In addition, a fully acrylate system will have a faster rate of polymerisation (than methacrylates) and, in combination with the increased functionality of the monomer mixture and polymerisation rate, this could be beneficial in reducing the oxygen retardation of polymerisation at the surface of the monolith.

NASI-based photopolymerised monoliths were analysed by SEM and it was shown that the material was rigid, was attached to the glass column and did not shrink on drying (see Figure 2:22 A)) In addition, the surface of the material did not have a polymerised 'skin', but instead had a typical polyHIPE morphology (see Figure 2:22 B)). Back pressures with water at a flow rate of 10 mL/min were recorded to be on average 24 bar with the column attached to the HPLC system and 8 bar without, which is comparable to PHP8, although the NASI-based monolith was not observed to crack after extensive use. These back pressures are considerably lower than the more elastomeric PHP1 and PHP9 monoliths produced and are indicative of a more rigid monolithic material.

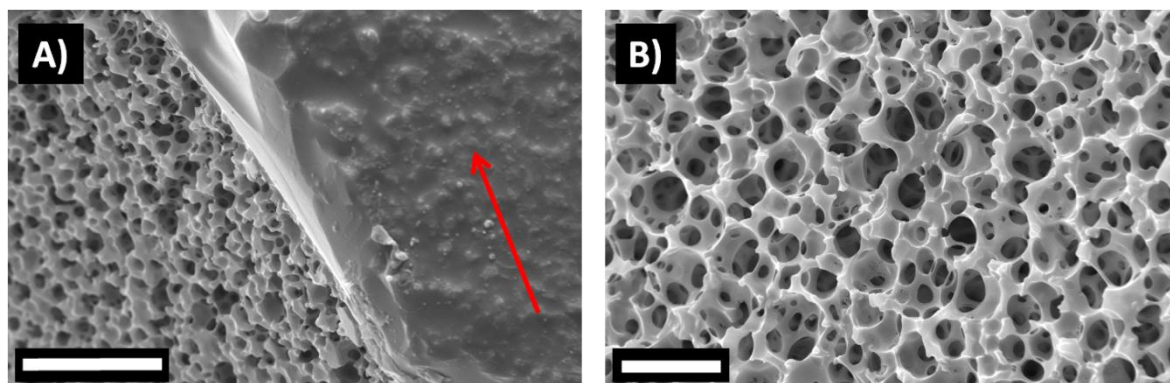


Figure 2:22 – SEM images of NASI-based photopolymerised HPLC columns (PHP11) A) Red arrow indicates to the glass column, scale bar 50  $\mu\text{m}$ . B) The surface morphology of the monolith, scale bar 20  $\mu\text{m}$ .

Following the successful preparation of NASI-based monoliths, GMA-based monoliths were prepared with 20 vol. % (v/v of monomer phase) GMA, following the same principle of increasing the functionality of the crosslinker from a tri-acrylate (trimethylolpropane triacrylate) to a penta-/hexa-acrylate (dipentaerythritol penta-/hexa-acrylate). SEM analysis of PHP10 photopolymerised monoliths showed similarities to the NASI-based monolith in terms of surface morphology and attachment to the glass column (see Figure 2:23). This indicates that the increase in polymerisation rate from the increased monomer functionality of the crosslinker has a greater effect than the addition of a slower reactive monomer (GMA) and also that the increase in functionality of the crosslinker did increase the rigidity of GMA-based monolithic materials.

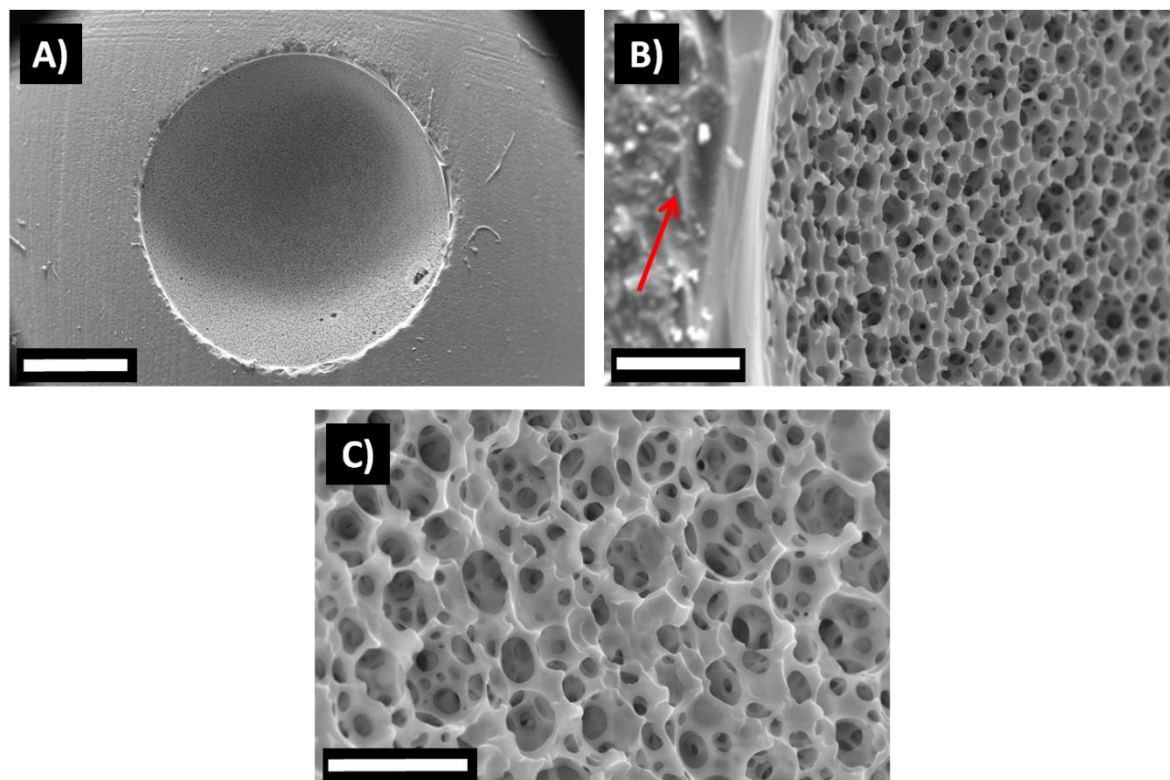


Figure 2:23 –SEM images of PHP10 photopolymerised monolithic columns. A) The glass column with monolith (centre), scale bar 1 mm. B) Red arrow indicates the glass column, scale bar 50  $\mu\text{m}$ . C) The surface morphology of the GMA-based monolithic column, scale bar 20  $\mu\text{m}$ .

Back pressures with UHP water at a flow rate of 10 mL/min for PHP10 monoliths were 16 bar with the column and monolith attached to the HPLC solvent delivery system and 15 bar without. These back pressures are considerably lower than is observed for the GMA-based monoliths prepared with only the tri-acrylate crosslinker (see above, section 2.4.2.4). This is attributed to the lack of polymerised skin on the surface of the monolith as well as the increased rigidity of the material. The pressure drop across these materials is also considerably lower than GMA-co-EGDMA thermally polymerised monoliths, which could be possibly due to the inhomogeneous morphology of these thermally polymerised materials[8]. Continuous use of the column did not result in any obvious cracks within the

monolith as has been observed with other photopolymerised GMA-based monoliths (see above, section 2.4.2.4).

Investigation into how the pressure drop across this monolithic column is affected by the flowrate would be beneficial into elucidating the permeability of the monolith (from the Darcy equation, see Equation 2:2)[49], as well as if, indeed, the pressure drop is linear with flow rate, indicating a rigid monolithic material with a laminar flow regime[8]. It has been observed for photopolymerised GMA-based polyHIPE materials that the degree of interconnectivity increases on increasing the internal phase volume of the emulsions (see section 2.4.2.1). It would also be interesting to observe the effect of changing the porosity of these materials on the pressure drop and permeability.

$$\Delta P = \frac{\eta u_F L}{B_0} \quad \text{Equation 2:2}$$

Where,  $\Delta P$  represents the change in pressure,  $\eta$ , the viscosity of the mobile phase,  $L$ , the length of the column,  $u_F$ , the superficial velocity and  $B_0$ , permeability.

Overall, open-void highly porous GMA-based photopolymerised materials have been successfully prepared and implemented as a continuous flow-through system, which could be used potentially as a flow-through enzyme bioreactor[50].

#### **2.4.2.5 Preparation of Photopolymerised GMA-co-TRIM PolyHIPE Material**

GMA-co-EGDMA polyHIPE materials could not be prepared by photopolymerisation within the PTFE moulds used for the formation of mixed methacrylate/acrylate materials (see section 2.4.2.1 and 2.4.2.2), although it was



observed that GMA-co-EGDMA HIPE could be polymerised within a 10 mm diameter glass column (see section 2.4.2.4). The monoliths were rigid although the morphology was inhomogeneous. Following from the observed increase in rigidity and improved surface morphology of GMA-based materials prepared with a penta-/hexa-acrylate crosslinker rather than a tri-acrylate crosslinker, which was attributed to the increase in the crosslink density and polymerisation rate of the emulsion[29] respectively (see section 2.4.2.4), it was investigated if increasing the crosslinker functionality from a di-methacrylate to a tri-methacrylate would have any effect on the morphology of the polymerised materials. GMA/TRIM photopolymerised emulsion-templated porous polymers could be successfully prepared within 35 mm diameter PTFE moulds (which were used for the mixed methacrylate and acrylate system), in a matter of minutes. Figure 2:24 shows the morphology of a GMA/TRIM photopolymerised polyHIPE material. As can be seen, an open-void morphology of micro-sized voids with micro-sized interconnecting windows is obtained, a marked difference to the inhomeogenous mainly close-void morphology of thermally polymerised GMA/EGDMA polyHIPEs prepared within this thesis and by Krajnc *et al.*[7, 8]. This is attributed to the rapid cure of the emulsion, effectively 'locking' the emulsion morphology prior to the extensive Ostwald ripening that can occur in the slower thermal polymerisation techniques.

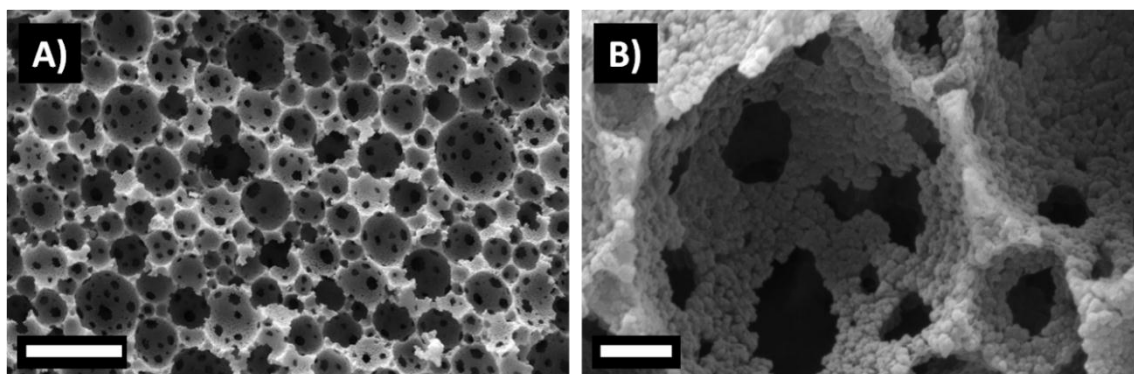


Figure 2:24 – SEM images of GMA – TRIM photopolymerised polyHIPE A) Scale bar 20  $\mu\text{m}$  B) Scale bar 2  $\mu\text{m}$

Commercially available GMA/EGDMA monoliths, namely CIM (Convective Interaction Media) columns from BIA Separations have been used as enzyme reactors[51] and for the separation of biomolecules[52]. CIM disks comprise a high content ( $>4 \text{ mmol/g}$ ) of epoxy groups, low surface areas ( $\sim 7 \text{ m}^2/\text{g}$ ), a porosity of  $\sim 64 \%$  and through-pores of around  $1.5 \mu\text{m}$ , which allows the transfer of relatively large biomolecules through the monolith[20, 53]. They can be prepared up to a diameter of 25 mm without affecting the distribution of pore sizes across the monolith due to heat transfer during this bulk polymerisation process[20]. In comparison, photopolymerised GMA/TRIM polyHIPEs comprise of a high content ( $4.8 \text{ mmol/g}$ ) of epoxy groups, surface area of  $9.9 \text{ m}^2/\text{g}$  (measured by BET analysis), higher porosity of  $80 \%$  and have interconnecting windows of the order of a few micrometres. In addition, polyHIPEs are observed to have fewer problems of heat transfer during polymerisation[54] and large polyHIPEs, with an internal diameter mould of  $14 \text{ cm} \times 4.5 \text{ cm}$  for thermally polymerised styrene/divinyl benzene polyHIPEs can be prepared[55]. GMA/TRIM monoliths have been successfully prepared with diameters up to 35 mm, although analysis of the interconnective window diameter distribution across this monolith needs to be undertaken, via mercury intrusion



porosimetry analysis. Overall, photopolymerised GMA/TRIM polyHIPE monoliths have advantages over commercially available products that are currently used as enzyme reactors and for bioseparations.

## 2.5 Conclusion

In conclusion, photopolymerised GMA-based emulsion-templated porous polymers with open-void and typical polyHIPE morphologies have been successfully prepared. Porosities and void sizes of these materials are 73 – 95 %, and 9.6 – 17.4  $\mu\text{m}$  respectively. Photopolymerisation of the HIPE within a 35 mm length PTFE mould allowed for the characterisation of these materials via mercury intrusion porosimetry. Average window size increased from 0.6 to 4.7  $\mu\text{m}$  and the degree of interconnectivity from 0.07 to 0.37 on increasing the nominal porosity of the material from 73 to 89 %. Calculated porosities were within 2 % of the nominal porosities showing these photopolymerised materials are templated directly from their respected emulsions, similar to thermally initiated polyHIPEs. Photoinitiation proved to have several advantages over the thermal initiation of HIPEs, namely the polymerisation of monomers without the need to remove inhibitors and rapid cure of the emulsion, resulting in a dual effect of i) dramatically reducing the preparation time for these materials and ii) the ability to prepare functional polyHIPEs from more unstable HIPEs. GMA could be incorporated up to 30 volume % with respect to the monomer phase without affecting the morphology of the polyHIPE. FTIR analysis showed the presence of vibrational bands at 908 and 856  $\text{cm}^{-1}$ , characteristic of epoxy groups indicating that these materials could be functionalized post-polymerisation.

GMA-based photopolymerised polyHIPEs were then developed for the preparation of highly porous rigid monolithic rods for continuous flow applications. This was achieved through the surface functionalization of a borosilicate glass chromatography column with 3-(trimethoxysilyl)propyl methacrylate and the *in situ* polymerisation of a GMA-based HIPE. The functionality of the crosslinker used had a dramatic effect on the rigidity and surface morphology of the monolith prepared. Only with the crosslinker dipentaerythritol penta-/hexa-acrylate was a rigid, GMA-based monolith produced with a monolith surface morphology that was typical of a polyHIPE. These GMA-based photopolymerised polyHIPEs could be used for covalent enzyme immobilization and as a continuous-flow bioreactor.

## 2.6 Bibliography

1. Hainey P, Huxham IM, Rowatt B, Sherrington DC, and Tetley L. *Macromolecules* 1991;24(1):117-121.
2. Cameron NR. *Polymer* 2005;46(5):1439-1449.
3. Stefanec D and Krajnc P. *React Funct Polym* 2005;65(1-2):37-45.
4. Barbetta A, Cameron NR, and Cooper SJ. *Chem Commun* 2000(3):221-222.
5. Krajnc P, Stefanec D, and Pulko I. *Macromol Rapid Commun* 2005;26(16):1289-1293.
6. Krajnc P, Stefanec D, Brown JF, and Cameron NR. *J Polym Sci Pol Chem* 2005;43(2):296-303.
7. Krajnc P, Leber N, Stefanec D, Kontrec S, and Podgornik A. *J Chromatogr A* 2005;1065(1):69-73.
8. Junkar I, Koloini T, Krajnc P, Nemec D, Podgornik A, and Strancar A. *J Chromatogr A* 2007;1144(1):48-54.
9. Pierre SJ, Thies JC, Dureault A, Cameron NR, van Hest JCM, Carette N, Michon T, and Weberskirch R. *Adv Mater* 2006;18(14):1822-1826.
10. Gokmen MT, Van Camp W, Colver PJ, Bon SAF, and Du Prez FE. *Macromolecules* 2009;42(23):9289-9294.
11. Peters EC, Svec F, and Freché JMJ. *Adv Mater* 1999;11(14):1169-1181.
12. Gauthier MA, Gibson MI, and Klok HA. *Angew Chem Int Edit* 2009;48(1):48-58.
13. Svec F and Huber CG. *Anal Chem* 2006;78(7):2100-2107.
14. Tunc Y, Golgelioglu C, Hasirci N, Ulubayram K, and Tuncel A. *J Chromatogr A* 2010;1217(10):1654-1659.
15. Vlakh EG and Tennikova TB. *J Sep Sci* 2007;30(17):2801-2813.
16. Uttamlal M, Sloan WD, and Millar D. *Polym Int* 2002;51(11):1198-1206.

17. Brunauer S, Emmett PH, and Teller E. J Am Chem Soc 1938;60:309-319.
18. <http://rsbweb.nih.gov/ij/>. Last accessed on 3/3/2011.
19. Barbetta A and Cameron NR. Macromolecules 2004;37(9):3188-3201.
20. Svec F, Tennikova TB, and Deyl Z. monolithic materials preparation, properties and applications. Journal of Chromatography Library, vol. 67: Elsevier, 2003.
21. Barbetta A, Dentini M, Leandri L, Ferraris G, Coletta A, and Bernabei M. React Funct Polym 2009;69(9):724-736.
22. Cummins D, Wyman P, Duxbury CJ, Thies J, Koning CE, and Heise A. Chem Mater 2007;19(22):5285-5292.
23. Kimmins SD and Cameron NR. Adv Funct Mater 2011;21:211-225
24. Kovacic S, Stefanec D, and Krajnc P. Macromolecules 2007;40(22):8056-8060.
25. Carnachan RJ, Bokhari M, Przyborski SA, and Cameron NR. Soft Matter 2006;2(7):608-616.
26. Cameron NR and Sherrington DC. Macromolecules 1997;30(19):5860-5869.
27. Lee JY, Tan B, and Cooper AI. Macromolecules 2007;40(6):1955-1961.
28. Cameron NR, Sherrington DC, Albiston L, and Gregory DP. Colloid Polym Sci 1996;274(6):592-595.
29. Decker C. Prog Polym Sci 1996;21(4):593-650.
30. Decker C. Macromol Rapid Commun 2002;23(18):1067-1093.
31. Decker C. Polym Int 1998;45(2):133-141.
32. Decker C, Zahouily K, Decker D, Nguyen T, and Viet T. Polymer 2001;42(18):7551-7560.
33. Yan QZ, Lu GD, Zhang WF, Ma XH, and Ge CC. Adv Funct Mater 2007;17:3355-3362.

34. Cao L. Carrier-bound Immobilized Enzymes, Principles, Applications and Design: Wiley-VCH, 2005.
35. Cao LQ. Curr Opin Chem Biol 2005;9(2):217-226.
36. Cao LQ, van Langen L, and Sheldon RA. Curr Opin Chem Biol 2003;14(4):387-394.
37. Torres-Bacete J, Arroyo M, Torres-Guzman R, de la Mata I, Castillon MP, and Acebal C. J Chem Technol Biotechnol 2001;76(5):525-528.
38. Fernandez-Trillo F, van Hest JCM, Thies JC, Michon T, Weberskirch R, and Cameron NR. Adv Mater 2009;21(1):55-59.
39. Kahveci MU, Beyazkilic Z, and Yagci Y. J Polym Sci Pol Chem 2010;48(22):4989-4994.
40. Williams CG, Malik AN, Kim TK, Manson PN, and Elisseeff JH. Biomaterials 2005;26(11):1211-1218.
41. Zhong C, Wu J, Reinhart-King CA, and Chu CC. Acta Biomaterialia 2010;6(10):3908-3918.
42. He B, Wan E, and Chan-Park MB. Chem Mater 2006;18(17):3946-3955.
43. Ruckenstein E. Concentrated emulsion polymerization. Polymer Synthesis / Polymer Catalysis, vol. 127. Berlin 33: Springer-Verlag Berlin, 1997. pp. 1-58.
44. Ruckenstein E and Li HQ. Polym Compos 1997;18(3):320-331.
45. Hermanson GT. Bioconjugate Techniques. Elsevier, 2008. pp. 946-947.
46. Bokhari M, Carnachan RJ, Cameron NR, and Przyborski SA. J Anat 2007;211(4):567-576.
47. Bokhari M, Carnachan R, Cameron N, and Przyborski S. J Anat 2008;212(1):92-92.

48. Bokhari M, Carnachan RJ, Przyborski SA, and Cameron NR. *J Mater Chem* 2007;17(38):4088-4094.
49. Guiochon G. *J Chromatogr A* 2007;1168:101-168.
50. Krenkova J and Svec F. *J Sep Sci* 2009;32(5-6):706-718.
51. Bencina M, Babic J, and Podgornik A. *J Chromatogr A* 2007;1144(1):135-142.
52. Barut M, Podgornik A, Brne P, and Strancar A. *J Sep Sci* 2005;28(15):1876-1892.
53. Mihelic I, Nemec DA, Podgornik A, and Koloini T. *J Chromatogr A* 2005;1065(1):59-67.
54. Svec F. *J Chromatogr A* 2010;1217(6):902-924.
55. Cameron NR, Sherrington DC, Ando I, and Kurosu H. *J Mater Chem* 1996;6(5):719-726.

## 3 Functionalization of GMA-based Emulsion-Templated Porous Polymers

### 3.1 Introduction

Functional polymers can be prepared by the homopolymerization, copolymerization or grafting of a reactive monomer [1-3]. Poly(glycidyl methacrylate) is an important functional polymer mainly from its ability to react with a range of nucleophiles[1]. This has led to the preparation of porous GMA polymers for use as bioreactors or for protein separation [4-6]. PolyHIPE materials have advantageous properties in comparison with other monolithic porous materials mainly higher porosity and the ability to prepare large monoliths [7-9]. This has led recently to interest in preparing GMA-based polyHIPE materials. These materials have been prepared by the copolymerisation of GMA with EGDMA and DVB via thermal or photopolymerisation as well as the grafting of GMA from a polyHIPE surface [10-15]. These materials have been observed to be capable of functionalization with nucleophiles and they have been used for protein separation[12].

The work described here focuses on the preparation of functional GMA polyHIPEs for covalent enzyme immobilization; the epoxy group of the GMA is required to be available for functionalization. Investigation was undertaken into the functionalization of the GMA polyHIPEs with amine nucleophiles; this was monitored by elemental analysis and X-ray photoelectron spectroscopy (XPS). In addition to this, a bis-amino terminated polyethylene glycol, a hydrophilic homobifunctional linker group was immobilized onto the polyHIPE. This was monitored with XPS,  $^1\text{H}$  high resolution magic angle (HR-MAS) solid

state nuclear magnetic resonance (NMR) spectroscopy, Fmoc number determination, Kaiser test and attachment of a fluorescent probe to assess the possibility of using this group as a spacer group for the attachment of enzymes.

## 3.2 Experimental Section

### 3.2.1 Materials

*O,O'*-Bis(3-aminopropyl)polyethylene glycol (Sigma-Aldrich;  $M_n \sim 1500$ ), tetrahydrofuran (Fisher Scientific, laboratory reagent grade), buffer tablets pH 9.2 (borate) (Fisher Scientific), fluorescein 5(6)-isothiocyanate (Sigma; ~90 %), morpholine (Sigma-Aldrich; ≥99 %), tris(2-aminoethyl)amine (Aldrich; 96 %), 9-fluorenylmethyl chloroformate (Aldrich, 97 %), piperidine (Sigma-Aldrich, 99 %), *N,N*-dimethylformamide (Sigma-Aldrich, ≥ 99.8 %), dichloromethane (Fisher Scientific, analytical grade), chloroform-*d* (Sigma-Aldrich, 99.8 atom % D), ethanol (Fisher Scientific, > 99 % (GLC)), *N,N*-diisopropylethylamine (Sigma-Aldrich, 99.5 %), methanol (Fisher Scientific, HPLC grade), ninhydrin (Sigma, ≥ 99 %) hydrochloric acid (Fisher Scientific, Laboratory grade (~36 %), ethylene glycol dimethacrylate (Aldrich; 98 vol. %), glycidyl methacrylate (Fluka, 97 %), 2-ethylhexyl acrylate (Aldrich; 98 %), Synperonic PEL 121 (triblock copolymer of poly(propylene oxide) and poly(ethylene oxide), with a HLB number of 0.5) (Croda), calcium chloride hexahydrate (Fluka, ≥ 99 %), trimethylolpropane triacrylate (Aldrich, technical grade), Hypermer B246 (triblock copolymer of poly(12-hydroxystearic acid) and poly(ethylene glycol) with a HLB number of 6) (Univar Ltd.), diphenyl(2,4,6-trimethylbenzoyl)phosphine oxide / 2-hydroxy – 2 – methylpropiophenone, blend (Aldrich), were all used as supplied.



### 3.2.2 GMA/EGDMA HIPE preparation and thermal polymerisation

For the preparation of thermally polymerised GMA-based polyHIPE materials see section 2.2.5.

### 3.2.3 Photopolymerised GMA-based polyHIPE preparation

For the preparation of photopolymerised GMA-based polyHIPE materials see section 2.2.2.

### 3.2.4 Functionalisation of GMA-based PolyHIPE materials

#### 3.2.4.1 *O, O'-Bis (3-aminopropyl) polyethylene glycol*

##### 3.2.4.1.1 Thermally polymerised GMA/EGDMA polyHIPE

100 mg (0.48 mmol of epoxy groups<sup>\*</sup>) of powdered GMA/EGDMA thermally polymerised polyHIPE (see section 2.2.5 for preparation) was added to a 30 mL solution of 1.88 g (1.25 mmol) of *O, O'-Bis(3-aminopropyl)polyethylene glycol* in pH 9.2 borate buffer and stirred at room temperature for 24 hours. The polyHIPE material was then washed with ultra high purity water (6 × 50 mL). The polyHIPE material was then freeze dried for 24 hours.

##### 3.2.4.1.2 Photopolymerised GMA-based polyHIPE

200 mg (0.15 mmol of epoxy groups<sup>\*</sup>) of powdered photopolymerised GMA-based polyHIPE (see section 2.2.2 for preparation) was added to 40 mL solution of 1.5 g (1

---

<sup>\*</sup> Assuming all the GMA used to prepare the polyHIPE is available for functionalization.

mmol) of *O,O'*-Bis(3-aminopropyl)polyethylene glycol in tetrahydrofuran (THF) and stirred at room temperature for 24 hours. The polyHIPE material was then washed with THF (3 × 50 mL) followed by ultra high purity water (6 × 50 mL). The polyHIPE material was then freeze dried for 24 hours.

#### 3.2.4.2 *Morpholine and Tris(2-aminoethyl)amine (Trisamine)*

##### 3.2.4.2.1 Method 1

The modification of polyHIPE materials with morpholine and trisamine followed the modification of epoxy-containing polystyrene microspheres with morpholine by Biçak *et al.*[16]. 1.5 g (7.2 mmol of epoxy groups\*) powdered thermally polymerised GMA/EGDMA polyHIPE (for preparation see section 2.2.5) was added to 20 mL of a 50 % (v/v) (115 mmol) morpholine (or (67 mmol) tris(2-aminoethyl)amine) / THF solution and stirred at 0 °C for 10 minutes. The mixture was then stirred for 2 hours at room temperature. Finally the mixture was heated to 80 °C for 10 minutes. The polyHIPE was then filtered and washed with THF (2 × 50 mL), water (2 × 50 mL), ethanol (2 × 10 mL) and diethyl ether (10 mL) and dried *in vacuo* at 55 °C for 24 hours.

##### 3.2.4.2.2 Method 2

1 g (0.77 mmol of epoxy groups\*) powdered photopolymerised GMA-based polyHIPE (PHP1, see Table 2:1 for formulation) was added to 80 mL of a 12.5 % v/v (115 mmol) morpholine (or (67 mmol) trisamine) / THF solution at 0 °C and stirred for 10 minutes. The mixture was then stirred for 2 hours at room temperature. The polyHIPE

was washed with THF (2 × 50 mL), water (2 × 50 mL), ethanol (2 × 10 mL) and diethyl ether (10 mL) and dried *in vacuo* at 55 °C for 24 hours.

#### 3.2.4.2.3 Method 3

1 g (0.77 mmol of epoxy groups<sup>\*</sup>) powdered photopolymerised GMA-based polyHIPE (PHP1, see Table 2:1 for formulation) was added to 80 mL of a 12.5 % v/v (115 mmol) morpholine (or (67 mmol) trisamine) / THF solution at room temperature and stirred for 10 minutes. The mixture was then stirred for 24 hours at reflux. The polyHIPE was washed with THF (2 × 50 mL), water (2 × 50 mL), ethanol (2 × 10 mL) and diethyl ether (10 mL) and dried *in vacuo* at 55°C for 24 hours.

### 3.2.5 Quantification of Amine Loading

#### 3.2.5.1 *O,O'-Bis(3-aminopropyl)polyethylene glycol - Determination of amine loading from Fmoc number determination*

The method for the determination of amine loading followed the method by Badyal *et al.*[17]. *O,O'*-Bis(3-aminopropyl)polyethylene glycol functionalized GMA/EGDMA polyHIPE (30 mg, 0.144 mmol of amine groups<sup>†</sup>), 9-Fluorenylmethyl chloroformate (Fmoc-Cl) (75 mg, 0.3 mmol), *N,N*-diisopropylethylamine (DIPEA) (50 µL, 0.29 mmol) and dichloromethane (1 mL) were loaded into a 10 mL glass vial fitted with a screw cap. The mixture was shaken on a roller shaker for 1.5 hours. The polyHIPE was

---

<sup>†</sup> Assuming all the GMA within the polyHIPE was functionalized with *O,O'*-bis(3-aminopropyl) polyethylene glycol in a one-to-one reaction.

then filtered under reduced pressure and washed with dichloromethane (10 × 5mL) and dried *in vacuo* at 50 °C for 24 hours.

Deprotection of the Fmoc-amine groups involved the addition of 10 mg (0.048 mmol of Fmoc protected amine groups<sup>‡</sup>) of the dried Fmoc-protected polyHIPE to a 5 mL volumetric flask, followed by 400 µL of a 20 % (0.81 mmol) piperidine/*N,N*-dimethylformamide (DMF) solution and shaking for 30 minutes at room temperature. Methanol was then added to the volumetric flask to obtain a 5 mL solution. A portion of the solution (200 µl) was then removed and diluted 25 times with methanol. Absorbance readings of the diluted solution were recorded on a UV-Vis spectrometer at 301 nm (related to the piperidine adduct deprotection product) and 322 nm (background reading). The Fmoc loading was calculated from the Beer-Lambert law (see equation 3:1). The Fmoc procedure was performed in duplicate in order to obtain an average Fmoc number. A normalised Fmoc value is recorded from the value obtained from taking into consideration the molecular weight of the Fmoc group.

$$\text{Loading in mmol g}^{-1} = \left( \frac{\text{UV value}}{7800} \right) \times \text{Dilution} \times \left( \frac{\text{Flask volume (mL)}}{\text{Wt.of sample (g)}} \right)$$

Equation 3:1 Calculation of the loading of Fmoc onto polyHIPE via the absorbance of the piperidine Fmoc adduct.

### 3.2.5.2 Determination of Morpholine Loading

Dried morpholine functionalized polyHIPE material (0.2 g) was added to 5 mL of 0.5 M hydrochloric acid solution and left to stand in the solution overnight. The mixture

<sup>‡</sup> Assuming all the amine groups that are present within the polyHIPE were protected with *O,O'*-bis(3-aminopropyl) polyethylene glycol.

was then filtered and 3 mL of this filtrate was then titrated with a dilute (0.05M) NaOH solution[16].

### 3.2.6 Qualification of Amine Loading

#### 3.2.6.1 Ninhydrin (Kaiser Test[18])

The following qualitative test for the presence of primary amine groups with ninhydrin, so called Kaiser test[18], was adapted from Coin *et al.*[19]. 50 mg of powdered *O,O'*-bis(3-aminopropyl)polyethylene glycol functionalised GMA/EGDMA polyHIPE was added to 1.5 mL of 1.0 mol dm<sup>-3</sup> ninhydrin solution in ethanol. This was stirred at room temperature for 5 minutes and then heated at 70 °C for 15 minutes. The polyHIPE was then washed with five aliquots of 15 mL volumes of ethanol and the polyHIPE was dried *in vacuo* at 55 °C for 24 hours. GMA/EGDMA polyHIPE was used as a control for this ninhydrin reaction.

#### 3.2.6.2 Fluorescein 5(6) – isothiocyanate (FITC)

50 mg of *O,O'*-bis(3-aminopropyl)polyethylene glycol functionalised GMA/EGDMA was added to 10 mL of 26 µmol dm<sup>-3</sup> fluorescein 5(6)-isothiocyanate solution in pH 9.2 borate buffer and was stirred at room temperature for 24 hours in a 20 mL glass vial covered with aluminium foil. The material was then washed with pH 9.2 borate buffer (2 × 50mL) and ethanol (2 × 10 mL) and then dried *in vacuo* at 55 °C for 24 hours. Unfunctionalized (GMA/EGDMA) powdered polyHIPE was used as a control material for analysis purposes. After functionalization with FITC the polyHIPEs were placed under a UV lamp of wavelength 254 nm for visualisation.

### 3.2.7 Instrumental

#### 3.2.7.1 *Fourier Transform Infrared Spectroscopy (FTIR)*

FTIR spectra were acquired on a Nicolet Nexus FTIR spectrometer with STI golden gate. 16 scans were taken for background and for the spectra with a resolution of  $4\text{ cm}^{-1}$ . The spectra were baseline-corrected. The aim of this analysis was to observe the presence of an acrylate carbonyl group ( $1730\text{ cm}^{-1}$ ) and epoxy groups ( $908\text{ cm}^{-1}$ ) of the polyHIPE and any subsequent functionalization of this material.

#### 3.2.7.2 *X-ray Photoelectron Spectroscopy (XPS)*

Samples were prepared as mentioned in section 2.2.5, 3.2.4.1.1 and 3.2.4.2.1. All samples were placed under vacuum at  $50\text{ }^{\circ}\text{C}$  for 24 hours prior to XPS analysis. XPS was run on a Kratos AXIS ULTRA XPS used in FAT (fixed analyser transmission) mode using mono-chromated Al  $K\alpha$  X-ray source ( $1486.6\text{ eV}$ ) operated at  $15\text{ mA}$  emission and  $12\text{ kV}$  anode potential –  $180\text{ W}$ . This was ‘charge corrected’ to C  $1s$  peak at  $285\text{ eV}$ . XPS energy range was calibrated using copper  $2p$ / gold  $4f$  and silver  $3d$  peaks. A wide survey scan and high resolution scan was performed on each sample. The wide angle scan was over all energy ranges that allowed for detection of all elemental photoelectron peaks (i.e.  $1400 - 0\text{ eV}$ , except hydrogen and helium).

XPS analysis was performed by Emily Smith at the open-access Nottingham XPS facility funded by EPSRC grant EP/F019750/01. Casa XPS™ software was used to view data obtained[20].

### 3.2.7.3 Nuclear Magnetic Resonance (NMR) Spectroscopy

All NMR analysis was performed using the facilities at Durham University and subsequent analysis was undertaken using the software Mestrenova©[21].

#### 3.2.7.3.1 *O,O'*-Bis(3-aminopropyl)polyethylene glycol

NMR spectra were acquired on a Varian 400 spectrometer with CDCl<sub>3</sub> as solvent.

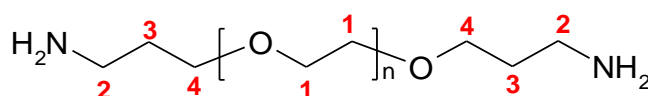


Figure 3:1 – *O,O'*-Bis(3-aminopropyl)polyethylene glycol

<sup>1</sup>H NMR: (400 MHz, CDCl<sub>3</sub>), δ ppm = 3.63 (s, 2H, H-1), 3.54 (t, 2H, J 6.2 Hz, H-4), 2.78 (t, 2H, J 6.8 Hz H-2), 1.72 (m, 2H, H-3)

#### 3.2.7.3.2 High Resolution Magic Angle Spinning (HR-MAS) NMR Spectra of PEGylated PolyHIPE

HR-MAS NMR spectra was carried out on a Varian 500 spectrometer with CDCl<sub>3</sub> as solvent, with the use of a Varian nanoprobe. A few mgs of dried powdered PEGylated polyHIPE was added to the sample tube, prior to the addition of 40 µL of CDCl<sub>3</sub>. PEGylated polyHIPE was allowed to swell within the CDCl<sub>3</sub> for 30 minutes prior to analysis. Samples were spun at the magic angle of ~ 54° at a spin rate of 1000 Hz to reduce signal broadening within the <sup>1</sup>H NMR Spectrum. GMA/EGDMA polyHIPE was also analysed via <sup>1</sup>H HR-MAS NMR spectroscopy as a comparison to the PEGylated material.

Durham University NMR facility carried out both the  $^1\text{H}$  and two dimensional  $^1\text{H}$  correlation spectroscopy (COSY) HR-MAS NMR experiments.

#### **3.2.7.4 *UV-Vis Spectrophotometer***

Varian Cary 100 Spectrophotometer was used for the calculation of Fmoc number and FITC absorbance at Durham University.

#### **3.2.7.5 *Elemental Analysis***

CHN elemental analysis was carried out using an Exeter Analytical Inc. CE-440 Elemental Analysis at Durham University.

#### **3.2.7.6 *Freeze Dryer***

PolyHIPE materials were frozen in liquid nitrogen for 20 minutes prior to being placed in a Christ Alpha 2-4 LSC freeze dryer.

### **3.3 Results and Discussion**

#### **3.3.1 Functionalization of GMA-based PolyHIPEs with Tris(2-aminoethyl)amine and Morpholine**

Tris(2-aminoethyl)amine (trisamine) was used as a model amine for the covalent attachment onto the polyHIPE (see figure 3:2 reaction 2) due to the high content of nitrogen within the molecule that would lead to accurate determination of loading via



elemental analysis. Morpholine was used as a complementary amine to also monitor the loading of the molecule on the polyHIPE material (see Figure 3:2, reaction 1). In addition to elemental analysis of morpholine immobilized polyHIPEs, a back-titration was undertaken, utilizing the basic nature of the morpholine group to also quantify the loading. Both trisamine and morpholine have been used for functional polyHIPEs to assess the level of functionalization post-polymerisation[22-25].

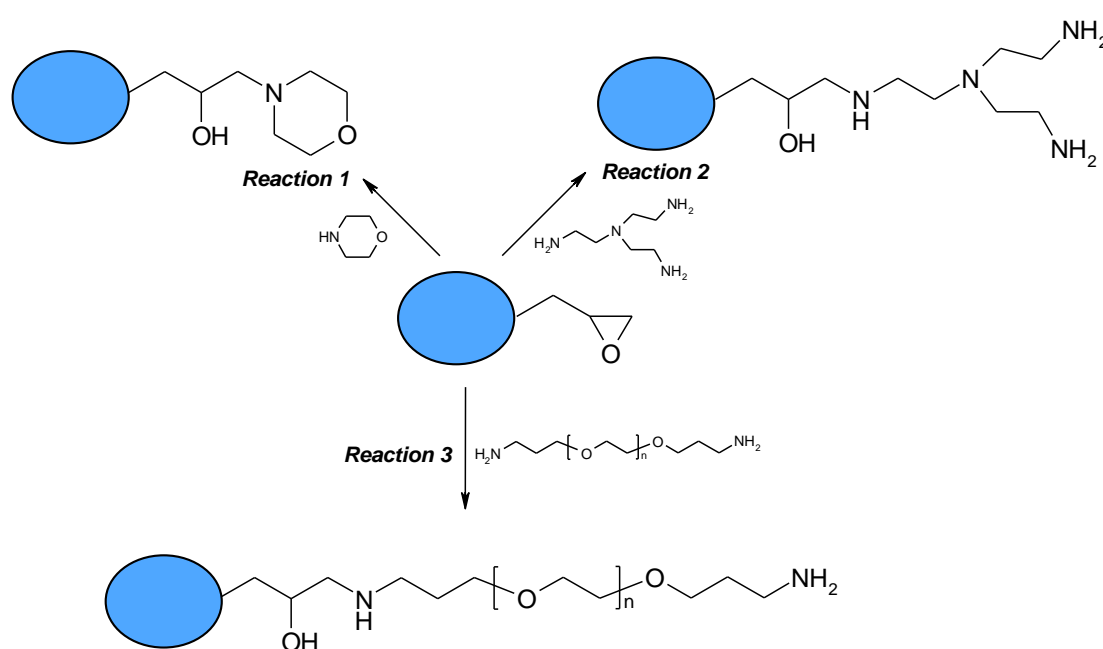


Figure 3:2 – Schematic of the functionalization of GMA-based polyHIPEs with amine nucleophiles. Reaction 1 morpholine, reaction 2 tris(2-aminoethyl) amine and reaction 3 *O,O'*-bis(3-aminopropyl)polyethylene glycol

FTIR analysis of GMA/EGDMA polyHIPE showed the distinctive methacrylate carbonyl peak at  $1724\text{ cm}^{-1}$  and, in addition to this, epoxy peaks were also present at  $906$  and  $845\text{ cm}^{-1}$  (see Figure 3:3 red spectrum). Following the functionalization of the polyHIPE with trisamine for 2 hours at room temperature it was noticeable that there was a dramatic reduction in the intensity of these epoxy peaks due to the ring opening of the epoxy

group of GMA, although these peaks are still present, indicating that there are residual epoxy groups after the functionalization of the polymer (see Figure 3:3 black spectrum).

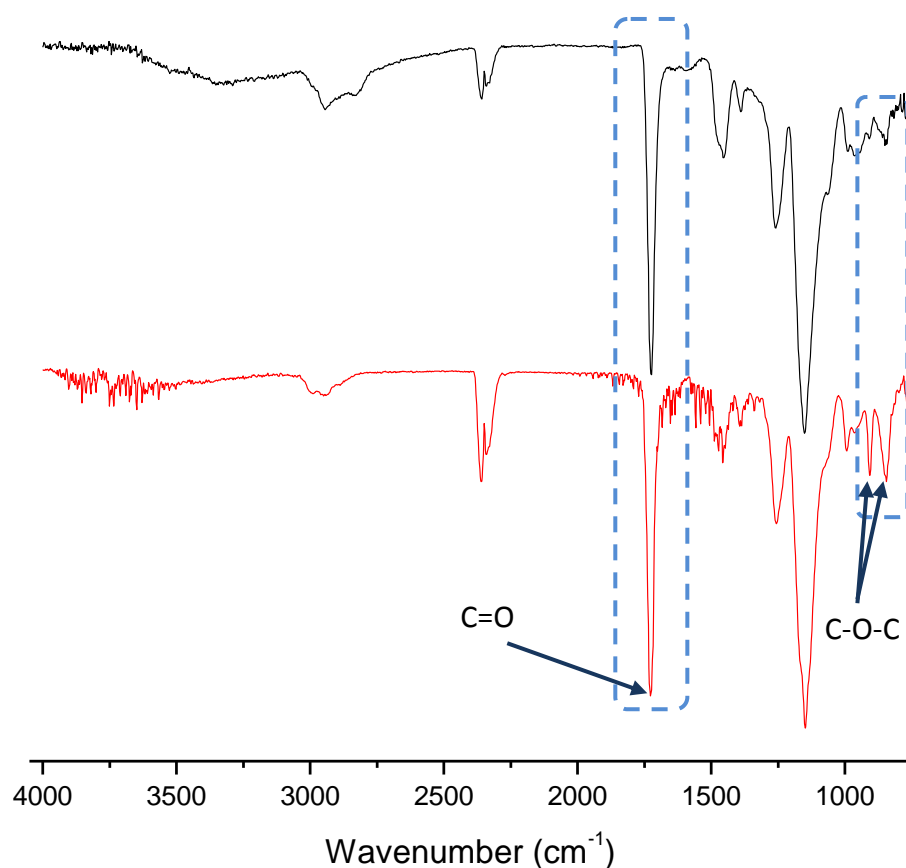


Figure 3:3 – FTIR spectra: above (black) GMA/EGDMA functionalized with tris(2-aminoethyl)amine (see section 4.2.4.1 for reaction), below (red) GMA/EGDMA thermally polymerised polyHIPE

Elemental analysis of the functionalization was undertaken to quantify the loading of trisamine and morpholine on the polyHIPE. Table 3:1 shows the results of reaction of GMA/EGDMA with morpholine and trisamine following the method in section 3.2.4.2.1, i.e. reacting the thermally polymerised polymer with the amine nucleophile for two hours at room temperature. As can be seen both morpholine and trisamine are present on the polyHIPE with 1.71 and 1.18 mmol g<sup>-1</sup>, although this is considerably less than the epoxy

content ( $4.8 \text{ mmol g}^{-1}$ ) of the polyHIPE. Hence, conversions of only 35 and 25 % for morpholine and trisamine respectively were achieved. Back-titration of the morpholine-functionalized polyHIPE was in good agreement with the elemental analysis for the quantification of loading of the molecule onto the polymer, indicating that this is a viable method for the quantification of loading.

Table 3:1 - Reaction 3.2.4.1 GMA/EGDMA thermally polymerised polyHIPE functionalized with morpholine and trisamine

Amine Nucleophile	% N <sup>a</sup>	mmol g <sup>-1</sup>	Conversion (%) <sup>d</sup>
Morpholine	2.40	$1.71^b$ ( $1.68$ ) <sup>c</sup>	36 (35) <sup>c</sup>
Trisamine	6.59	$1.18^b$	25 <sup>e</sup>

a) Results from elemental analysis. b) Calculated from elemental analysis. c) Calculated from titre (see section 3.3.5.2) d) Assumed all epoxy groups from GMA were available for post polymerization functionalization. Conversion was calculated from the ratio of the loading of amine nucleophile to epoxy content of polyHIPE material. e) Assuming no additional crosslinking

Functionalization of photopolymerised GMA-based polyHIPE materials (10 % v/v of monomer phase, PHP1, see Table 2:1 for formulation) was also undertaken. Table 3:2 shows that the epoxy groups are available for post-polymerisation modification, with  $0.32 \text{ mmol g}^{-1}$  (calculated from back-titration) and  $0.40 \text{ mmol g}^{-1}$  (calculated from elemental analysis) loading of morpholine and trisamine respectively (for functionalization see section 3.2.4.2.2). The discrepancy between the loading of morpholine as determined via elemental analysis in comparison to back-titration is attributed to the very low nitrogen content of the recorded elemental analysis (error is  $\sim 0.3 \%$ ). Conversion of the epoxy groups is again low, up to 54 % with trisamine. When the reaction was conducted at reflux for 24 hours (see section 3.2.4.2.3), high conversion of the epoxy group with both morpholine and trisamine was observed, up to 89 % for morpholine (see Table 3:3). Again the difference in values from back-titration and elemental analysis are attributed to the

error in the elemental analysis measurement at such low recorded percentage of nitrogen. Conversion of epoxy groups with trisamine and morpholine is comparable to other functional polyHIPE materials[24, 25]. Hydrolysis of epoxy groups from GMA-based polyHIPEs during polymerisation has been observed by Barbetta *et al.*[13]. The hydrolysis of epoxy groups prior to polymerisation was not investigated, although if epoxy groups did hydrolyse on polymerisation, this could lead to lower reported conversions of epoxy groups.

Table 3:2 - Reaction 3.2.4.2.2 GMA-based photopolymerised polyHIPE (PHP1) functionalized with morpholine and trisamine.

Amine Nucleophile	% N <sup>a</sup>	mmol g <sup>-1</sup>	Conversion (%) <sup>d</sup>
Morpholine	0.10	0.07 <sup>b</sup> (0.32) <sup>c</sup>	9 (43) <sup>c</sup>
Trisamine	2.26	0.40 <sup>b</sup>	54 <sup>e</sup>

a) Results from elemental analysis. b) Calculated from elemental analysis. c) Calculated from titre (see section 3.3.5.2) d) Assumed all epoxy groups from GMA were available for post polymerization functionalization. Conversion was calculated from the ratio of the loading of amine nucleophile to epoxy content of polyHIPE material. e) Assuming no additional crosslinking

Table 3:3 - Reaction 3.2.4.2.3 GMA-based photopolymerised polyHIPE (PHP1) functionalized with morpholine and trisamine.

Amine Nucleophile	% N <sup>a</sup>	mmol g <sup>-1</sup>	Conversion (%) <sup>d</sup>
Morpholine	0.74	0.53 <sup>b</sup> (0.66) <sup>c</sup>	72 (89) <sup>c</sup>
Trisamine	3.44	0.61 <sup>b</sup>	82 <sup>e</sup>

a) Results from elemental analysis. b) Calculated from elemental analysis. c) Calculated from titre (see section 3.2.5.2) d) Assumed all epoxy groups from GMA were available for post polymerization functionalization. Conversion was calculated from the ratio of the loading of amine nucleophile to epoxy content of polyHIPE material. e) Assuming no additional crosslinking

### 3.3.1.1 X-ray Photoelectron Spectroscopy (XPS) of Trisamine Functionalized

#### GMA/EGDMA polyHIPE

X-ray photoelectron spectroscopy (XPS), also known as electron spectroscopy for chemical analysis (ESCA), is a surface sensitive technique that can detect and quantify elements within different chemical environments[26, 27]. It is a technique that has been used extensively for analysis of the top few nanometres (1-10 nm) of polymer substrates[27, 28]. XPS is a result of the photoelectric effect, in which a photon of frequency  $\nu$  can result in the emission of an electron from an atom. The kinetic energy of the emitted electron is related to the binding energy by:

$$E_{\text{kinetic}} = h\nu - E_{\text{binding}} \quad \text{Equation 3:2}$$

where,  $E_{\text{kinetic}}$  is the kinetic energy of the ejected electron,  $h$  is Planck's constant,  $\nu$  is the frequency of the incident radiation and  $E_{\text{binding}}$  is the binding energy.

The technique is used for elemental determination as the energy of the electrons that are ejected from core orbitals is characteristic of atomic species apart from small shifts in energies due to their local environments, which gives rise to the characterisation of atoms within different chemical environments[26, 27, 29].

GMA/EGDMA and functionalized GMA/EGDMA polyHIPEs were analysed by XPS to quantify the amount of nitrogen on the materials' surfaces as well as to determine the chemical environment of atoms at the surface. Figure 3:4 shows typical wide-scan XPS spectra from the surface (1-10 nm[27]) of functionalized and unfunctionalized GMA/EGDMA polyHIPE materials. Using this data Table 3:4 lists the calculated atomic composition of the materials' surfaces relative to the respective C 1S peak in Figure 3:4.

The atomic composition data of the trisamine functionalized GMA/EGDMA polyHIPE surface (see Table 3:4 column B)) in comparison to the unfunctionalized GMA/EGDMA polyHIPE surface (see Table 3:4 column A)) shows a 20 × increase in the N 1s peak. This is indicative of the successful covalent surface functionalization of the polyHIPE with trisamine.

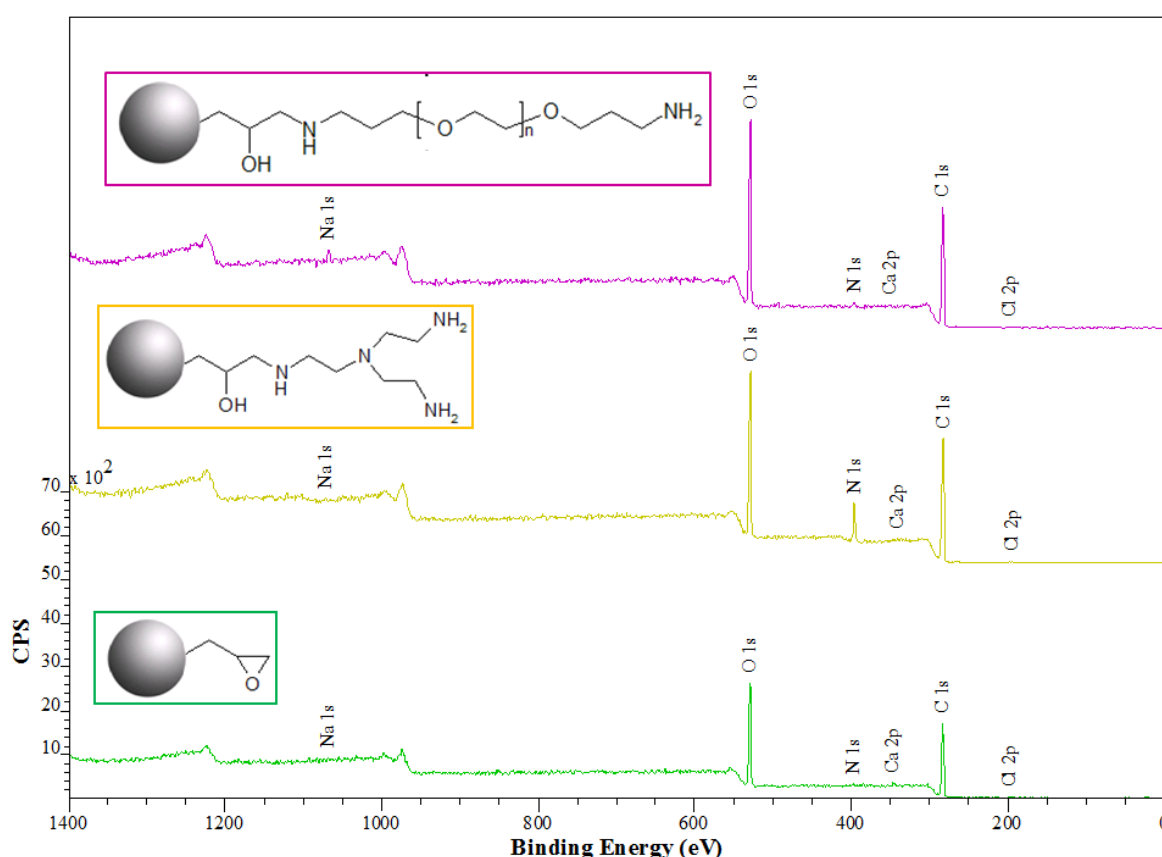


Figure 3:4 - XPS spectra from the surface of polyHIPE materials, above (pink spectrum) *O,O'*-Bis(3-aminopropyl)polyethylene glycol functionalized polyHIPE surface; middle: (yellow spectrum) tris(2-aminoethyl) amine functionalized polyHIPE surface; bottom: (green spectrum) GMA/EGDMA polyHIPE surface. Atoms corresponding to the peaks in the respective spectra have been shown.

Table 3:4 - XPS data showing the averaged relative atomic composition of A) GMA/EGDMA polyHIPE surface, B) tris(2aminoethyl) amine functionalized polyHIPE surface. Three repeats were taken for each sample.

Atomic %	A)	B)
O 1s	$28.8 \pm 0.7$	$24.0 \pm 0.1$
C 1s	$69.6 \pm 0.8$	$67.8 \pm 0.3$
Ca 2p	$0.6 \pm 0.1$	$0.0 \pm 0.0$
Cl 2p	$0.5 \pm 0.1$	$0.2 \pm 0.1$
N 1s	$0.4 \pm 0.7$	$8.0 \pm 0.2$
Na 1s	$0.1 \pm 0.2$	$0.0 \pm 0.1$

Figure 3:5 shows the high-resolution XPS spectrum from a GMA/EGDMA polyHIPE surface showing the C 1S peak. There are three distinct chemical environments corresponding to the C 1S peak. C1 component (285.0 eV, full width half maximum (FWHM) 1.3 eV) is assigned to C-C, C-H and C=C bonds; C2 (286.5 eV, FWHM 1.2 eV) is assigned to hydroxyl and ether bonds (C-OH and C-O-C) and C3 (288.7eV, FWHM 1.4 eV) to carbonyl bonds (C=O)[30, 31]. The chemical shifts of the C1 S peak is representative of polymerised GMA-co-EGDMA and is similar in comparison to high resolution XPS spectrum of C 1S peak of poly(methyl methacrylate)[30].

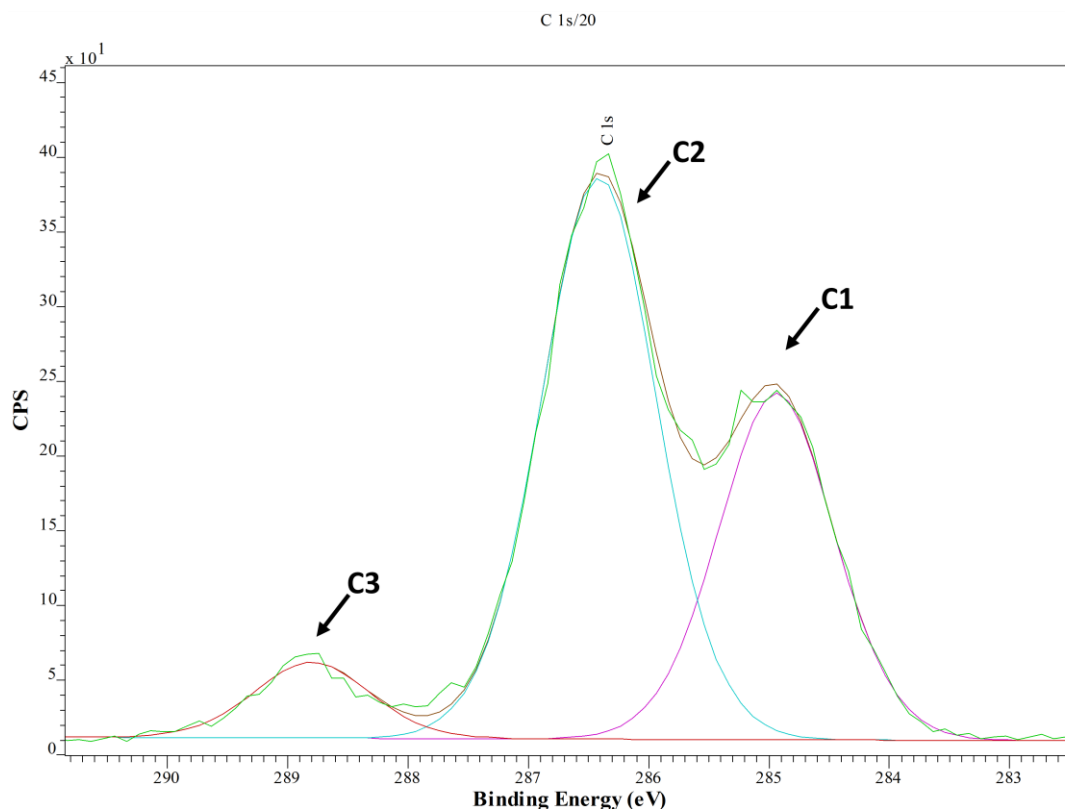


Figure 3:5 – High-resolution XPS spectrum from a GMA/EGDMA polyHIPE surface showing the C 1s peak. Internal structures corresponding to atoms in different chemical environments have been shown. CPS is counts per second.

The N 1s peak in the high-resolution XPS spectrum from the trisamine functionalized polyHIPE surface shows that nitrogen is in two chemical environments, binding energies of 398.9 eV (FWHM 1.3eV) and 401.4 eV (FWHM 1.4 eV) in a ratio of 3:1 was obtained (see Figure 3:6). The two chemical environments correspond to non-protonated ( $\text{NH}_2$ ) and hydrogen bonded / protonated ( $\text{---NH}_2/\text{NH}_3^+$ ) amine species[31, 32]. As trisamine is present in excess compared to the epoxy content of the polyHIPE, it is assumed that the functionalized material would have pendant primary amine groups. The high-resolution XPS spectrum of the N 1s peak is indicative of this assumption. The chemical shift of the N 1s peak complements the wide survey XPS scan in indicating the successful surface functionalization of GMA/EGDMA with trisamine.



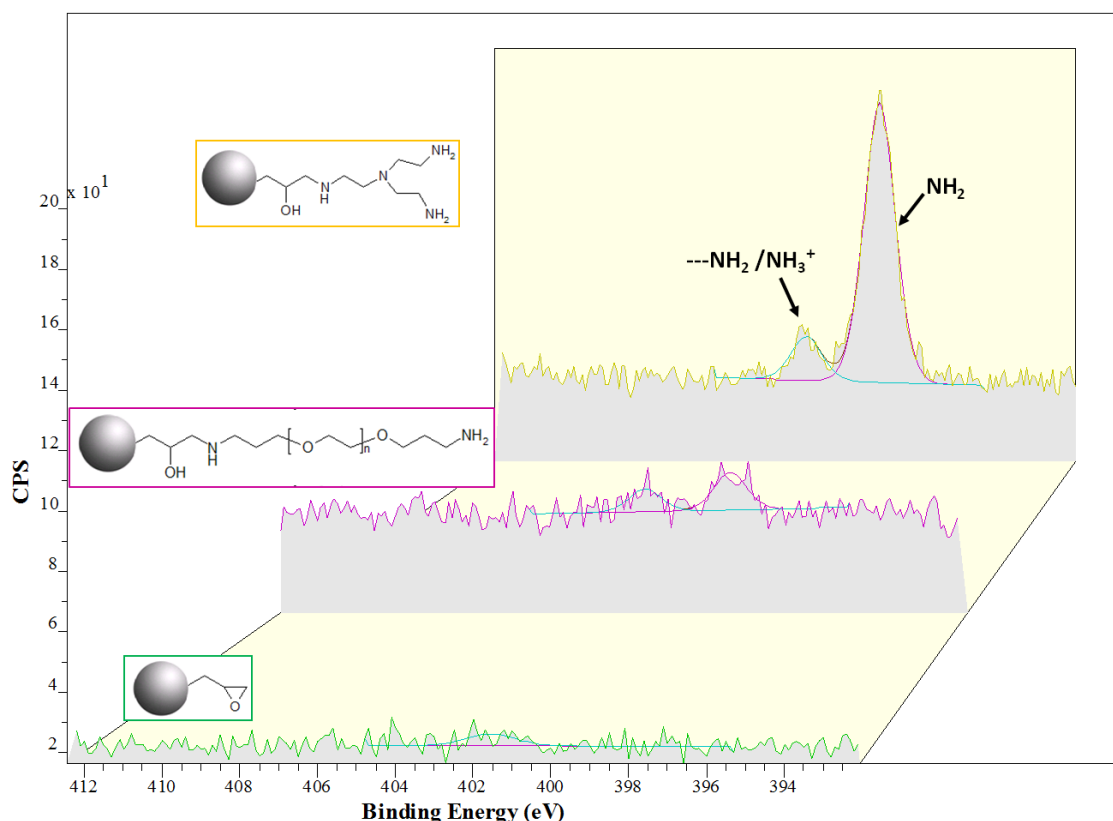


Figure 3:6 - XPS spectrum from surface of polyHIPE materials showing N 1S peak above: (yellow spectra) tris(2-aminoethyl) amine functionalized polyHIPE surface; middle: (pink spectra) *O,O'*-Bis(3-aminopropyl)polyethylene glycol functionalized polyHIPE surface; bottom: (green spectra) GMA/EGDMA polyHIPE surface. Internal structures corresponding to atoms in different chemical environments have been shown.

Overall the XPS, FTIR, elemental analysis and back-titration data for both thermally polymerised and photopolymerised GMA-based materials indicate that this material can be functionalized post-polymerisation with amine nucleophiles up to a conversion of 89 %.

### 3.3.2 Functionalization of GMA-based PolyHIPEs with *O,O'*-Bis (3-aminopropyl) polyethylene glycol

Thermally and photopolymerised GMA-based polyHIPEs were functionalized with the hydrophilic homobifunctional linker group, *O,O'*-bis(3-aminopropyl)polyethylene

glycol (see Figure 3:2, reaction 3). This was investigated because linker groups from insoluble supports are observed to increase the stability of enzymes[33]. It is well known that a high density of PEG on a surface prevents the adhesion of enzymes onto the respective surface, due to the high exclusion volume of the PEG chains in aqueous solution[34]. PEG has also been used for the chemical modification of proteins (called PEGylation)[35, 36] and PEG chains grafted onto poly(styrene-divinylbenzene) beads (called TentaGel™) have been used extensively for solid phase peptide synthesis (SPPS)[37, 38]. In addition to these observations, PEG linker groups from insoluble solid supports have also been used for the covalent attachment of enzymes[33]. This led to the investigation of the functionalization of GMA-based polyHIPEs with this linker group. A range of techniques were used to quantify and qualify the molecules attachment to the polyHIPEs.

#### ***3.3.2.1 Functionalization of PEGylated PolyHIPE with Ninhydrin (Kaiser Test[18])***

The Kaiser test[18] is a qualitative assay that is used extensively in SPPS for the detection of primary amines[19]. The reaction involves the addition of ninhydrin to the compound in question (see Figure 3:7, reaction 1). A positive test (amine groups present) results in the formation of a deep blue coloration in the crosslinked polymer[39]. Advantages of this technique are that it is relatively quick, and small quantities of amine groups can be detected[19].

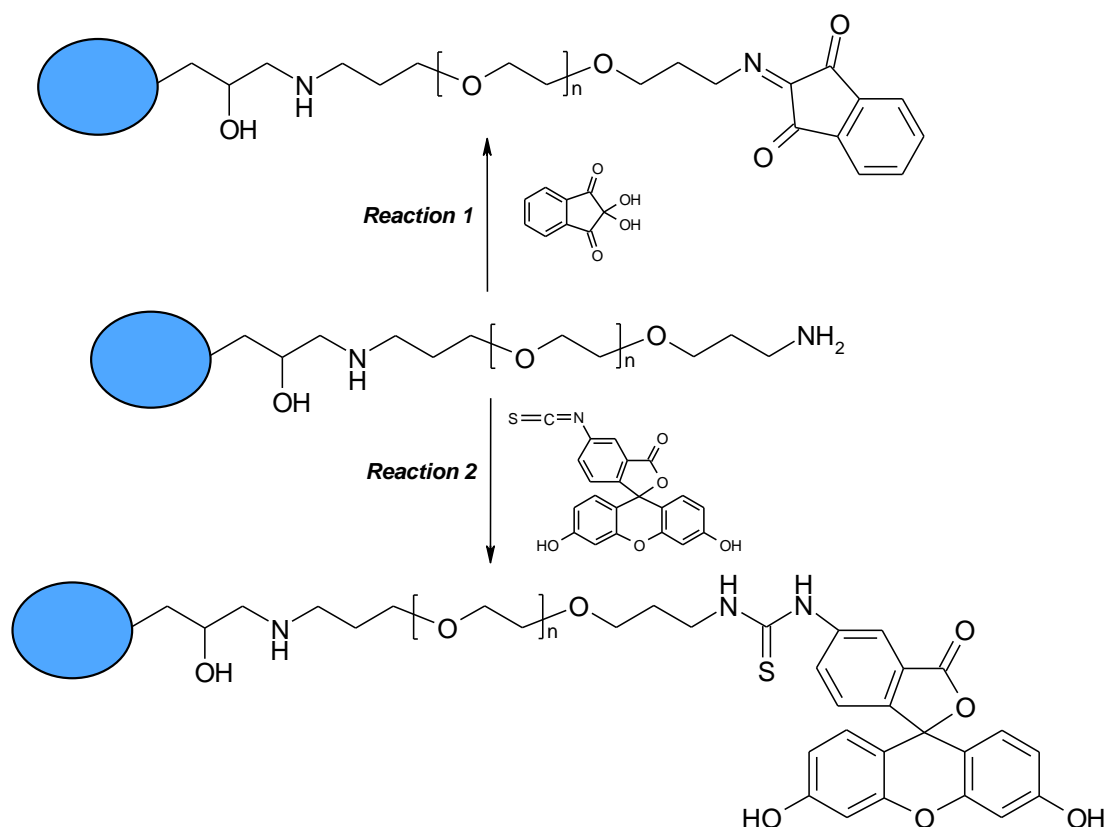


Figure 3:7 – Schematic of functionalization of PEGylated polyHIPE. Reaction 1 with ninhydrin and reaction 2 with fluorescein isothiocyanate

PEGylated GMA/EGDMA polyHIPEs were reacted with ninhydrin and GMA/EGDMA (unfunctionalized) polyHIPEs were used as a control. As can be seen in Figure 3:8 the PEGylated polyHIPE material changed to a deep blue colour on the addition of ninhydrin, indicating the presence of primary amines within the material[19, 39], in comparison to the control which was white in colour indicating that there was no adsorption of ninhydrin on to these polyHIPE materials.

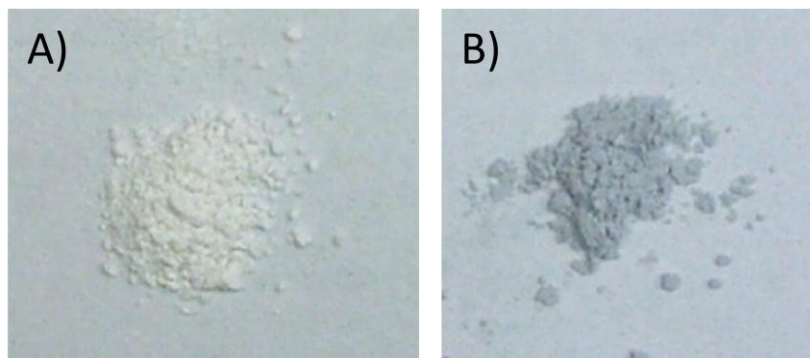


Figure 3:8 – Powdered polyHIPE materials following their reaction with ninhydrin (Kaiser test[18])  
A) GMA/EGDMA polyHIPE (control) B) PEGylated polyHIPE

### 3.3.2.2 Functionalization of PEGylated PolyHIPE with Fluorescein 5(6)-isothiocyanate

Work by Fernandez-Trillo *et al.* showed the possibility of observing the reversible attachment of a fluorescently labelled polymer onto a polyHIPE material by imaging the material on irradiation with UV light[40]. Taking inspiration from this work, a fluorescent probe, fluorescein 5(6)-isothiocyanate (FITC) was reacted with PEGylated polyHIPE to indicate the presence or absence of amine groups within the material. FITC selectively reacts with amine nucleophiles under alkaline conditions forming thiourea bonds (see Figure 3:7, reaction 2)[41].

The powdered PEGylated polyHIPE when reacted with FITC shows the typical green colour on irradiating the sample with UV light, due to the fluorescence of the fluorescein moiety[42] (see Figure 3:9 B)). This is in contrast to the control (GMA/EGDMA polyHIPE), where no emission is observed on irradiating the material with UV light, thus indicating that FITC is covalently attached to the PEG chains on the functionalized polyHIPE. This qualitative result complements the Kaiser test (see above) in showing the successful attachment of the linker group, *O,O'*-bis(3-aminopropyl)polyethylene glycol to the

GMA/EGDMA polyHIPE with pendant primary amine groups that are available for further functionalization.

Attempts were made to quantify the loading of FITC onto the polyHIPE material by observing the absorbance of the FITC pH 9.2 borate buffer solutions on a UV-vis spectrophotometer, after the reaction with PEGylated polyHIPE and with the control. However, these results were deemed to be inaccurate which was attributed to the fast rate of photobleaching of FITC[43, 44].

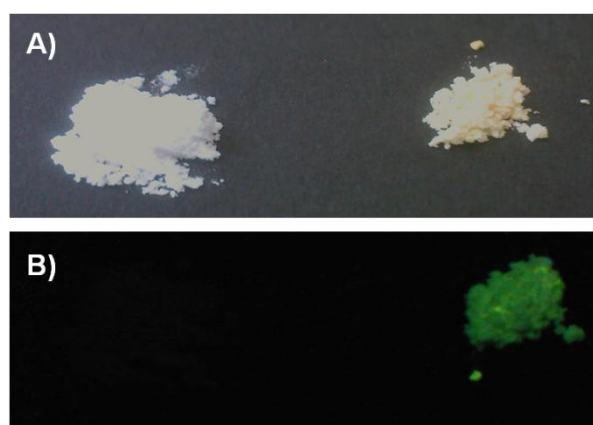


Figure 3:9 – Reaction of powdered thermally polymerised polyHIPE material with FITC A) Image in natural light, left: GMA/EGDMA PolyHIPE (control); right: PEGylated polyHIPE. B) Image taken with samples illuminated under UV light ( $\lambda = 254\text{nm}$ ) left: GMA/EGDMA polyHIPE (control); right: PEGylated polyHIPE

Photopolymerised monolithic GMA-based polyHIPEs (PHP1) were functionalized with *O,O'*-bis(3-aminopropyl)polyethylene glycol, although the reaction was carried out in THF, rather than pH 9.2 borate buffer. PHP1 polyHIPEs are hydrophobic, leading to difficulty in wetting of the material with an aqueous system. Cameron *et al.*[45] observed that for homogeneous functionalization of a monolithic polyHIPE the material must swell within the solvent system used for the reaction. THF was used as the solvent not only because it swelled the polyHIPE, but also it is a 'good' solvent for PEG[46], therefore allowing the

PEG to be in a more expanded conformation, increasing the likelihood of a 1:1 reaction of this linker group (when in excess) with the epoxy groups within the polyHIPE.

FITC was reacted with PEGylated PHP1 in an alkaline aqueous buffer system. As can be seen in Figure 3:10 B) the typical green fluorescent colour of FITC[42] is visible when the material was irradiated under UV light. Green fluorescence was not observed for the control; again, this indicates that the FITC is covalently bound to pendant primary amine groups from the *O,O'*-bis(3-aminopropyl)polyethylene glycol linker group on the monolith.

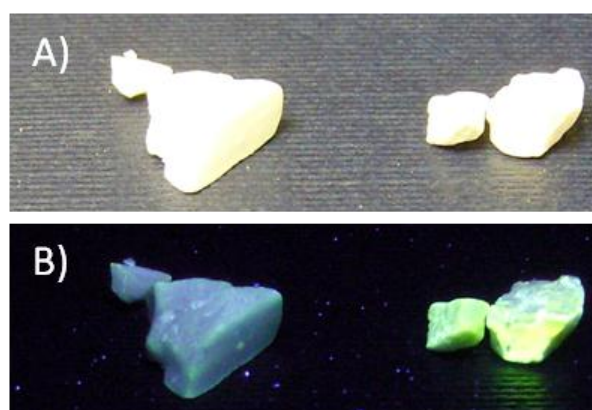


Figure 3:10 - Reaction of monolithic photopolymerized polyHIPE material with FITC A) Image in natural light, left: GMA/EGDMA polyHIPE (control); right: PEGylated polyHIPE. B) Image taken with samples illuminated under UV light ( $\lambda = 254\text{nm}$ ) left: GMA/EGDMA polyHIPE (control); right: PEGylated polyHIPE

### 3.3.2.3 Fmoc Number Determination and Element Analysis (CHN)

Quantification of the loading of *O,O'*-bis(3-aminopropyl)polyethylene glycol on thermally polymerised GMA/EGDMA polyHIPEs was undertaken by i) measuring the loading of Fmoc onto accessible amine groups of the linker group and ii) measuring the percentage of nitrogen from elemental analysis (CHN). PEGylated polyHIPE was protected with 9-fluorenylmethyl chloroformate (Fmoc-Cl) (see Figure 3:11). The polyHIPE was then

deprotected (see Figure 3:11) and the absorbance at 301 nm of the Fmoc piperidine derivative was measured with a UV-vis spectrophotometer. Loading of Fmoc was determined using the Beer-Lambert law (see section 3.2.5.1). Fmoc loading was determined to be  $0.12 \text{ mmol g}^{-1}$ . Elemental analysis (CHN) gives the percentage of nitrogen as 0.31 % within the PEGylated polyHIPE material, thus indicating a loading of  $0.11 \text{ mmol g}^{-1}$  of *O,O'*-bis(3-aminopropyl)polyethylene glycol onto the polyHIPE in good agreement with Fmoc number of  $0.12 \text{ mmol g}^{-1}$ . Overall these results show that the conversion of the epoxy group ( $4.8 \text{ mmol g}^{-1}$ ) is only 2 %. This could possibly be due to the high exclusion volume of the PEG chains in aqueous solution on the polyHIPE material preventing other PEG chains from attaching to adjacent epoxy groups on the materials surface[34].

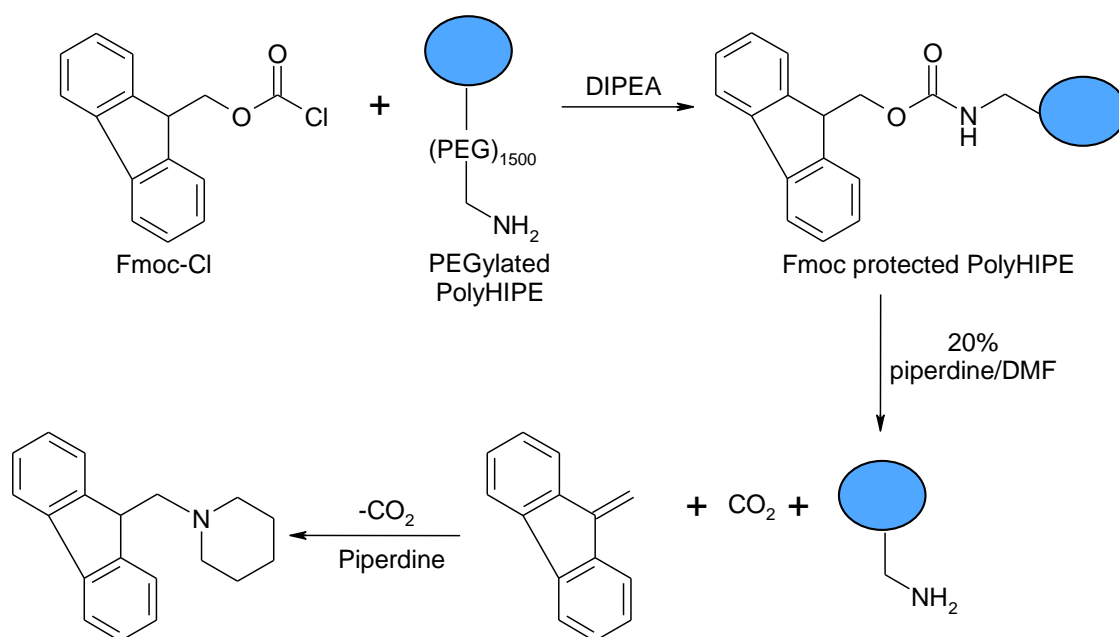


Figure 3:11 – Schematic showing the derivatisation of amine groups on *O,O'*-bis(3-aminopropyl)polyethylene glycol functionalized (PEGylated) GMA/EGDMA polyHIPE powder with 9-fluorenylmethyl chloroformate (Fmoc-Cl), followed by deprotection with 20 % piperidine / N,N-dimethylformamide (DMF) solution to obtain the piperidine adduct, which absorbs at  $\lambda=301 \text{ nm}$  (UV). Blue circles represent bulk GMA/EGDMA polyHIPE matrix. DIPEA = N,N-diisopropylethyamine.

### 3.3.2.4 X-ray Photoelectron Spectroscopy (XPS)

Table 3:5 lists the calculated atomic composition of PEGylated GMA/EGDMA and unfunctionalized GMA/EGDMA polyHIPE surface relative to the respective C 1S peak in the wide survey scan XPS spectra (see Figure 3:4). Analysis of the atomic composition of the *O,O'*-bis(3-aminopropyl)polyethylene glycol functionalized GMA/EGDMA polyHIPE surface (see Table 3:5 column B)) in comparison to the unfunctionalized GMA/EGDMA polyHIPE surface (see Table 3:5 column A)) shows a  $3.5 \times$  increase in the N 1S peak. The low nitrogen content on the PEGylated polyHIPEs surface is suggested to be due to the low loading of bis-amino PEG. Nonetheless, the small increase in nitrogen content is indicative of the covalent surface functionalization of the polyHIPE with PEG.

The high resolution XPS spectrum of the *O,O'*-bis(3-aminopropyl)polyethylene glycol functionalized polyHIPE surface indicates that the N 1S peak is in two chemical environments (399.0 eV and 401.7 eV, see Figure 3:6) corresponding to non-protonated ( $\text{NH}_2$ ) and hydrogen bonded / protonated ( $\text{---NH}_2/\text{NH}_3^+$ ) amine species[31, 32]. This is similar to the observation with trisamine functionalized polyHIPE, although the intensity of the peak is much lower due to the lower loading of PEG.

Table 3:5 - XPS data showing the averaged relative atomic composition of A) GMA/EGDMA polyHIPE surface, B) *O,O'*-bis(3-aminopropyl)polyethylene glycol functionalized polyHIPE surface. Three repeats were taken for each sample.

Atomic %	A)	B)
O 1s	$28.8 \pm 0.7$	$27.3 \pm 0.7$
C 1s	$69.6 \pm 0.8$	$70.7 \pm 1.3$
Ca 2p	$0.6 \pm 0.1$	$0.1 \pm 0.1$
Cl 2p	$0.5 \pm 0.1$	$0.1 \pm 0.1$
N 1s	$0.4 \pm 0.7$	$1.4 \pm 0.1$
Na 1s	$0.1 \pm 0.2$	$0.3 \pm 0.3$



### 3.3.2.5 *High Resolution Magic Angle Spinning (HR-MAS) Nuclear Magnetic Resonance (NMR) Spectroscopy*

Problems are associated with carrying out  $^1\text{H}$  and  $^{13}\text{C}$  NMR spectroscopy of solid samples. This arises mainly from line broadening as a result of dipolar coupling due to the anisotropy of solids[47]. Swelling of a crosslinked polymer in a 'good' solvent and spinning the polymer at a moderate speed of (1-3 kHz) at the magic angle ( $\sim 54^\circ$ ) relative to the magnetic field ( $B_0$ ) is known to reduce significantly the line broadening, resulting in high resolution NMR spectra[48]. This technique is particularly useful for obtaining information about the functionalization of crosslinked polymers, as moieties attached to the surface of insoluble supports are more mobile than the support itself[48, 49]. Hence, when the insoluble support is swollen, the local environment of these moieties approaches that in an isotropic solution, reducing the line broadening of these peaks[47]. Line widths of less than 4 Hz for compounds immobilized onto insoluble supports have been observed with the use of this technique for  $^1\text{H}$  NMR spectra[50, 51].

A crosslinked polymer with pendant PEG chains (TentaGel™) is particularly well suited to HR-MAS NMR spectroscopy due to the high mobility of the PEG chain ends[48, 52, 53]. In addition to this, 2D HR-MAS NMR spectroscopy of solvent swollen gels has also been observed[54], and recently Van Camp *et al.*[55] have shown that cryogels functionalized with PEG can be monitored with 1D and 2D HR-MAS NMR spectroscopy.

Utilizing this technique, the functionalization of GMA/EGDMA polyHIPE material with *O,O'*-bis(3-aminopropyl)polyethylene glycol was monitored. Firstly, a  $^1\text{H}$  NMR spectrum of *O,O'*-bis(3-aminopropyl)polyethylene glycol was taken to determine the chemical shifts of the peaks as well as the splitting pattern, in order to aid characterization of the

functionalized polyHIPE material. As can be seen in Figure 3:12, the  $^1\text{H}$  NMR spectrum of *O,O'*-bis(3-aminopropyl)polyethylene glycol at 400 MHz in  $\text{CDCl}_3$  shows a singlet at 3.63 ppm, corresponding to the glycol protons, and additional triplet and quintet peaks at 2.78 ppm and 1.72 ppm corresponding to  $\text{CH}_2\text{-CH}_2\text{-NH}_2$  and  $\text{CH}_2\text{-CH}_2\text{-NH}_2$  protons on the terminus of either end of the polymer chain.

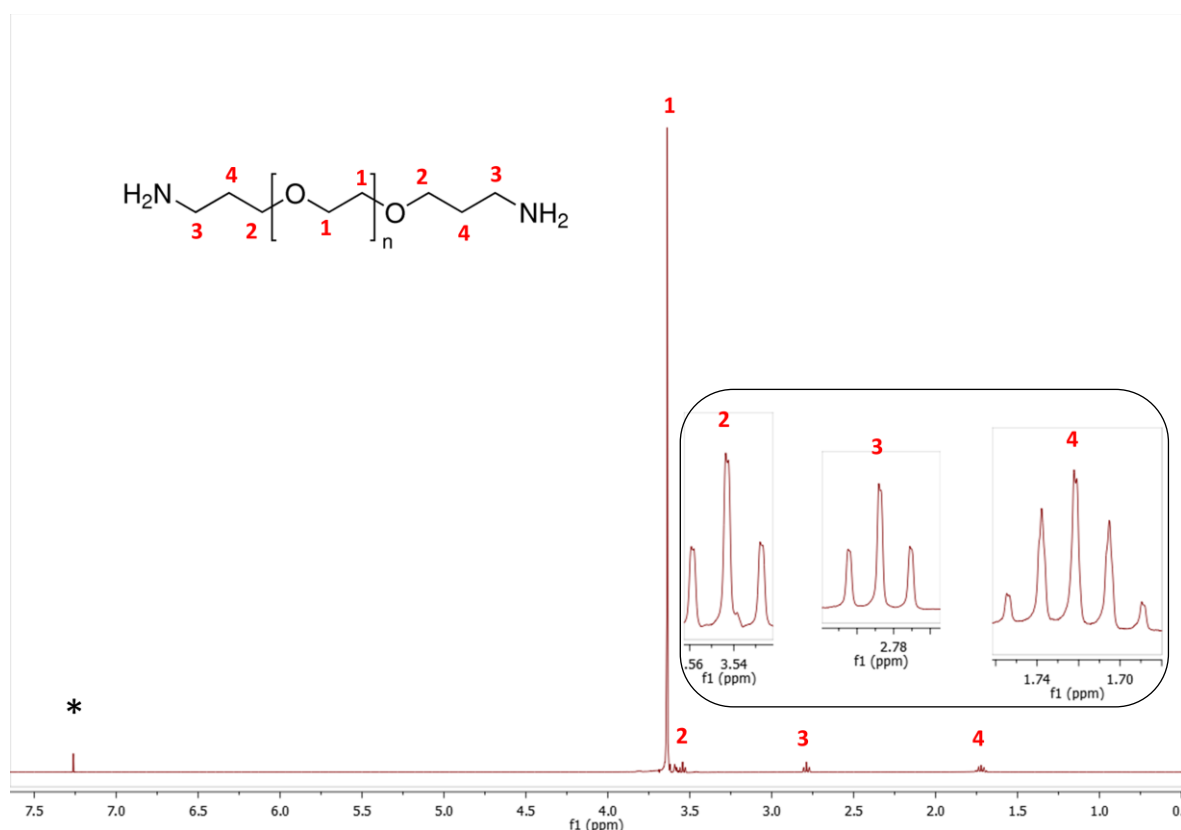


Figure 3:12 –  $^1\text{H}$  NMR spectrum of *O,O'*-bis(3-aminopropyl)polyethylene glycol at 400 MHz in  $\text{CDCl}_3$ . Inset (left) is molecular structure of *O,O'*-bis(3-aminopropyl)polyethylene glycol, numbered to indicate relevant protons that match peaks within the NMR spectrum. Inset (right) is a magnified spectrum of the peaks at 3.54, 2.78 and 1.72 ppm. Solvent peaks are indicated by an \*.

*O,O'*-Bis(3-aminopropyl)polyethylene glycol functionalized GMA/EGDMA polyHIPE was swollen in  $\text{CDCl}_3$  for 30 minutes prior to acquisition of the  $^1\text{H}$  HR-MAS NMR spectrum. As can be seen in Figure 3:13, the polymer backbone is still clearly visible within the spectrum (indicated by \* in Figure 3:13, and blue spectra in Figure 3:14 and 3:15). Peaks

are present from the *O,O'*-bis(3-aminopropyl)polyethylene glycol chain immobilized on the polyHIPE surface; a singlet at 3.64 ppm corresponding to the glycol protons is significantly more intense than the peak corresponding to the polymer backbone, which is indicative of the increase in the local mobility of the PEG chain attached to the polyHIPE surface[47]. In addition to this peak, a triplet at 2.82 ppm corresponding to  $\text{CH}_2\text{-CH}_2\text{-NH}_2$  on the terminus of the PEG chain is also visible within the spectra (see Figure 3:13 inset spectra and Figure 3:15). This peak is not observed in the spectrum of the polymer backbone indicating that it is not due to solvents or any impurities within the material (see Figure 3:15). These peaks are in good agreement with the solution phase NMR spectrum of this linker group except that a quintet is expected to be visible around 1.72 ppm, although a water solvent peak could be masking this peak.

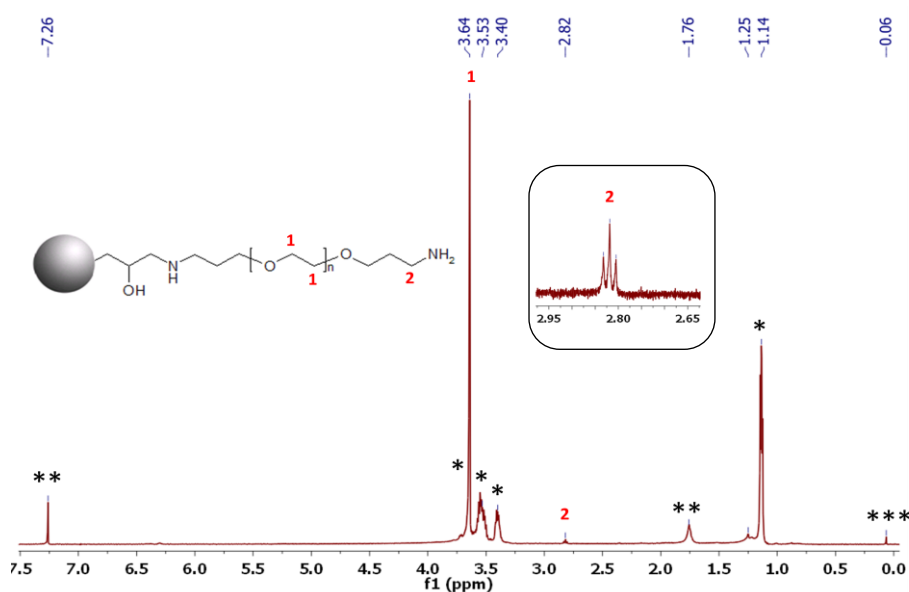


Figure 3:13 -  $^1\text{H}$  HR-MAS NMR spectrum of swollen *O,O'*-bis(3-aminopropyl)polyethylene glycol functionalized (PEGylated) GMA/EGDMA polyHIPE at 500 MHz in  $\text{CDCl}_3$ . Inset (left) is molecular structure of *O,O'*-bis(3-aminopropyl)polyethylene glycol functionalized (PEGylated) GMA/EGDMA polyHIPE, numbered to indicate relevant protons that match peaks in the NMR spectrum. Inset (right) is a magnified spectra of the peak at 2.82 ppm. Peaks corresponding to the polyHIPE matrix are indicated by \*. Solvent peaks are indicated by \*\*. Impurities are indicated \*\*\*.

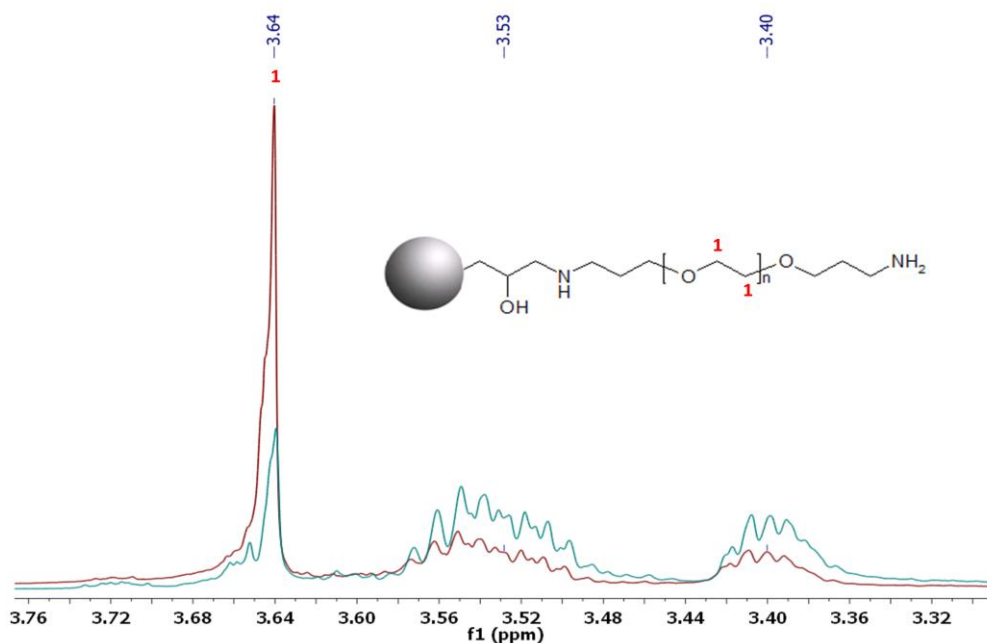


Figure 3:14 -  $^1\text{H}$  HR-MAS NMR spectra of swollen polyHIPEs at 500 MHz in  $\text{CDCl}_3$ . Blue spectrum is GMA/EGDMA polyHIPE. Red spectrum is *O,O'*-bis(3-aminopropyl)polyethylene glycol functionalized (PEGylated) GMA/EGDMA polyHIPE. Inset is molecular structure of *O,O'*-bis(3-aminopropyl)polyethylene glycol functionalized (PEGylated) GMA/EGDMA polyHIPE, numbered to indicate relevant protons that match peaks with the (red) NMR spectrum.

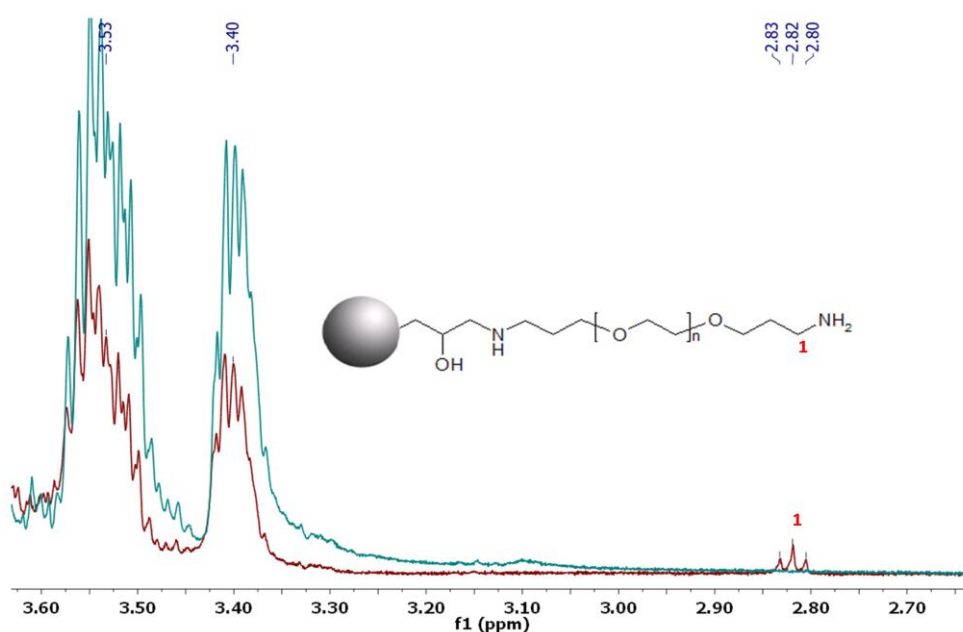


Figure 3:15 -  $^1\text{H}$  HR-MAS NMR spectra of swollen polyHIPEs at 500 MHz in  $\text{CDCl}_3$ . Blue spectra is GMA/EGDMA polyHIPE. Red spectra is *O,O'*-Bis(3-aminopropyl)polyethylene glycol functionalized (PEGylated) GMA/EGDMA polyHIPE. Inset (left) is molecular structure of *O,O'*-Bis(3-aminopropyl)polyethylene glycol functionalized (PEGylated) GMA/EGDMA polyHIPE, numbered to indicate relevant protons that match peaks within the (red) NMR spectra.

2D  $^1\text{H}$  NMR correlation spectroscopy (COSY) HR-MAS NMR spectroscopy was undertaken on solvent swollen PEGylated polyHIPE materials to access the through-bond proton coupling of the PEG chains. As can be seen in Figure 3:16, the peak at 2.82 ppm is coupled to the peak at 1.76 ppm. This indicates that the peak at 1.76 ppm corresponds to  $\text{CH}_2\text{-CH}_2\text{-NH}_2$  on the terminus of the functionalized PEG chain, which is masked in the 1D NMR spectrum by the water solvent peak. As far as can be determined this is the first example of the successful application of 1D and 2D  $^1\text{H}$  HR-MAS NMR spectroscopy for the assessment of the functionalization of polyHIPE materials.

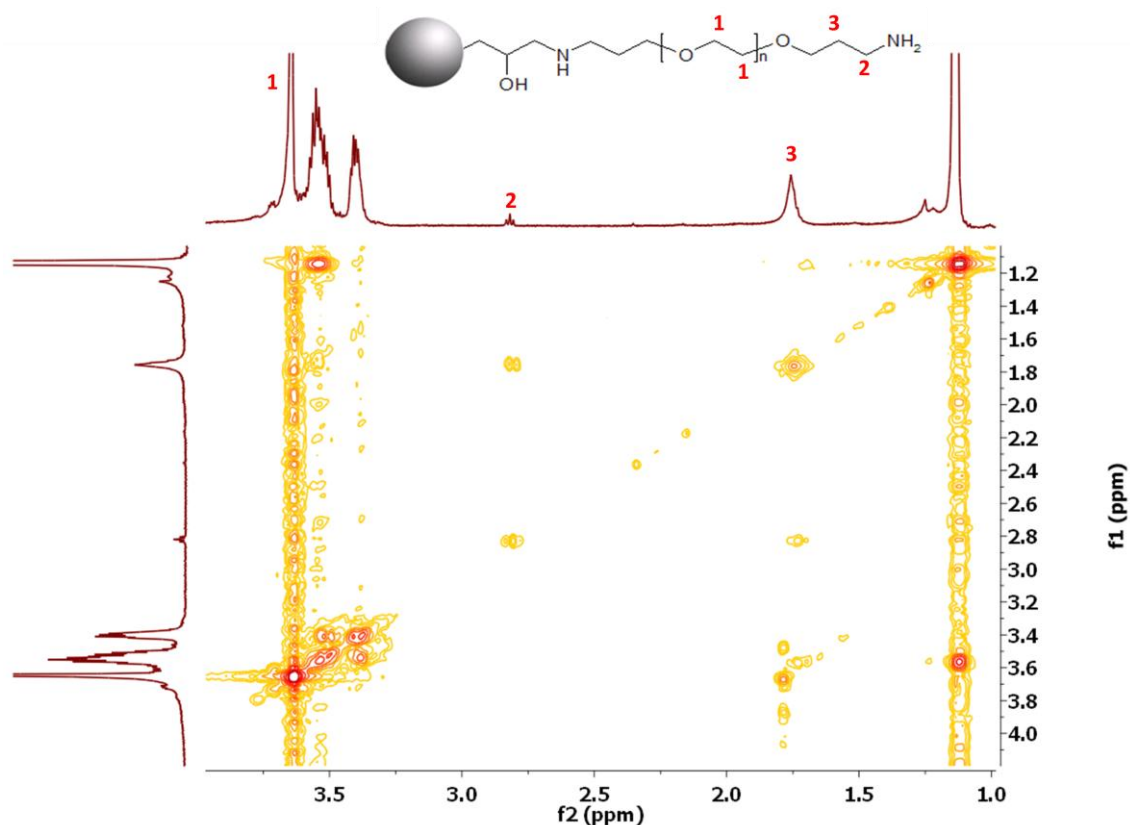


Figure 3:16 – Two dimensional COSY  $^1\text{H}$  HR-MAS NMR spectrum of swollen *O,O'*-bis(3-aminopropyl)polyethylene glycol functionalized (PEGylated) GMA/EGDMA polyHIPE at 500MHz in  $\text{CDCl}_3$ . The molecular structure of *O,O'*-bis(3-aminopropyl)polyethylene glycol functionalized (PEGylated) polyHIPE, numbered to indicate relevant protons that match peaks within the two dimensional COSY NMR spectra.

### 3.4 Conclusion

Thermally and photopolymerised polyHIPE materials have been shown to be post-functionalized with a range of nucleophiles. Loading of trisamine and morpholine at 1.18 and 1.71 mmol/g respectively was obtained for GMA/EGDMA polyHIPE after two hours of reaction at room temperature. Conversions were low with GMA/EGDMA polyHIPE (25 and 36 %), this was also shown to be the case for photopolymerised GMA-based polyHIPE materials. It was observed that higher, near quantitative conversion (up to 89 %) of epoxy groups could be achieved by conducting the reaction under reflux for 24 hours. This is in agreement with findings from the functionalization of other polyHIPE materials with trisamine and morpholine[24, 25]. It is envisaged that these materials could be used for the covalent attachment of enzymes, via the amine group from lysine residues that are commonly present on the surface of enzymes.

Attachment of a hydrophilic homobifunctional PEG linker group was successful, albeit with only ~ 2 % conversion of epoxy groups after reaction for 24 hours. This was attributed to the large exclusion volume of PEG chains preventing other PEG chains in solution covalently attaching to the polyHIPE surface[34].  $^1\text{H}$  HR-MAS NMR spectroscopy showed that attachment of *O,O'*-bis(3-aminopropyl)polyethylene glycol was successful, as indicated by the increase in intensity at 3.6 ppm as a result of glycol protons of the PEG chains, as well as a triplet peak at 2.6 ppm corresponding to  $\text{CH}_2\text{-NH}_2$  of the linker groups. In addition to this, a Kaiser test and reaction with a fluorescent probe, FITC, indicated that unreacted primary amine groups were present for further functionalization.

### 3.5 Bibliography

1. Gauthier MA, Gibson MI, and Klok HA. *Angew Chem Int Edit* 2009;48(1):48-58.
2. McCormack CL and Lowe AB. *Acc. Chem. Res.* 2004;37(5):312-325.
3. Matyjaszewski K and Tsarevsky NV. *Nature Chem.* 2009;1(4):276-288.
4. Peters EC, Svec F, and Freché JMJ. *Adv Mater* 1999;11(14):1169-1181.
5. Krenkova J and Svec F. *J Sep Sci* 2009;32(5-6):706-718.
6. Benes MJ, Horak D, and Svec F. *J Sep Sci* 2005;28(15):1855-1875.
7. Tunc Y, Golgelioglu C, Hasirci N, Ulubayram K, and Tuncel A. *J Chromatogr A* 2010;1217(10):1654-1659.
8. Svec F. *J Chromatogr A* 2010;1217(6):902-924.
9. Vlakh EG and Tennikova TB. *J Sep Sci* 2007;30(17):2801-2813.
10. Cummins D, Duxbury CJ, Quaedflieg P, Magusin P, Koning CE, and Heise A. *Soft Matter* 2009;5(4):804-811.
11. Junkar I, Koloini T, Krajnc P, Nemec D, Podgornik A, and Strancar A. *J Chromatogr A* 2007;1144(1):48-54.
12. Krajnc P, Leber N, Stefanec D, Kontrec S, and Podgornik A. *J Chromatogr A* 2005;1065(1):69-73.
13. Barbetta A, Dentini M, Leandri L, Ferraris G, Coletta A, and Bernabei M. *React Funct Polym* 2009;69(9):724-736.
14. Yao CH, Qi L, Jia HY, Xin PY, Yang GL, and Chen Y. *J Mater Chem* 2009;19(6):767-772.
15. Cummins D, Wyman P, Duxbury CJ, Thies J, Koning CE, and Heise A. *Chem Mater* 2007;19(22):5285-5292.
16. Biçak N, Gazi M, Galli G, and Chiellini E. *J Polym Sci Pol Chem* 2006;44(23):6708-6716.

17. Badyal JP, Cameron AM, Cameron NR, Oates LJ, Oye G, Steel PG, Davis BG, Coe DM, and Cox RA. *Polymer* 2004;45(7):2185-2192.
18. Kaiser E, Colescot.RI, Bossinge.Cd, and Cook PI. *Anal Biochem* 1970;34(2):595-&.
19. Coin I, Beyermann M, and Bienert M. *Nat Protoc* 2007;2(12):3247-3256.
20. <http://www.casaxps.com/>. Last accessed on 3/3/2011.
21. <http://mestrelab.com/software/>. Lst accessed on 3/3/2011.
22. Cameron NR. *Polymer* 2005;46(5):1439-1449.
23. Pulko I and Krajnc P. *Chem Commun* 2008(37):4481-4483.
24. Leber N, Fay JDB, Cameron NR, and Krajnc P. *J Polym Sci Pol Chem* 2007;45(17):4043-4053.
25. Stefanec D and Krajnc P. *Polym Int* 2007;56:1313-1319.
26. Woodruff DP and Delchar TA. *Modern techniques of Surface Science*. Cambridge University Press, 1986. pp. 96-113.
27. Jones RAL and Richards RW. *Polymers at Surfaces and Interfaces*. Cambridge: Cambridge University Press, 1999. pp. 101-106.
28. Clark DT and Feast WJ. *Polymer Surfaces*. John Wiley and Sons, 1978. pp. 309-350.
29. Hollas JM. *Modern Spectroscopy*. John Wiley and Sons, Ltd, 2005. pp. 309-313.
30. Green PF, Christensen TM, Russell TP, and Jerome R. *J Chem Phys* 1990;92(2):1478-1482.
31. Truica-Marasescu F and Wertheimer MR. *Plasma Processes Polym* 2008;5(1):44-57.
32. Graf N, Yegen E, Gross T, Lippitz A, Weigel W, Krakert S, Terfort A, and Unger WES. *Surf Sci* 2009;603(18):2849-2860.



33. Wang YH and Hsieh YL. *J Polym Sci Pol Chem* 2004;42(17):4289-4299.
34. Harris JM. *Poly(ethylene glycol) chemistry: biotechnical and biomedical applications*. Plenum Press, 1992.
35. Veronese FM and Pasut G. *Drug Discov Today* 2005;10(21-24):1451-1458.
36. Harris JM and Chess RB. *Nat Rev Drug Discovery* 2003;2(3):214-221.
37. Ingenito R, Bianchi E, Fattori D, and Pessi A. *J Am Chem Soc* 1999;121(49):11369-11374.
38. Guillier F, Orain D, and Bradley M. *Chem Rev* 2000;100(6):2091-2157.
39. Maddar A, Farcy N, Hosten NGC, De Muynck H, De Clercq PJ, Barry J, and Davis AP. *Eur J Org Chem* 1999(11):2787-2791.
40. Fernandez-Trillo F, van Hest JCM, Thies JC, Michon T, Weberskirch R, and Cameron NR. *Adv Mater* 2009;21(1):55-59.
41. Hermanson GT. *Bioconjugate Techniques*. Elsevier, 2008. pp. 396-403.
42. Lakowicz JR. *Principles of Fluorescence Spectroscopy*. Springer, 2006.
43. Song LL, Hennink EJ, Young IT, and Tanke HJ. *Biophys J* 1995;68(6):2588-2600.
44. Panchuk-Voloshina N, Haugland RP, Bishop-Stewart J, Bhalgat MK, Millard PJ, Mao F, and Leung WY. *J Histochem Cytochem* 1999;47(9):1179-1188.
45. Cameron NR, Sherrington DC, Ando I, and Kurosu H. *J Mater Chem* 1996;6(5):719-726.
46. Dinc CO, Kibarar G, and Guner A. *J Appl Polym Sci* 2010;117(2):1100-1119.
47. Shapiro MJ and Gounarides JS. *Prog Nucl Magn Reson Spectrosc* 1999;35(2):153-200.
48. Ando I and Asakura T. *Solid State NMR of Polymers*. Elsevier, 1998. pp. 509-588.

49. Iqbal S, Rodriguez-Llansola F, Escuder B, Miravet JF, Verbruggen I, and Willem R. *Soft Matter* 2010;6(9):1875-1878.
50. Keifer PA. *J Org Chem* 1996;61(5):1558-1559.
51. Keifer PA. *Drug Discov Today* 1997;2(11):468-478.
52. Bayer E, Albert K, Willisch H, Rapp W, and Hemmasi B. *Macromolecules* 1990;23(7):1937-1940.
53. Pursch M, Schlotterbeck G, Tseng LH, and Albert K. *Angew Chem Int Edit* 1996;35(23-24):2867-2869.
54. Anderson RC, Stokes JP, and Shapiro MJ. *Tetrahedron Lett* 1995;36(30):5311-5314.
55. Van Camp W, Dispinar T, Dervaux B, Du Prez FE, Martins JC, and Fritzing B. *Macromol Rapid Commun* 2009;30(15):1328-1333.

## **4 Enzyme Immobilization onto GMA-based Emulsion-Templated Porous Polymers**

### **4.1 Introduction**

Enzymes catalyse reactions resulting in much higher rates in comparison to uncatalysed reactions, due to the spatial orientation of amino acid residues within the active site of the enzyme[1]. Enzymes are also stereo- and regio-specific, react under relatively mild conditions[2] and can be used on industrial scales[3]. Examples of such enzymes are lipases, which naturally hydrolyse fatty esters. These have been utilized in the synthesis of a range of pharmaceutical intermediates and also bulk chemicals [4-9]. Proteases, whose natural function is the hydrolysis of amide bonds, can catalyse the formation of peptide bonds via either thermodynamic or kinetic control [2, 10, 11], and are being researched intensely for the production of di- and oligo-peptides[11-14]. Protease-catalysed peptide synthesis has several advantages over solid phase peptide synthesis, mainly milder reaction conditions and increased enantioselectivity [2].

Immobilization has many advantages over using the enzyme in solution, namely the ease of handling, increase in stability, the ability to remove the enzyme from the product by simple filtration and the reduction in cost from the ability to reuse immobilized enzymes[1, 15]. Spacer groups between the support surface and the enzyme can be beneficial in increasing the stability of enzyme and retaining its activity on immobilization, in comparison to direct immobilization[15-19].

Recently, polyHIPEs have been investigated as a potential material for the covalent immobilization of enzymes[20-23]. Although polyHIPE materials have a relatively low surface area and the loading of enzyme onto the material was observed to be several times lower than that of a commercially available product, they have been shown to have higher activities and can be re-used several times without any reduction in activity, which was attributed to a greater accessibility of the enzyme to the substrate in comparison to the commercially available product[20].

Our work is focusing on the immobilization of two hydrolases, lipase from *Candida Antarctica* (CAL) (EC 3.1.1.3) and proteinase K (pro K) (EC 3.4.21.64) from *Tritirachium album* onto GMA-based emulsion-templated porous polymers. Lipase loading onto the polymer was assessed by a Bradford assay and also by monitoring the activity of the enzyme solution before and after immobilization, together with washings of the polymer. Activity of CAL immobilized polyHIPEs was determined by a discontinuous photometric assay monitoring the hydrolysis of 4-nitrophenyl acetate. Pro K immobilized polyHIPEs' activity was monitored with a continuous electrochemical assay, monitoring the hydrolysis of N-acetyl-L-tyrosine ethyl ester monohydrate.

## 4.2 Experimental Section

### 4.2.1 Materials

See section 2.2.1 for list of materials used for the preparation of polyHIPE materials. Sodium phosphate monobasic (Sigma-Aldrich, ReagentPlus®, ≥ 99.0 %), sodium hydroxide (Sigma-Aldrich, reagent grade, ≥ 98 %), glutaraldehyde (Sigma-Aldrich, 50 wt. % in H<sub>2</sub>O), sodium cyanoborohydride (Fluka, purum, ≥ 95.0 %), *O,O'*-bis(3-

aminopropyl)polyethylene glycol (Sigma-Aldrich;  $M_n \sim 1500$ ), tetrahydrofuran (Fisher Scientific, laboratory reagent grade), lipase from *Candida Antarctica* (Sigma,  $\geq 1.0$  units/mg), proteinase K from *Tritirachium album* (Sigma, lyophilized powder,  $\geq 30$  units/mg protein), proteinase K, immobilized on Eupergit® C from *Tritirachium album* (Sigma, powder (granular),  $\geq 1500$  U/g), bovine serum albumin (Bio-rad, 2.15 mg/ml standard solution in  $H_2O$ ), Bradford Reagent (Bio-rad, concentrated solution, contains Coomassie brilliant blue, methanol, and phosphoric acid), 4-nitophenyl acetate (Fluka,  $\geq 99.0$  %), N-acetyl-L-tyrosine ethyl ester monohydrate (Aldrich, 99 %), methanol (Fisher, 99.8 %), cellulose acetate syringe filters (Cronus®, 0.45  $\mu m$  porosity, 13 mm diameter), Cuvette semi-micro disposable polystyrene cuvettes of 4.0 mL capacity and 10 mm path length (Fisher Scientific), were used as supplied unless stipulated otherwise.

All phosphate buffers used throughout this thesis were prepared prior to use with sodium phosphate monobasic. Concentrations of sodium phosphate monobasic buffer and pH were adjusted accordingly. Buffers were stored at 4 °C prior to use and were discarded after one month.

#### **4.2.2 GMA/EGDMA HIPE Preparation and Thermal Polymerisation**

For the preparation of thermally polymerised GMA-based polyHIPE materials see section 2.2.5.

#### **4.2.3 Photopolymerised GMA-based polyHIPE preparation**

For the preparation of photopolymerised GMA-based polyHIPE materials see section 2.2.2

#### 4.2.4 Functionalization of GMA-based PolyHIPE materials

##### 4.2.4.1 *O,O'-Bis-(3-aminopropyl) polyethylene glycol*

For the preparation of *O,O'*-bis(3-aminopropyl) polyethylene glycol functionalized photopolymerised GMA-based polyHIPEs see section 3.2.4.1.2.

#### 4.2.5 Enzyme Immobilization onto GMA-based Emulsion-Templated Porous Polymers

##### 4.2.5.1 *Lipase from Candida Antarctica*

Powdered polyHIPE was added to a 1 mg/mL solution of lipase from *Candida Antarctica* (CAL) in 20 mM pH 8.0 phosphate buffer (10 mg of polyHIPE per 1 mL of CAL solution) and stirred at room temperature for 24 hours. PolyHIPE material was washed with 20 mM pH 8.0 phosphate buffer (5 × 10 mL) and 20 mM pH 7.0 phosphate buffer (5 × 10 mL). PolyHIPE was then stored at 4 °C in pH 7.0 phosphate buffer until further use.

##### 4.2.5.2 *Proteinase K from Tritirachium Album*

###### 4.2.5.2.1 GMA/EGDMA thermally polymerised and GMA-based photopolymerised polyHIPE material

Followed the procedure in section 4.2.5.1 with proteinase K (pro K) as enzyme instead of CAL.

###### 4.2.5.2.2 PEGylated photopolymerised GMA-based polyHIPE material

Aminated (PEGylated) polyHIPE material was 'activated' with glutaraldehyde prior to immobilization of pro K [24-26]. Powdered PEGylated polyHIPE material (400 mg) was

added to 20 mL of a 10 % glutaraldehyde solution and stirred at 30 °C for 3 hours. Powdered glutaraldehyde-functionalized polyHIPE was then washed with 20 mM pH 8.0 phosphate buffer (5 × 10 mL) and was then added to a 1 mg/mL solution of pro K in 20 mM pH 8.0 phosphate buffer (10 mg of polyHIPE per 1 mL of pro K solution) and stirred at 4°C for 48 hours. Reduction of imine groups followed the protocol from Hermanson[27], whereby 10 µL of 5M sodium cyanoborohydride in 20 mM pH 8.0 phosphate buffer was added to the mixture and stirred for 2 hours at room temperature. PolyHIPE material was then washed with 20 mM pH 8.0 phosphate buffer (5 × 10 mL) and 20 mM pH 7.0 phosphate buffer (5 × 10 mL). PolyHIPE was then stored at 4 °C in pH 7.0 phosphate buffer until further use.

#### **4.2.6 Enzyme Loading**

##### **4.2.6.1 *Bradford Protein Assay***

The determination of the enzyme content was carried out from an adaptive method from Bradford[28]. Bio-rad dye reagent (containing Coomassie® Blue G-250, phosphoric acid and methanol) was removed from 4 °C storage and allowed to warm to ambient temperature and the dye reagent was passed through Whatman #1 filter paper to remove particulates prior to the start of the assay. Dye-reagent was then diluted fourfold with UHP H<sub>2</sub>O. Various dilutions from 0.1 to 1 mg/mL were undertaken with UHP H<sub>2</sub>O with a 2.15 mg/mL bovine serum albumin (BSA) standard. 100 µL of the BSA diluted solutions were added to 2.5 mL of diluted filtered dye reagent within 3 mL quartz cuvettes and mixed. The cuvettes were incubated at room temperature for a minimum of 5 minutes and for no longer than 1 hour. A blank of 100 µL UHP H<sub>2</sub>O added to 2.5 mL

diluted dye reagent was used to zero the UV-vis spectrophotometer. Various dilutions of the BSA standard were measured at 595 nm. A calibration curve was then used to determine the quantity in mg/mL of lipase in the solution after immobilization onto the polyHIPE material. This was then used to determine the loading of CAL onto the polyHIPE material.

#### **4.2.6.2 Determination from CAL solutions**

Lipase loading onto the polymer was determined from monitoring the activity of the lipase solution before addition to the GMA/EGDMA polyHIPE, after the addition to the polyHIPE, the washings of the polyHIPE and blank rate of activity with buffer. The loading followed the immobilization of the lipase onto the polymer described in section 4.2.5.1. Hydrolysis of 4-nitrophenyl acetate (4-NPac) was carried out at 25.0 °C and pH 8.0 and was monitored at 400 nm with the use of a temperature controlled UV-vis spectrophotometer. Each 4.0 mL polystyrene cuvette contained 2.97 mL 20 mM pH 8.0 phosphate buffer and 30 µL of a 1 mg/mL lipase solution (in 20 mM pH 8.0 phosphate buffer) before immobilization onto the polyHIPE, the lipase solution after immobilization onto the polyHIPE, the first 10 mL 20 mM pH 8.0 phosphate buffer washing of the polyHIPE, the second 10 mL 20 mM pH 8.0 phosphate buffer washing of the polyHIPE, or 20 mM pH 8.0 phosphate buffer (blank). All cuvettes with various solutions were placed within a temperature block and incubated at 25.0 °C for 25 minutes prior to the addition of 100 µL of 7.25 mg/mL 4-NPac solution in absolute ethanol.

It was assumed that: the lipase solution before was equivalent to the total amount of enzyme used (in mg), the activity of the lipase in the solution after reaction with polyHIPE



was not affected by the immobilization and the activity of the lipase that was adsorbed onto the polymer was not affected. Following these assumptions, the ratio of the magnitude of the enzyme activity with 4-NPac was related to the lipase solution used before immobilization. For example, an activity of half of the enzyme solution used before immobilization corresponds to a solution with 0.5 mg/ml of enzyme.

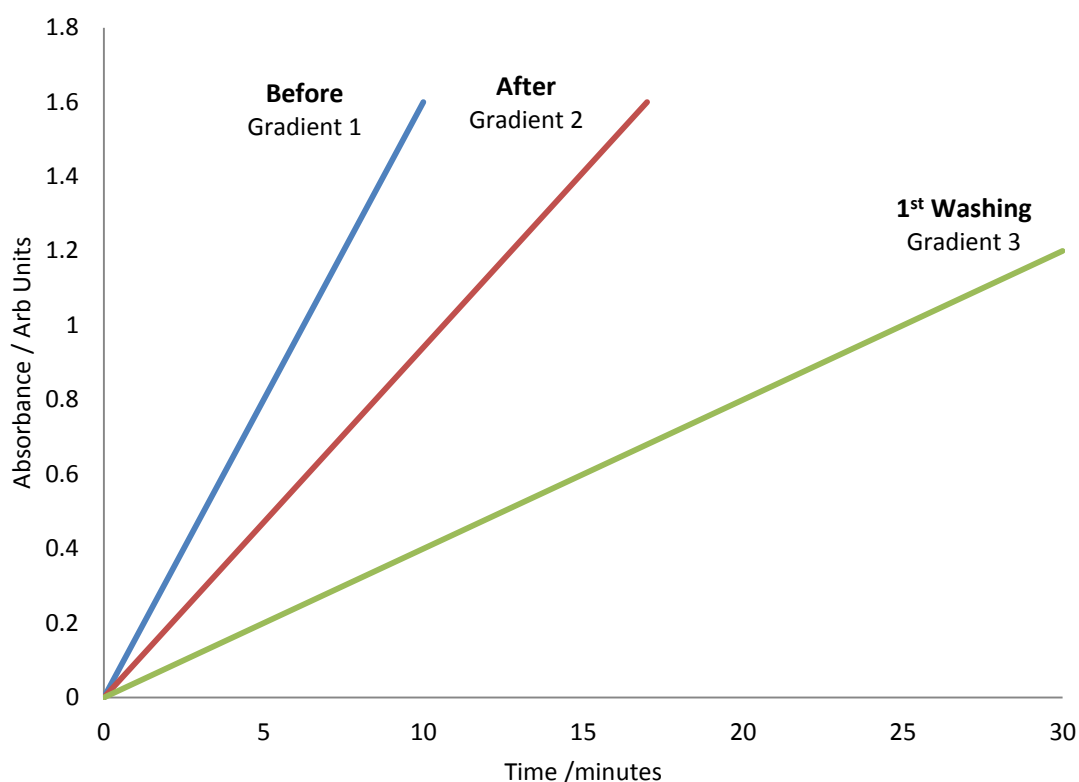


Figure 4:1 – Graphical illustration showing a typical data set for the hydrolysis of 4-NPac, where blank rate of hydrolysis has been subtracted. Blue line represents the lipase solution before immobilization onto the polymer, red line represents the lipase solution after immobilization, green line represents the 1<sup>st</sup> washing of the polyHIPE material.

The following equation was used for the determination of lipase loading onto GMA/EGDMA polyHIPE material:

$$\text{Enzyme Loading (wt \% per gramme PHP)} = \left[ \frac{(A - B - C)}{\text{weight of PHP (g)}} \right] \times 100\% \quad \text{Equation 4:1}$$

Where,

$$A = \left( \left( \frac{\text{grad.1}}{\text{grad.1}} \times 1 \text{ mg/mL} \right) \times \text{vol. ENZ soln.} \right) \quad \text{Equation 4:2}$$

$$B = \left( \left( \frac{\text{grad.2}}{\text{grad.1}} \times 1 \text{ mg/mL} \right) \times \text{vol. ENZ soln.} \right) \quad \text{Equation 4:3}$$

$$C = \left( \left( \frac{\text{grad.3}}{\text{grad.1}} \times 1 \text{ mg/mL} \right) \times \text{vol. washing soln.} \right) \quad \text{Equation 4:4}$$

The experiment was carried out in duplicate to determine the loading of lipase onto the polyHIPE material. A minimum of six repeats were taken for each solution including blank 20 mM pH 8.0 potassium buffer. Error within the value was determined from the standard deviation of the values determined for the enzyme loading from repeat experiments.

#### 4.2.7 Enzymatic Assay

##### 4.2.7.1 CAL discontinuous photometric assay

Prior to the start of the assay the spectrophotometer was blanked at 400 nm with 3 mL of 20 mM pH 8.0 phosphate buffer. 50 mg of CAL-immobilized polyHIPE material was placed within 4 mL polystyrene disposable cuvettes. 3 mL of 20 mM pH 8.0 phosphate buffer was added to the cuvettes and the mixtures were incubated at 25.0 °C for 25 minutes within a temperature block. The assay was started on the addition of 100 µL of 7.25 mg/mL 4-NPac in absolute ethanol to the cuvettes at 25.0 °C. Cuvettes were then removed from the temperature block at specific two minute time intervals from 2 min. to 14 min. The mixtures were filtered through 13 mm diameter 0.45 µm porosity

cellulose acetate syringe filters to remove any particulates. 100  $\mu\text{L}$  of this filtered solution was then added to 900  $\mu\text{L}$  of 20 mM pH 8.0 phosphate buffer in a 1.6 mL volume polystyrene cuvette and the absorbance of the solution was monitored at 400 nm. At least three repeats were carried out for each time interval. Activity of the immobilized lipase was determined from the Beer-Lambert equation using an extinction coefficient of  $18380 \text{ L mol}^{-1} \text{ cm}^{-1}$  for 4-nitrophenol[29].

#### **4.2.7.2 Pro K continuous titrametric assay**

Pro K assay followed titrimetric assay by Ebeling *et al.*[30]. The assay for pro K was the hydrolysis of N-acetyl-L-tyrosine ethyl ester monohydrate (ATEE) at pH 9.0 and 30 °C. An autotitrator was used for the electrochemical pH-stat assay. The Radiometer TIM 856 autotitrator consisted of an electrode, pH meter, a motor-driven 25 mL volume burette, and a magnetically stirred reaction vessel with water jacket. An external water bath and piston pump were used to control the temperature of the reaction vessel.

The following reagents were prepared: 50 % (w/w) methanol solution in UHP water, 50 mM ATEE in 50 % (w/w) methanol solution, 500 mM calcium chloride solution in UHP water, 60 mM sodium hydroxide solution in UHP water. To a stirred thermostatted reaction vessel powdered pro K immobilized polyHIPE material or pro K immobilized Eupergit C beads (between 50 – 600 mg), 12.0 mL of UHP water and 4.0 mL of calcium chloride solution was added and incubated at 30 °C for 20 minutes. This was then followed by the addition of 4.0 mL of 50 mM ATEE in 50 % (w/w) methanol solution in UHP water. The pH stat was then pre-dosed with 60 mM sodium hydroxide until a pH 9.0

was reached prior to the start of the assay. Equation 4:5 was used for the calculation of the activity (in units) of the immobilized enzyme per g of polyHIPE material.

$$\text{Units/g polyHIPE} = \frac{(\text{Molarity of NaOH}) \times (\text{Vol. NaOH}) \times (1000)}{(\text{g polyHIPE}) \times (T)} \quad \text{Equation 4:5}$$

where, one unit (U) is defined as the hydrolysis of 1.0  $\mu\text{mol}$  of ATEE per minute at pH 9.0 at 30°C, T is the time taken for the assay (in min.).

## 4.2.8 Instrumental

### 4.2.8.1 UV-Vis Spectrophotometer

Varian Cary 100 Spectrophotometer was used for the calculation of enzyme loading and the activity of lipase immobilized onto GMA/EGDMA polyHIPE at Durham University.

### 4.2.8.2 pH-Stat Autotitrator

Radiometer TIM 856 pH-Stat autotitrator was used for Pro K continuous titrimetric assay at Durham University.

## 4.3 Results and Discussion

### 4.3.1 Lipase Immobilization onto GMA/EGDMA PolyHIPE Material

The most commonly used immobilization strategy is to adsorb the enzyme onto the carrier material. This is a low-cost process and is used in the preparation of the commercially available product, Novozyme® 435 [15, 31]. However, it has a significant

drawback; enzyme can leach from the support on re-use, resulting in the reduction in the activity of the material over time [20].

Epoxy-containing polymeric materials have been used extensively for the covalent attachment of enzymes, with the advantage of the ability to re-use the material several times with minimal reduction in activity in comparison to adsorbed enzyme materials[1, 15, 32, 33].

Recently, polyHIPE materials have been utilized for the covalent immobilization of enzymes and their use as bioreactors[20-23]. This led to the investigation into the direct immobilization of lipase, via primary amine groups present on lysine residues on the surface of the enzyme onto epoxy containing polyHIPE materials (see Figure 4:2 for schematic). These polyHIPE materials were prepared via the copolymerisation of GMA with EGDMA following the method of their preparation by Krajnc *et al.*[34].

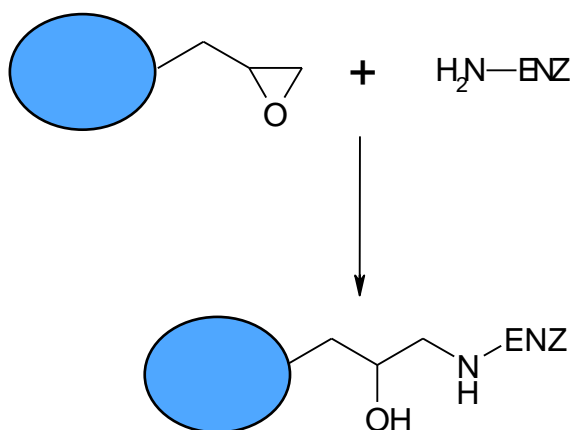


Figure 4:2 – Schematic of the direct immobilization of enzyme onto a GMA-based polyHIPE material

#### 4.3.1.1 Lipase loading onto GMA-based Emulsion-Templated Porous Polymers

There are several techniques for the quantification of protein concentration in solution; namely the Biuret[35], bicinchoninic acid (BCA) [36, 37], Lowry[38] and

Coomassie Blue dye-binding (Bradford) assay[28]. The Bradford assay was chosen for the quantification of lipase loading over the other methods due to the increased sensitivity and rapidity in comparison to the other methods[39]. There are three forms of the Coomassie Blue dye, a non-protonated anionic, protonated neutral and doubly protonated cationic form, with absorption maxima of 595 nm, 656 nm and 465 nm, respectively[40]. The protein stabilizes the blue, non-protonated anionic form of the Coomassie blue dye and the Bradford assay works by monitoring the absorbance of the protein-dye complex (at 595 nm) which is stable from 2 – 60 min. [28]. As Coomassie Blue G dye reagents have been observed to vary in quality from different suppliers, an absolute value of an absorbance related to a protein standard is not adequate, this is why a calibration curve of (standard) protein concentration *versus* absorbance of the Coomassie Blue G-250 bound protein was undertaken (see Figure 4:3) [41, 42]. Bovine serum albumin (BSA) was used as the protein standard due to its extended linear relationship of protein concentration with absorbance with the Coomassie Blue dye when compared with other standards[40]. In addition, it has been used previously as a standard protein for the quantification of lipase loading onto polyHIPE materials via the Bradford assay and it is commercially available in a purified form[21]. Lipase loading was then assessed from the lipase solution after immobilization onto the GMA/EGDMA polyHIPE material, using the calibration curve in Figure 4:3 for estimating the concentration of lipase in the solution after immobilization onto the polymer. The results obtained showed that the loading of the enzyme onto the polymer was 5.4, 6.6 and 7.5 wt. % per g of polyHIPE for CAL concentrations of 2 mg/mL, 3 mg/mL and 4 mg/mL, respectively.

Possible errors within the results obtained are mainly from the technique chosen for the quantification of the enzyme concentration. As the Bradford assay is affected by strong basic buffers, it has been shown that an increase of the pH of the protein dye complex can increase the absorbance at 595 nm, due to the increase in the anionic non-protonated form of Coomassie Blue[43]. As the enzyme solution that was used for the covalent attachment of the enzyme to the polyHIPE was in a pH 8.0 basic buffer, this could lead to an over-estimate of the lipase solution concentration after immobilization[41]. Another drawback of this technique in comparison to the biuret assay is sensitivity of the assay to the binding of the dye to different proteins [39, 41, 44]. The standard used has a significantly high absorbance with the dye in comparison with other proteins and this could lead to an under-estimation of the lipase concentration [28, 41, 45]. Hence, this technique is used as a semi-quantitative method for protein concentration determination.

The results obtained are considerably higher than other functional polyHIPE materials, which were observed to have loadings of 0.8 wt. % (determined via Bradford assay) [20], although this is possibly due to the increased concentration of functional groups. GMA/EGDMA polyHIPEs have 4.8 mmol/g of epoxy content (from the GMA content within the copolymer mixture), whereas NASI-based polyHIPEs have a much lower functional group content of only up to 1.2 mmol/g [20].

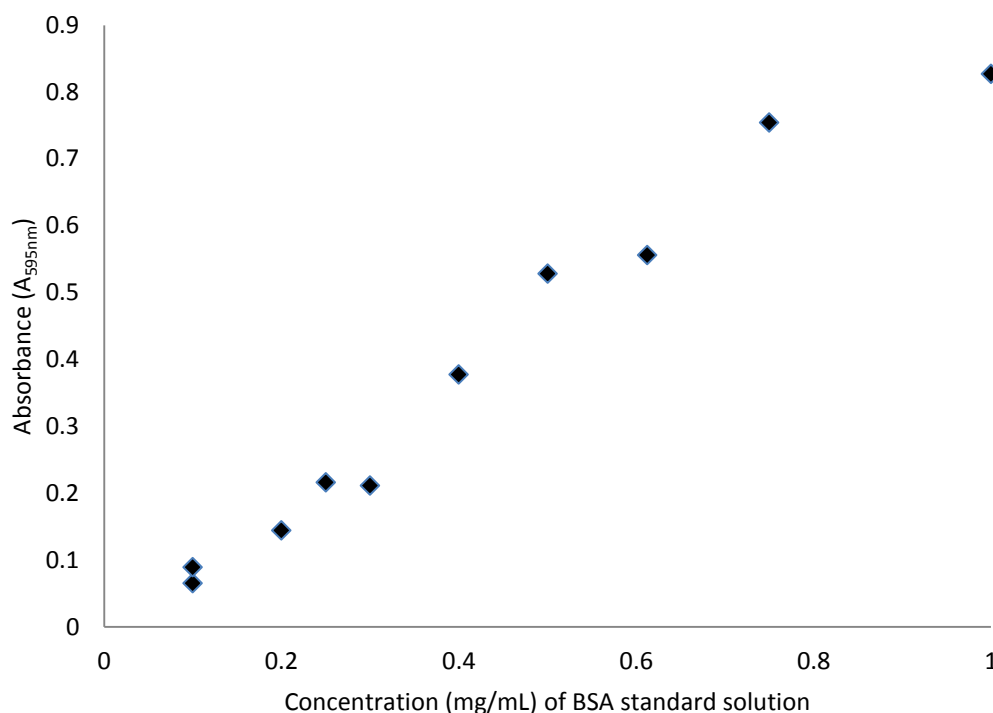


Figure 4:3 – Standard curve of 2.5 mL Bradford assay procedure with BSA standard.

In addition to estimating the quantification of lipase loading from the Bradford assay, the loading was also assessed by observing the activity of buffered lipase solutions used before immobilization onto the polymer, after immobilization and also washings of the polymer. This was undertaken to complement the Bradford assay. The assay that was used was one of the most common assays for lipase activity, the hydrolysis of 4-nitrophenyl acetate (4-NPac) forming the coloured 4-nitrophenol product, which has an absorbance maximum at 400 nm[46]. This assay was chosen as it allows for the continuous photometric measurement of the production of 4-nitrophenol with a spectrophotometer. The spectrophotometer used has a Peltier temperature block that allowed for accurate temperature control of the assay and also allowed for the monitoring of multiple samples at the same time. Figure 4:4 shows a typical graph from the hydrolysis of 4-NPac of the various solutions. A minimum of six repeats were taken for



each solution. Calculated value for the loading of lipase was  $5.6 \pm 0.6$  wt. % per g of GMA/EGDMA polyHIPE material. This value is in agreement with the values obtained from the Bradford assay.

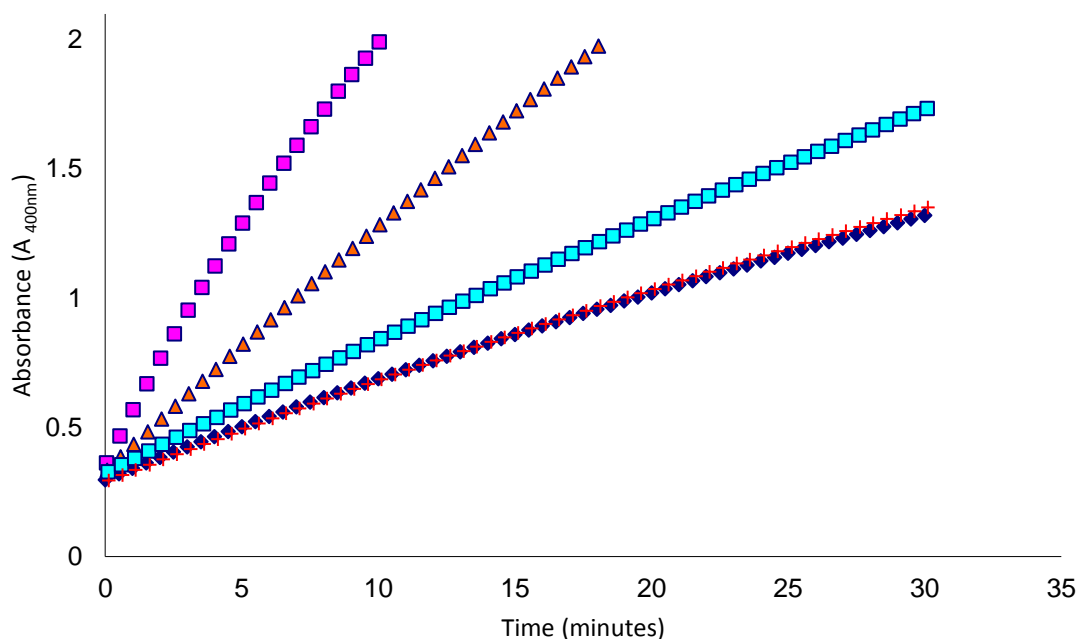


Figure 4:4 – Typical graph showing the hydrolysis of 100  $\mu$ L 4-nitrophenyl acetate (7.25 mg/mL in absolute ethanol) at 25°C in 2.97mL 20 mM pH 8.0 phosphate buffer with 30  $\mu$ L 1 mg/ml Lipase solution in 20 mM pH 8.0 phosphate buffer before immobilization onto GMA/EGDMA polyHIPE (represented by  $\blacksquare$ ), 30  $\mu$ L Lipase solution in 20 mM pH 8.0 phosphate buffer after immobilization onto polyHIPE material (represented by  $\blacktriangle$ ), 30  $\mu$ L from the 1<sup>st</sup> 10 ml 20 mM pH 8.0 phosphate buffer washing of GMA/EGDMA polyHIPE (represented by  $\blacksquare$ ), 30  $\mu$ L from the 2<sup>nd</sup> 10 ml 20 mM pH 8.0 phosphate buffer washing of GMA/EGDMA polyHIPE (represented by  $+$ ), and blank 30  $\mu$ L, 20 mM pH 8.0 phosphate buffer (represented by  $\blacklozenge$ )

#### 4.3.1.2 Enzymatic activity of Lipase Immobilized GMA/EGDMA PolyHIPE Material

Hydrolysis of 4-NPac was used as the assay for the lipase immobilized onto GMA/EGDMA polyHIPE. Figure 4:5 shows the images taken at different time intervals of the assay with immobilized enzyme, enzyme in solution and also two blanks, polyHIPE material (without immobilized enzyme) and buffer. The immobilized enzyme produces a

significant amount of yellow 4-nitrophenol product (see ii), Figure 4:5), indicating that some of the immobilized enzyme is still active after immobilization.

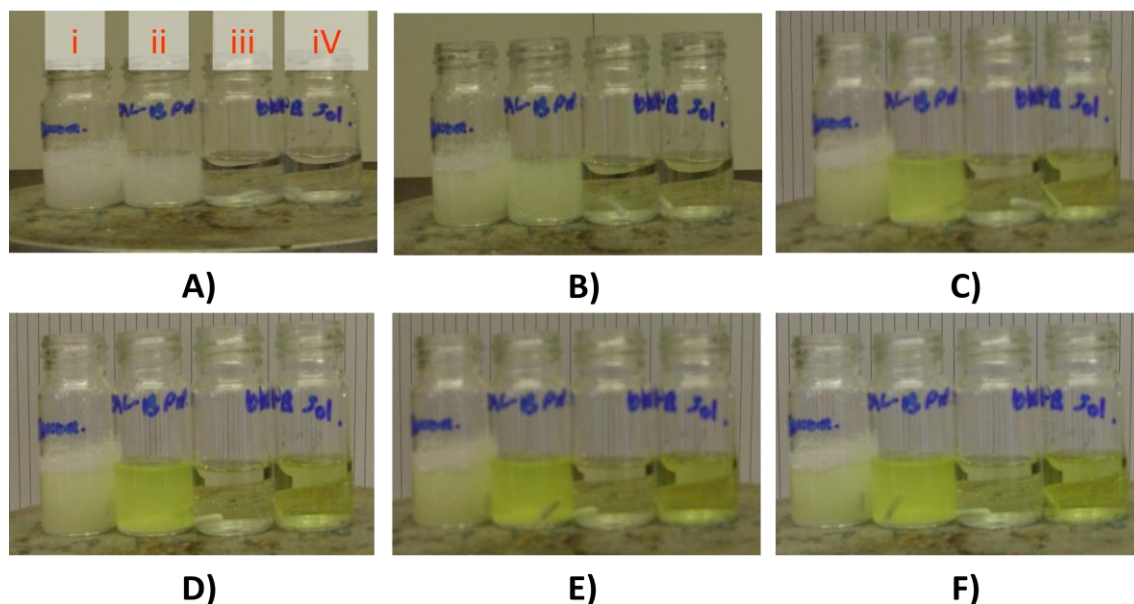


Figure 4:5 – Images showing the hydrolysis of pNPAc at room temperature of a stirred 3 mL 20 mM pH 8.0 phosphate buffer solution containing. i) 50 mg of GMA/EGDMA powdered polyHIPE (blank), ii) 50 mg of lipase immobilized GMA/EGDMA powdered polyHIPE, iii) 20 mM pH 8.0 phosphate buffer only (blank) and iv) 30  $\mu$ L of 1mg/mL lipase. A) Before the addition of pNPAc B) immediately C) 5 min. D) 10 min. E) 15 min. F) 20 min after the addition of 100  $\mu$ L 7.25 ml/mL 4-NPac in absolute ethanol.

Quantification of the activity of the immobilized lipase material was undertaken using a discontinuous photometric assay of the hydrolysis of 4-NPac. The assay was undertaken on a 3 mL scale (for use within cuvettes) with the addition of 50 mg of lipase immobilized polyHIPE material. The assay solution had to be filtered through hydrophilic cellulose acetate syringe filters prior to monitoring the absorbance of 4-nitrophenol, to remove particulates present within the solution from the powdered polyHIPE material. Filtered assay solution also had to be diluted tenfold due to the high absorbance at 400 nm from 4-nitrophenol over the time of the assay. At least three repeats were acquired for each time interval and cuvettes were incubated for a minimum of twenty minutes at 25.0  $^{\circ}$ C to

reduce errors in the measured activity from temperature differences within repeat experiments. The activity of the immobilized enzyme was assessed from the gradient between 2 to 10 minutes, as this was determined to be the linear part of the graph (see Figure 4:6). Overall, the activity was determined to be 1.5 U/g of polyHIPE material. This is over twenty five times lower than was expected for the amount of immobilized enzyme used as determined from the 5.6 wt. % loading and the activity of 0.819 U/mg (of powdered CAL) as determined from monitoring the activity of the 1 mg/mL lipase solution in 20 mM pH 8.0 phosphate buffer (see 4.3.1.1). This result indicates that the immobilization of the lipase resulted in the inactivation of the majority of the enzyme possibly due to microenvironmental effects.

The method described above for the assay of enzyme activity is quite inaccurate, sampling of the reaction could result in a reduction in 4-nitrophenol due to absorption onto the syringe filter membrane, and there are possible errors from dilution of the filtered solution (see Figure 4:6). Attempts were made to monitor the re-use of the immobilized lipase polyHIPE, however they were unsuccessful, due to the inaccuracy of the particular method, in addition to the amount of material that was lost through filtration through the syringe filters, which resulted in only one additional re-use of the immobilized enzyme that could be monitored (results not shown). A possible solution to the inaccuracies encountered with the discontinuous assay used would be to use a continuous photometric assay via the use of a flow-cell cuvette as used by Pierre *et al.* for monitoring the activity of immobilized lipase polyHIPE material[20].

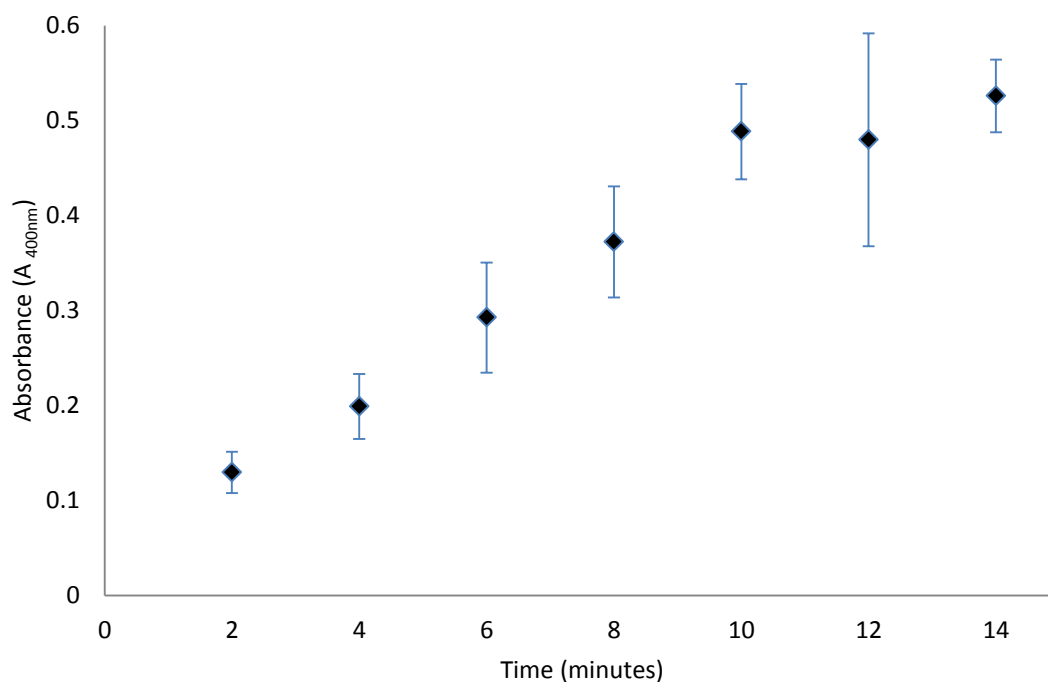
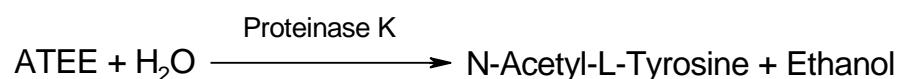


Figure 4:6 – Graph showing the hydrolysis of 4-nitrophenyl acetate at 25 °C with 20mM pH 8.0 phosphate buffer with immobilized lipase onto powdered GMA/EGDMA polyHIPE material. Each filtrate of immobilized enzyme solution at the particular time interval was diluted tenfold; i.e 900  $\mu$ L of 20 mM pH 8.0 phosphate buffer was added to 100  $\mu$ L of filtrate. At least three points were acquired for each time interval taken. Vertical error bars represent one standard deviation of the values recorded at the particular time interval.

### 4.3.2 Proteinase K Immobilization onto GMA-based PolyHIPE Materials

Immobilization of proteinase K onto GMA-based polyHIPEs was investigated as proteases can catalyse the synthesis of peptides and is a particular area of interest for the production of enantiomerically pure peptides without the need for solid phase peptide synthesis due to the advantages of mainly milder reaction conditions [2]. In addition to this, enzyme immobilization onto polyHIPE materials is a relatively under-studied area of research and only lipases have been studied to any extent [20-23]. It has been observed that immobilization of proteases can stabilise the enzyme in comparison to the enzyme used in solution[2].

The assay used for monitoring the activity of pro K immobilized polyHIPE material was the hydrolysis of N-acetyl-L-tyrosine ethyl ester at pH 9.0 (see reaction scheme below). This assay was chosen as it is a continuous electrochemical assay that would prevent some of the limitations that were observed for the discontinuous photometric assay for lipase immobilized polyHIPE materials.



Proteinase K was immobilized directly onto GMA/EGDMA thermally polymerised polyHIPE material and also GMA-based photopolymerised polyHIPE material using the same strategy as the immobilization of lipase onto the polymer, using the reaction between the primary amine groups present within lysine residues on the surface of the enzyme with epoxy groups present within the crosslinked polymer material (see Figure 4:2). Also, in addition to the direct immobilization of the enzyme onto the polymer, a hydrophilic linker group was also used for the covalent immobilization of the enzyme. The hydrophilic linker

group that was used was a 'short' chain homobifunctional poly(ethylene glycol) with pendant amine groups that was investigated in chapter 3 of this thesis (see section 3.3.2). Pro K was immobilized onto the PEGylated polyHIPE material via the 'activation' of the material with glutaraldehyde (see Reaction 1 and 2, Figure 4:7) [24-26]. Following this attachment the resulting material was reacted with sodium cyanoborohydride to reduce the imine groups present from the immobilization procedure (see Reaction 3, Figure 4:7) [27]. This reduction step is necessary as it has been observed that, when glutaraldehyde has been used for the attachment of enzymes onto insoluble carrier materials, it can improve the stability of the enzyme [47]. Sodium cyanoborohydride was used instead of sodium borohydride as it is a milder reducing agent that has been observed not to result in any reduction in activity when used in conjunction with proteins [27].

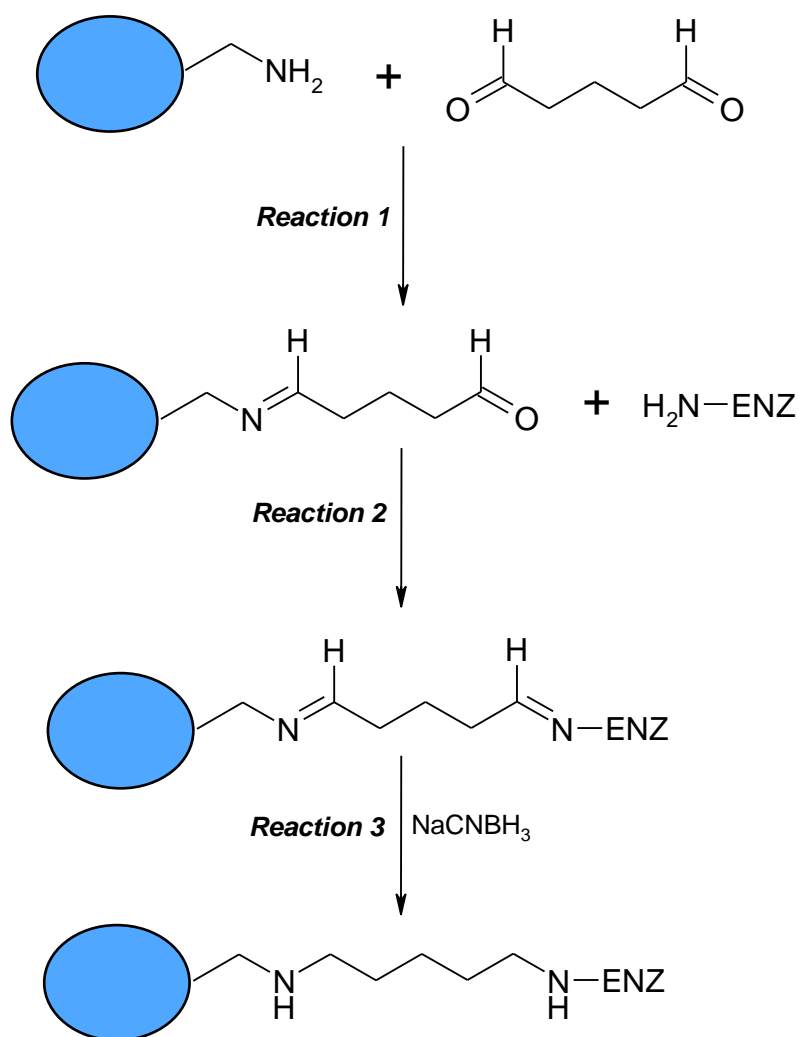


Figure 4:7 – Schematic of the immobilization of Pro K onto PEGylated polyHIPE material. Reaction 1 is the activation of the PEGylated polyHIPE with glutaraldehyde. Reaction 2 is the immobilization of pro K onto polyHIPE. Reaction 3 is the reduction of imine bonds with sodium cyanoborohydride.

A commercially available product, pro K immobilized onto Eupergit® C from Rohm and Haas, was investigated for comparison with the enzyme immobilized onto the GMA-based polyHIPE materials. Eupergit® C, is a beaded epoxy containing crosslinked polymer that has been used extensively for the covalent attachment of enzymes for use as bioreactors [32]. Results that were obtained showed that the activity of this particular enzyme was between 118 U/g and 199 U/g.

Determination of the loading of pro K on polyHIPE was attempted by measuring the absorbance of a pro K solution at 280 nm and using a predicted molar absorptivity of the proteinase K[48]. The results obtained were unreliable due to particulates present within the enzyme solutions. Filtration of this turbid enzyme solution gave varied results on repeating the procedure, possibly due to the adsorption of enzyme on the filters used.

Activity of proteinase K in solution was first calculated using the pH-stat assay and was observed to be 53 U/mg of lyophilized enzyme. The activity of pro K immobilized onto GMA/EGDMA, photopolymerised polyHIPE was 3.6 U/g and 0 U/g respectively. As the loading of the enzyme was not calculated it is difficult to determine whether the enzyme immobilized is inactivated or that a low loading of the enzyme for the material was responsible for the very low activities of these materials.

Activity of pro K immobilized onto GMA-based photopolymerised polyHIPE with the hydrophilic PEG linker group was significantly higher in comparison to the direct immobilization procedure. Activity was between 51 U/g and 78 U/g, indicating that the hydrophilic linker group did have a positive effect on the immobilization of the protease. Again, as the enzyme loading could not be accurately determined, it is not certain whether the higher activity of the PEGylated material is due to an increase in enzyme loading or due to a reduction in the inactivation of the enzyme on immobilization. The material was re-used two more times, washing the material with UHP water between assays, and activities of between 33 U/g to 55 U/g, and 19 U/g to 24 U/g respectively were found. The lowering of the activity between assays suggests either the leaching of the protease from the polyHIPE, indicative of some adsorbed enzyme or the inactivation of the enzyme on successive washes. As the assay solution and/or the washings of the



polymer were not assessed for enzyme content, either one or both of these processes could be occurring with the immobilized pro K polyHIPE material.

#### 4.4 Conclusion

CAL was immobilized onto GMA/EGDMA thermally polymerised polyHIPE with a loading of between 5.4 and 7.5 wt. % per g of polyHIPE for CAL concentrations between 2 mg/mL and 4 mg/mL as determined by Bradford assays. A loading of  $5.6 \pm 0.6$  wt. % per g of GMA/EGDMA polyHIPE material was determined by observing the activity of various lipase solutions used. These loadings are considerably larger than other loadings that have been reported within the literature for functional emulsion-templated porous polymers and this was attributed to the greater functional group content with the GMA/EGDMA polyHIPE in comparison to the other polyHIPE materials.

Pro K was immobilized directly onto GMA/EGDMA thermally polymerised polyHIPE material, in addition to the immobilization onto a homobifunctional PEG functionalized polyHIPE material that was 'activated' with glutaraldehyde prior to the immobilization of the enzyme. Activities of the pro K immobilized directly onto the polymer were considerably low (3.6 U/g and 0 U/g), and it could not be determined whether this was due to the inactivation of the enzyme on immobilization or that a low amount of the enzyme was immobilized. In addition to the direct immobilization the activities of the pro K immobilized onto the PEGylated polyHIPE were higher (51 and 78 U/g), although on washing of the polymer the activity of the immobilized enzyme decreased which could be indicative of adsorbed rather than covalently bound enzyme.

Overall, the particular low activity of both immobilized enzymes would initially suggest that GMA-based polyHIPE materials are not particularly well suited as a support for the immobilization of either enzyme used. However, it has been observed for other functional emulsion-templated porous polymers that these materials are well suited for the immobilization of enzymes[20-23]. Future work should focus on the development of the materials described in chapter 2 for use in a continuous flow set-up. This would allow the undertaking of a continuous photometric assay via the use of a UV flow-cell reducing the problems with the sampling technique used.

## 4.5 Bibliography

1. Bucholz K, Kasche V, and Bornscheuer U, T. Biocatalyst and Enzyme Technology: Wiley-VCH, 2005.
2. Illanes A. Enzyme Biocatalysis Principles and Applications, 2008.
3. Bornscheuer UT and Kazlauskas RJ. Hydrolases in Organic Synthesis Regio- and Stereoselective Biotransformations, 2nd Edition ed., 2006.
4. Anderson EM, Karin M, and Kirk O. Biocatal Biotransform 1998;16(3):181-204.
5. Sharma R, Chisti Y, and Banerjee UC. Biotechnol Adv 2001;19(8):627-662.
6. Kloosterman M, Elferink VHM, Vaniersel J, Roskam JH, Meijer EM, Hulshof LA, and Sheldon RA. Trends Biotechnol 1988;6(10):251-256.
7. Ladner WE and Whitesides GM. J Am Chem Soc 1984;106(23):7250-7251.
8. Matsumae H, Furui M, and Shibatani T. J Ferment Bioeng 1993;75(2):93-98.
9. Matsumae H, Furui M, Shibatani T, and Tosa T. J Ferment Bioeng 1994;78(1):59-63.
10. Capellas M, Caminal G, Gonzalez G, LopezSantin J, and Clapes P. Biotechnol Bioeng 1997;56(4):456-463.
11. Schellenberger V and Jakubke HD. Angew Chem Int Edit 1991;30(11):1437-1449.
12. Richards AO, Gill IS, and Vulfson EN. Enzyme Microb Technol 1993;15(11):928-935.
13. Gill I, Lopezfandino R, and Vulfson E. J Am Chem Soc 1995;117(23):6175-6181.
14. Bordusa F. Chem Rev 2002;102(12):4817-4867.
15. Cao L. Carrier-bound Immobilized Enzymes, Principles, Applications and Design: Wiley-VCH, 2005.

16. Nouaimi M, Moschel K, and Bisswanger H. *Enzyme Microb Technol* 2001;29(8-9):567-574.
17. Wang YH and Hsieh YL. *J Polym Sci Pol Chem* 2004;42(17):4289-4299.
18. Goddard JM and Hotchkiss JH. *Prog Polym Sci* 2007;32(7):698-725.
19. Bayramoglu G, Kaya B, and Arica MY. *Food Chem* 2005;92(2):261-268.
20. Pierre SJ, Thies JC, Dureault A, Cameron NR, van Hest JCM, Carette N, Michon T, and Weberskirch R. *Adv Mater* 2006;18(14):1822-1826.
21. Dizge N, Keskinler B, and Tanriseven A. *Colloid Surface B* 2008;66(1):34-38.
22. Dizge N, Aydiner C, Imer DY, Bayramoglu M, Tanriseven A, and Keskinler B. *Bioresour Technol* 2009;100(6):1983-1991.
23. Dizge N, Keskinler B, and Tanriseven A. *Biochem Eng J* 2009;44(2-3):220-225.
24. Miletic N, Rohandi R, Vukovic Z, Nastasovic A, and Loos K. *React Funct Polym* 2009;69(1):68-75.
25. Petro M, Svec F, and Fréchet JM. *Biotechnol Bioeng* 1996;49(4):355-363.
26. Hermanson GT. *Bioconjugate Techniques*. vol. 2nd Edition: Elsevier, 2008. pp. 134-135.
27. Hermanson GT. *Bioconjugate Techniques*. Elsevier, 2008. pp. 232-233.
28. Bradford MM. *Anal Biochem* 1976;72(1-2):248-254.
29. Bowers GN, McComb RB, Christensen RG, and Schaffer R. *Clin Chem* 1980;26(6):724-729.
30. Ebeling W, Hennrich N, Klockow M, Metz H, Orth HD, and Lang H. *Eur J Biochem* 1974;47(1):91-97.
31. Du W, Xu YY, Liu DH, and Zeng J. *J Mol Catal B-Enzym* 2004;30(3-4):125-129.
32. Katchalski-Katzir E and Kraemer DM. *J Mol Catal B-Enzym* 2000;10(1-3):157-176.

33. Boller T, Meier C, and Menzler S. *Org Process Res Dev* 2002;6(4):509-519.
34. Krajnc P, Leber N, Stefanec D, Kontrec S, and Podgornik A. *J Chromatogr A* 2005;1065(1):69-73.
35. Goshev I and Nedkov P. *Anal Biochem* 1979;95(2):340-343.
36. Smith PK, Krohn RI, Hermanson GT, Mallia AK, Gartner FH, Provenzano MD, Fujimoto EK, Goeke NM, Olson BJ, and Klenk DC. *Anal Biochem* 1985;150(1):76-85.
37. Brenner AJ and Harris ED. *Anal Biochem* 1995;226(1):80-84.
38. Lowry OH, Rosebrough NJ, Farr AL, and Randall RJ. *J Biol Chem* 1951;193(1):265-275.
39. Sapan CV, Lundblad RL, and Price NC. *Biotechnol Appl Biochem* 1999;29:99-108.
40. Compton SJ and Jones CG. *Anal Biochem* 1985;151(2):369-374.
41. Read SM and Northcote DH. *Anal Biochem* 1981;116(1):53-64.
42. Wilson CM. *Anal Biochem* 1979;96(2):263-278.
43. Stoscheck CM. *Anal Biochem* 1990;184(1):111-116.
44. Tal M, Silberstein A, and Nusser E. *J Biol Chem* 1985;260(18):9976-9980.
45. Gasparov VS and Degtyar VG. *Biochemistry-Moscow* 1994;59(6):563-572.
46. Eienthal R and Danson MJ. *Enzyme Assays: A Practical Approach*, 2nd Edition ed., Oxford University Press, 2009.
47. Bianchi D, Golini P, Bortolo R, and Cesti P. *Enzyme Microb Technol* 1996;18(8):592-596.
48. Pace CN, Vajdos F, Fee L, Grimsley G, and Gray T. *Protein Sci* 1995;4(11):2411-2423.

## 5 Conclusions and Future Work

As was mentioned in chapter 1, the aim of this thesis was to develop a highly porous open-void GMA-based emulsion-templated polymer, via the polymerisation of the continuous phase of a HIPE. These materials were then to be developed for use within a continuous flow set-up. The post-polymerisation functionalization of these materials with a range of amine nucleophiles was also to be investigated. Finally, these materials were to be used as a support for the covalent immobilization of enzymes, either directly onto the support or via a hydrophilic homobifunctional linker group from the support.

### 5.1 Preparation of GMA-based PolyHIPE Materials

Highly porous open-void morphology GMA-based emulsion-templated polymers were successfully prepared via the photoinitiated free radical polymerisation of the continuous phase of a w/o HIPE. It was observed that the ultrafast polymerisation, provided by the photoinitiation of these inherently unstable HIPEs was required to prepared GMA-based polyHIPEs with a homogeneous open-void morphology. Mercury intrusion porosimetry of these materials was possible due to relatively thick (35 mm in diameter) samples that were prepared via this technique, which was attributed to the photo-frontal polymerisation of these opaque emulsions.

GMA-based polyHIPEs prepared by copolymerisation with acrylate monomers were observed with mercury porosimetry to be a direct template from their respected emulsions. SEM analysis in conjunction with mercury porosimetry analysis showed that the degree of interconnectivity of these materials increased significantly from 0.07 to 0.37 on increasing the nominal porosity of the material from 73 % to 89 % (see section

2.4.2.1). GMA could be incorporated into the emulsion up to a concentration of 30 wt.% without affecting the morphology of the templated porous polymer (see section 2.4.2.2).

In addition to the preparation of emulsion-templated porous polymers via the photopolymerisation of the continuous phase of a HIPE, materials were also prepared with the addition of hydrophilic low molecular weight PEG-MA to a HIPE, producing a hydrophilic porous polymer. Future work needs to be carried out to investigate if the PEG-MA is covalently attached or adsorbed on to the support surface. Further work could be undertaken to investigate the preparation of functional hydrophilic porous polymers, via the addition of hydrophilic (meth)acrylate monomers such as (meth)acrylic acid to the HIPE. This could also be followed by investigation of covalent enzyme immobilization strategies onto this carboxylate functionalized material, such as the use of zero length linker groups such as carbodiimides and N,N'-carbonyl diimidazole[1].

A continuous flow set-up was successfully achieved via the development of the photopolymerised GMA-based emulsion-templated porous monolithic materials. This was accomplished via the functionalization of glass columns with methacrylate groups with subsequent photopolymerisation of the HIPE within the column. It was observed that the functionality of the crosslinker used was the most important factor for the preparation of these materials. For example, when TMPTA was used as the crosslinker, the monolith had a polymerised 'skin' on the surface, was not rigid and shrank on drying. In addition high back pressures were observed which indicated that the monolith was not rigid. In contrast, when a higher functional crosslinker, penta-/hexa-acrylate was used, a rigid material was prepared with low back pressures and without a polymerised skin on the surface of the monolith. Future work is required to further substantiate the claims that

the GMA-based polyHIPEs prepared with penta-/hexa- acrylate are rigid materials; this could be accomplished by the investigation if the back pressure is linear with flow rate through the monolithic material[2].

In addition to the preparation of GMA-based photopolymerised materials via the copolymerisation with acrylate monomers, a fully methacrylate-based polyHIPE was also prepared. This was accomplished via the usage of a trimethacrylate rather than dimethacrylate crosslinker. As was mentioned in chapter 2, these materials are potentially better supports in terms of higher porosity and hence lower back pressures for biomolecules than commercially available monolithic materials prepared via suspension polymerisation technique[3]. Further work needs to be undertaken on these materials, for example as thick monoliths (35 mm in diameter) can be prepared the average window size and window size distribution could be observed via mercury porosimetry, also FTIR analysis and post-polymerisation of the monolith has to be undertaken to assess the availability of the epoxy groups present within the material. In addition it would be beneficial to investigate if this polyHIPE could be used within the continuous flow system developed in chapter 2.

The porous polymers prepared within this thesis have inherently low surface areas, and it would be advantageous to increase the surface area of these materials for use as a bioreactor. High surface area polyHIPE materials have been prepared, of the magnitude of several hundreds of  $\text{m}^2/\text{g}$  for thermally initiated materials with the use of a high content of crosslinker with respect to the total monomer concentration and the use of a porogen creating an additional porosity on the surface of the templated macroporous material[4-7]. Recently, Yao *et al.* have prepared a GMA-based thermally initiated



emulsion-templated porous material with Pluronic triblock copolymers as surfactants similar to those used within this thesis for the preparation of GMA/TRIM photopolymerised material[8]. Investigation could be undertaken into the preparation of GMA-based photopolymerised materials with higher surface areas using both of these techniques. As the UV-initiation carried out within this thesis is undertaken at ambient temperature this would allow the use of low boiling point porogenic solvents, such as chloroform and hexane added to the continuous phase of the HIPE[9]. In addition, taking inspiration from GMA-EGDMA polyHIPEs prepared by Yao and coworkers[8], photopolymerised GMA-TRIM polyHIPEs could be prepared investigating the effect that surfactant concentration has on the morphology and surface area of the material.

## 5.2 Functionalization of GMA-based PolyHIPE Materials

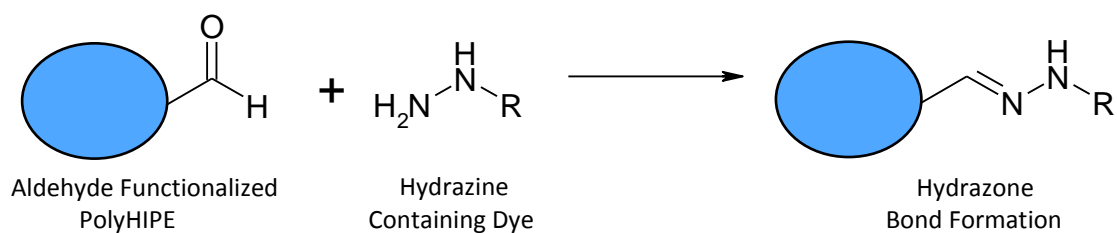
GMA-based polyHIPE materials were functionalized post-polymerisation with trisamine, morpholine and *O,O'*-bis(3-aminopropyl)polyethylene glycol. FTIR spectra indicated, through the reduction in intensity of the epoxy peaks at 906 and 845  $\text{cm}^{-1}$  on the reaction of the polyHIPE with trisamine, that the epoxy groups could be functionalized post-polymerisation (see section 3.3.1). However, it was also observed that these peaks did not disappear altogether, which suggested that some of the epoxy groups were not functionalized. This was also confirmed via the elemental analysis of trisamine and morpholine functionalized polyHIPEs, for example a conversion of only 25 and 36 % of the epoxy groups respectively was observed for thermally initiated GMA/EGDMA polyHIPE materials with reaction with the substrates following the procedure in section 3.2.4.2.1. However, when the reaction was carried out at reflux for 24 hours on

photopolymerized polyHIPE (PHP1) (for procedure see section 3.2.4.2.3) it was observed that much higher conversion was achieved of 72 and 82 % for trisamine and morpholine functionalized PHP1 respectively.

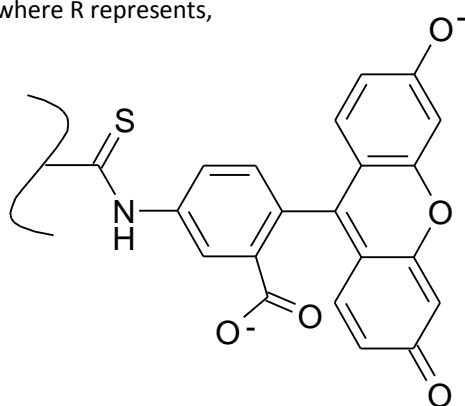
Hydrophilic homobifunctional linker group, *O,O'*-bis(3-aminopropyl)polyethylene glycol ( $M_n \sim 1500$ ) was successfully attached to GMA-based polyHIPEs. A positive Kaiser test and the attachment of a fluorescent dye which reacts preferentially with amine groups (FITC) indicated that primary amine groups were available after the covalent attachment of the spacer group to the porous polymer[10-13]. In addition, solid state  $^1\text{H}$  HR-MAS NMR spectroscopy also indicated the successful attachment of the *O,O'*-bis(3-aminopropyl)polyethylene glycol onto the material. Quantification of the attachment of PEG spacer group was accomplished via elemental analysis and also the attachment of Fmoc-Cl followed by the deprotection of primary amine groups and the quantification of the deprotected piperidine Fmoc adduct via UV spectrometry. A problem with the use of this spacer group was the low conversion of only  $\sim 2$  % of the epoxy groups, which was attributed to the high exclusion volume of PEG[14]. Further work would concentrate on the investigation into differing molecular weight PEG spacer groups and how this effects conversion. In addition, ethylene diamine could be used as the linker group to investigate the effect of the hydrophilicity (or hydrophobicity) on the immobilization of enzymes onto polyHIPE material.

As each step of a reaction procedure needs to be investigated to substantiate fully claims made, investigation into the 'activation' of the diamino PEG with glutaraldehyde (for subsequent covalent enzyme immobilization) must be undertaken. Possible qualitative colourmetric methods could include the covalent attachment of a hydrazine

functionalized fluorescent dyes from the formation of hydrazone bonds, for example, fluorescein-5-thiosemicarbazide, lissamine rhodamine B sulfonyl hydrazine or 7-amino-4-methyl-coumarin-3-acetic acid hydrazide (see Figure 5.1) [15]. In addition to the quantification with these dyes the use of non-fluorescein dyes (due to the high rate of photobleaching) could be used to determine the conversion of amine groups via the reduction in the absorbance of the dye solution after immobilization.  $^1\text{H}$  HR-MAS NMR spectroscopy could also be used to assess the functionalization of the polyHIPE material with glutaraldehyde.

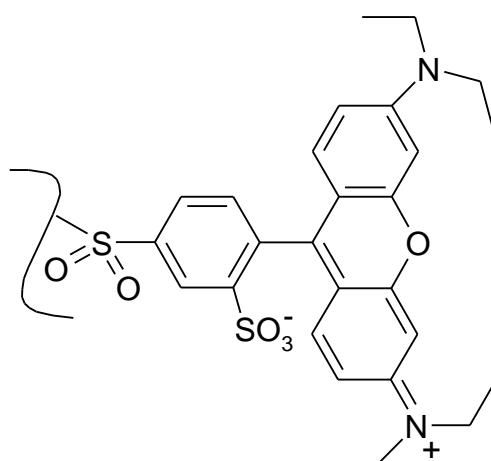


where R represents,

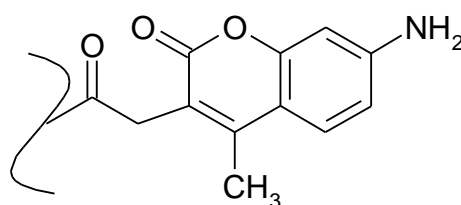


**Derivative**

Fluorescein



Rhodamine



Coumarin

Figure 5:1 – Schematic showing covalent attachment of hydrazine containing dyes with glutaraldehyde functionalized polyHIPE material for qualitative colourmetric analysis of the functionalization of the material.

Investigation could be undertaken into the attachment of a heterobifunctional linker group, such as PEG spacer groups which are terminated with a N-hydroxysuccinimide and a 'clickable' moiety on the other end, for example alkyne group. Bon *et al.* and Cummins *et al.* have shown that GMA-based polyHIPE materials can be functionalized via a copper catalyzed azide-alkyne cycloaddition click reaction, via the functionalization of epoxy group of the GMA with an azide residue (see Figure 5.2)[16, 17]. This functionalization procedure could be used for the materials prepared within this thesis. Following the functionalization of the polyHIPE with azide groups a heterobifunctional spacer group, terminated with an N-hydroxysuccinimide (NHS) group and an alkyne group could be 'clicked' onto the polyHIPE monolith[18]. Potentially, this would alleviate the need to use an excess of expensive linker group in the reaction procedure to assure a 1:1 reaction with epoxy groups. This could then be followed by the covalent attachment of enzymes onto the material via the reaction of lysine residues of the enzyme with the NHS group of the spacer group. Alternatively, this linker group could be covalently attached to an enzyme prior to being 'clicked' onto the polyHIPE, which has been observed by Fréchet *et al.* for azide Functionalized GMA/EGDMA beads with a similar linker group[19]. Overall this linking procedure could be beneficial taking advantage of the great specificity of click chemical reactions[20].

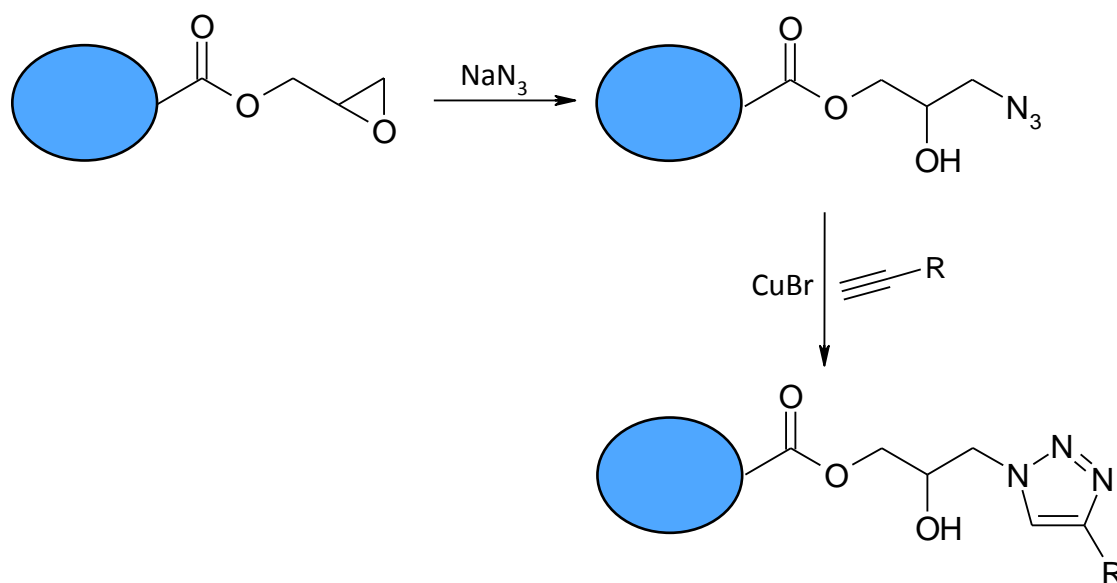


Figure 5:2 – Schematic showing the ring-opening of epoxy ring of GMA-based polyHIPE material with an azide, followed by further functionalization of the material via a Cu(I) catalyzed azide-alkyne click reaction

### 5.3 Covalent Enzyme Immobilization onto GMA-based PolyHIPE Materials

In conclusion, lipase from *Candida Antarctica* (CAL) and proteinase K (pro K) from *Tritirachium album* were immobilized onto GMA-based emulsion-templated porous polymers. The loading of CAL onto GMA-based polyHIPE was determined to be 5.4, 6.6 and 7.5 wt. % per g of polyHIPE for enzyme concentrations of 2, 3 and 4 mg/mL respectively via a Bradford assay and 5.6 wt. % for concentration of 1 mg/mL from spectrophotometric analysis of the decrease in activity of the enzyme solution used to the supernatant solution after immobilization and the washings of the polymer. Pro K was immobilized directly onto the polyHIPE in addition to a glutaraldehyde activated PEGylated photopolymerised polyHIPE material. Overall, the experimental procedures were problematic and future work would be needed to be carried out to address these issues. For example, a much more efficient and accurate method would be to utilize the

continuous flow photopolymerised system developed in chapter 2 with a flow cell cuvette allowing the continuous photometric analysis of enzyme activity as was used by Pierre *et al.*[21], in addition to the ability to measure the activity of the re-cycling of the enzyme without reduction in any polymeric material on re-use from filtration.

## 5.4 Bibliography

1. Hermanson GT. Bioconjugate Techniques. Elsevier, 2008. pp. 215-229.
2. Junkar I, Koloini T, Krajnc P, Nemec D, Podgornik A, and Strancar A. J Chromatogr A 2007;1144(1):48-54.
3. Bencina M, Babic J, and Podgornik A. J Chromatogr A 2007;1144(1):135-142.
4. Cameron NR and Barbetta A. J Mater Chem 2000;10(11):2466-2472.
5. Barbetta A and Cameron NR. Macromolecules 2004;37(9):3188-3201.
6. Barbetta A and Cameron NR. Macromolecules 2004;37(9):3202-3213.
7. Barbetta A, Dentini M, Leandri L, Ferraris G, Coletta A, and Bernabei M. React Funct Polym 2009;69(9):724-736.
8. Yao CH, Qi L, Jia HY, Xin PY, Yang GL, and Chen Y. J Mater Chem 2009;19(6):767-772.
9. Vlahk EG and Tennikova TB. J Sep Sci 2007;30(17):2801-2813.
10. Kaiser E, Colescot RL, Bossinge CD, and Cook PI. Anal Biochem 1970;34(2):595-&.
11. Coin I, Beyermann M, and Bienert M. Nat Protoc 2007;2(12):3247-3256.
12. Madder A, Farcy N, Hosten NGC, De Muynck H, De Clercq PJ, Barry J, and Davis AP. Eur J Org Chem 1999(11):2787-2791.
13. Hermanson GT. Bioconjugate Techniques. Elsevier, 2008. pp. 396-403.
14. Harris JM. Poly(ethylene glycol) chemistry: biotechnical and biomedical applications. Plenum Press, 1992.
15. Hermanson GT. Bioconjugate Techniques. Elsevier, 2008. pp. 412-439.
16. Gokmen MT, Van Camp W, Colver PJ, Bon SAF, and Du Prez FE. Macromolecules 2009;42(23):9289-9294.



17. Cummins D, Duxbury CJ, Quaedflieg P, Magusin P, Koning CE, and Heise A. *Soft Matter* 2009;5(4):804-811.
18. Tsarevsky NV, Bencherif SA, and Matyjaszewski K. *Macromolecules* 2007;40(13):4439-4445.
19. Slater M, Snauko M, Svec F, and Fréchet JMJ. *Anal Chem* 2006;78(14):4969-4975.
20. Sumerlin BS and Vogt AP. *Macromolecules* 2010;43(1):1-13.
21. Pierre SJ, Thies JC, Dureault A, Cameron NR, van Hest JCM, Carette N, Michon T, and Weberskirch R. *Adv Mater* 2006;18(14):1822-1826.

# Conferences, Seminars, Publications and Awards

## A1.1 Conferences

### A1.1.1 Oral Contribution

- International Workshop “Macroporous polymers” (5<sup>th</sup> -7<sup>th</sup> May 2009, Imperial College London) - Covalent Enzyme Immobilization onto Emulsion-Templated Porous Polymers
- 2<sup>nd</sup> North East Process Industry Cluster (NEPIC) symposium – “Sustainable Chemical Processes” (30<sup>th</sup> June 2009, Chemistry Department, Durham University) - Covalent Enzyme Immobilization onto Emulsion-Templated Porous Polymers
- RSC Macro Group Young Researchers Meeting – (29<sup>th</sup> -30<sup>th</sup> April 2010, School of Chemistry, University of Nottingham) – Covalent Enzyme Immobilization onto Emulsion-Templated Porous Polymers

### A1.1.2 Poster Presentations

- RSC Symposium - “Advances in Biocatalysis” (21<sup>st</sup> April 2009, University College London, UK) - Covalent Enzyme Immobilization onto Emulsion-Templated Porous Polymers
- 42<sup>nd</sup> IUPAC Congress – “Chemistry Solutions” (2<sup>nd</sup> -7<sup>th</sup> August 2009, SECC, Glasgow, UK) - Covalent Enzyme Immobilization onto Emulsion-Templated Porous Polymers

- 238<sup>th</sup> American Chemical Society (ACS) National Meeting (16<sup>th</sup> – 20<sup>th</sup> August 2009, Washington DC, USA) – Covalent Enzyme Immobilization onto Emulsion-Templated Porous Polymers
- Polymer IRC Spring Meeting (28<sup>th</sup> March 2010, Durham University, UK)- Covalent Enzyme Immobilization onto Emulsion-Templated Porous Polymers
- RSC Perkin Division Northeast Region Organic Chemistry Symposium – (15<sup>th</sup> April 2010, Chemistry Department, Durham University, UK) – Covalent Enzyme Immobilization onto Emulsion-Templated Porous Polymers
- MACRO 2010 43<sup>rd</sup> IUPAC World Polymer Congress – “Polymer Science in the Service of Society” (11<sup>th</sup> -16<sup>th</sup> July 2010, SECC, Glasgow, UK) – Covalent Enzyme Immobilization onto Emulsion-Templated Porous Polymers
- Soft Matter/Polymer symposium (16<sup>th</sup> July 2010, Durham University, UK) – Covalent Enzyme Immobilization onto Emulsion-Templated Porous Polymers
- The Institute of Materials, Minerals and Mining (IOM<sup>3</sup>) Applied Polymer Science Group Meeting (16<sup>th</sup> September 2010, Van Mildert College, Durham University, UK) – Emulsion-Templated Porous Polymers

#### **A1.1.3 Attended**

- High Polymer Research Group 50<sup>th</sup> Anniversary Meeting – “Polymer Science: The Next Fifty Years” (25<sup>th</sup> – 29<sup>th</sup> April 2010, Shrigley Hall Hotel, Pott Shrigley, Cheshire, UK)

## A1.2 Seminars

- IRC Polymer Course Interdisciplinary Research Centre (IRC) Polymer Science and Technology Course (2007):
  - Polymer Physics
  - Basic Polymer Science (Part 1)

## A1.3 Publications

- *Review*: Scott D. Kimmins and Neil R. Cameron, “Functional Porous Polymers by Emulsion Templating: Recent Advances”, *Adv Funct Mater*, **2011**, 21, 211-225 DOI: 10.1002/adfm.201001330
- *Communication*: Elaine Lovelady, Scott D. Kimmins, Junjie Wu and Neil R. Cameron, “Emulsion Templated Porous Polymers by Thiol-Ene and Thiol-Yne Chemistry”, *Polymer Chemistry*, **2011**, 2, 559-562 DOI: 10.1039/c0py00374c
- *Preprint*: Scott D. Kimmins, Paul Wyman, Neil R. Cameron and Jens C. Thies, “Covalent Enzyme Immobilization onto Emulsion-Templated Porous Polymers”, Preprint ACS PMSE Div., **2009**, 101, 1371-1372.

## A1.4 Awards

- 2<sup>nd</sup> Prize for Oral Contribution: North East Polymer Association (NEPA) Young Persons Lecture Competition (24<sup>th</sup> February 2010, Chemistry Department, Durham University, UK) – Emulsion-Templated Porous Polymers
- Durham University Teaching Induction for Postgraduates: Preparing to Teach – Demonstrating (2007)

- Durham University Teaching Induction for Postgraduates: Preparing to Teach – Assessment in the Sciences (2007)